EFFECT OF HYDROPHILIC SEGMENT LENGTH ON SIZE AND STABILITY OF CORE CROSSLINKED MICELLES

by

RABİA ARSLAN

B.S., Chemistry, Fatih University, 2011

Submitted to the Institute for Graduate Studies in
Science and Engineering in partial fulfillment of
the requirements for the degree of
Master of Science

Graduate Program in Chemistry

Boğaziçi University

2014

EFFECT OF HYDROPHILIC SEGMENT LENGTH
ON SIZE AND STABILITY
OF CORE CROSSLINKED MICELLES

APPROVED BY:

Assoc. Prof. Rana Sanyal ……...….
(Thesis Supervisor)

Assoc. Prof. Amitav Sanyal …..……..

Assoc. Prof. Burak Esat ……

DATE OF APPROVAL: 06.01.2014

To my dear family

ACKNOWLEDGEMENTS

I would like to express my most sincere gratitude to my thesis supervisor Assoc. Prof. Rana Sanyal for her endless patience, attention and scientific guidance throughout this study. I appreciate her support and useful comments throughout my laboratory work.

I wish to express my thanks to Assoc. Prof. Amitav Sanyal for his scientific advices and his helpful discussions regarding all my research in this laboratory.

I wish to express my thanks to Assoc. Prof. Burak Esat for his careful and constructive review of the final manuscript.

I would like to extend my thanks to Burcu Sümer Bolu, for her care, endless patience and support during my whole research and laboratory works.

I also thank my labmates, Özgül Gök, Filiz Çalık and Nazlı Böke for their friendship and endless support and Sadık, Yasemin, Aslı, Merve, Duygu, Tuğçe, Laura, Betül, Sedef, Özlem, Fatma, Janset, Harun, Hasan Can, Sesil, Yavuz and my hoodmate Nergiz Cengiz for their companionship. I would like to thank all my friends and all the members of the faculty in the Chemistry Department.

Finally, my deepest thanks go to my husband Mehmet for his endless love, support and encouragement throughout these years.

ABSTRACT

EFFECT OF HYDROPHILIC SEGMENT LENGTH ON SIZE AND STABILITY OF CORE CROSSLINKED MICELLES

Polymeric micelles are being extensively studied in recent years for their potential use as drug carriers. They consist of hydrophilic and hydrophobic segments and due to the solubility difference between these segments, polymeric micelles are self-assembled into core-shell nanostructures formed in aqueous solution. The hydrophobic reservoir of micelles are capable of hosting low water soluble drug molecules, thus so-prepared micellar constructs have been widely utilized in preparation of sustained/controlled drug releasing platforms. In order to improve the stability of micelles and to achieve a more gradual release profile crosslinking strategies can be employed. In this thesis, several amphiphilic linear polymer-dendron conjugates have been synthesized via Huisgen type 'click' reaction using biodegradable, hydrophobic polyester dendron and biocompatible, hydrophilic p(PEGMA)-based copolymers. These conjugates differ from each other in terms of length of hydrophilic segment while the hydrophobic dendron part is constant. Since, the periphery of the dendron contains alkene units, core of the micelles were crosslinked using thiol-ene 'click' chemisty to increase the stability of the micelles. The micelle formation of conjugates were investigated in aqueous media, studying size and stability. The results demonstrated that as increasing the polymer length of the conjugates, critical micelle concentrations and size distributions did not change which means that stability of the micelles remained same.

ÖZET

ÇEKİRDEĞİ ÇAPRAZ BAĞLANMIŞ MİSELLERDEKİ HİDROFİLİK SEGMENT UZUNLUĞUNUN BOYUT VE STABİLİTE ÜZERİNDEKİ ETKİSİ

Polimerik miseller potansiyel ilaç taşıma sistemi özelliğinden dolayı son yıllarda yaygın olarak kullanılmaktır. Miselleri oluşuran hidrofilik ve hidrofobik kısımlar, aralarındaki çözünürlük farkından dolayı su içerisinde kendiliğinden çekirdek-kabuk yapısı oluştururlar. Hidrofobik çekirdek kısım suda çözünürlüğü az olan ilaç molekülleri için rezervuar görevi görürken, kabuk kısmı bütün sistemin sudaki çözünürlüğünü sağlar. Bu sayede, polimerik miseller devamlı ve kontrollü ilaç salınım platformlarının hazırlanmasında sıkça kullanılırlar. Misellerin stabilitesi, kandaki dolaşım süresinin artmasında ve kontrollü ilaç salınımının gerçekleşmesinde önemli yere sahiptir. Bu yüzden daha kararlı miseller elde edebilmek için birçok strateji geliştirilmiştir. Bunlardan birtanesi de çekirdeği çapraz bağlama yöntemidir. Bu tezde, çeşitli amfifilik polimer-dendron konjugatları, bio-çözünür hidrofobik dendron ve bio-uyumlu hidrofilik polimer kullanılarak, Huisgen tipi ‘klik’ reaksiyonu aracılığıyla sentezlenmiştir. Konjugasyonlar değişik zincir uzunluğuna sahip polimerler ile uç grupları alken birimleri içeren dendronlar arasında olmuştur ve misel oluşum çalışmaları, sulu ortam içinde incelenmiştir. Misel stabilitesini arttırmak için, iç kısım tiyol-en ‘klik’ kimyası kullanılarak çapraz bağlanmıştır ve çekirdeği çapraz bağlanmamış misellerle ebat ve stabilite açısından karşılaştırılmıştır. Konjugatların hidrofilik zincir uzunluğu değiştirilerek elde edilen misellerin, boyut ve stabilite üzerindeki etkisi incelenmiştir.

TABLE OF CONTENTS

LIST OF FIGURES

LIST OF TABLES

LIST OF SYMBOLS

J	Coupling constant

LIST OF ACRONYMS/ABBREVIATIONS

Bis-MPA	2,2-bis(hydroxymethyl)propionic acid
$CDCl_3$	Deuterated Chloroform
CH_2Cl_2	Dichloromethane
CMC	Critical Micelle Concentration
CuAAC	Copper catalyzed azide alkyne cycloaddition
DCC	Dicyclohexylcarbodiimide
DDS	Drug Delivery System
DLS	Dynamic Light Scattering
DMAP	N,N Dimethylaminopyridine
EPR	Enhanced Permeability and Retention
Et_2O	Diethyl ether
FT-IR	Fourier Transform Infrared
G_1	Generation 1 dendron
G_2	Generation 2 dendron
G_3	Generation 3 dendron
NMR	Nuclear Magnetic Resonance
PAMAM	Poly(amido amine)
PEA	Poly Ethyl Acrylate
PEG	Poly(ethylene glycol)
PEO	Poly(ethylene oxide)
PCL	poly-ε-caprolactone
PMDETA	N,N,N',N',N''-Pentamethyldiethylenetriamine
STEM	Scanning Transmission Electron Microscope
TEA	Triethylamine
THF	Tetrahydrofuran

1. INTRODUCTION

1.1. Polymeric Micelles in Targeted Drug Delivery

Cancer is a widespread group of diseases involving uncontrolled cell growth and invasion by abnormal cells to nearby parts of the body. According to the International Agency for Research on Cancer (IARC), 12.7 million new cancer cases were seen throughout the world in 2008. Around 5.6 million of new cases were assigned to developed countries and 7.1 million in developing countries (Figure1.1). This estimated number corresponds to 7.6 million cancer deaths (21,000 deaths a day) [1]. Each year the number of new cancer cases and deaths are increasing continuously.

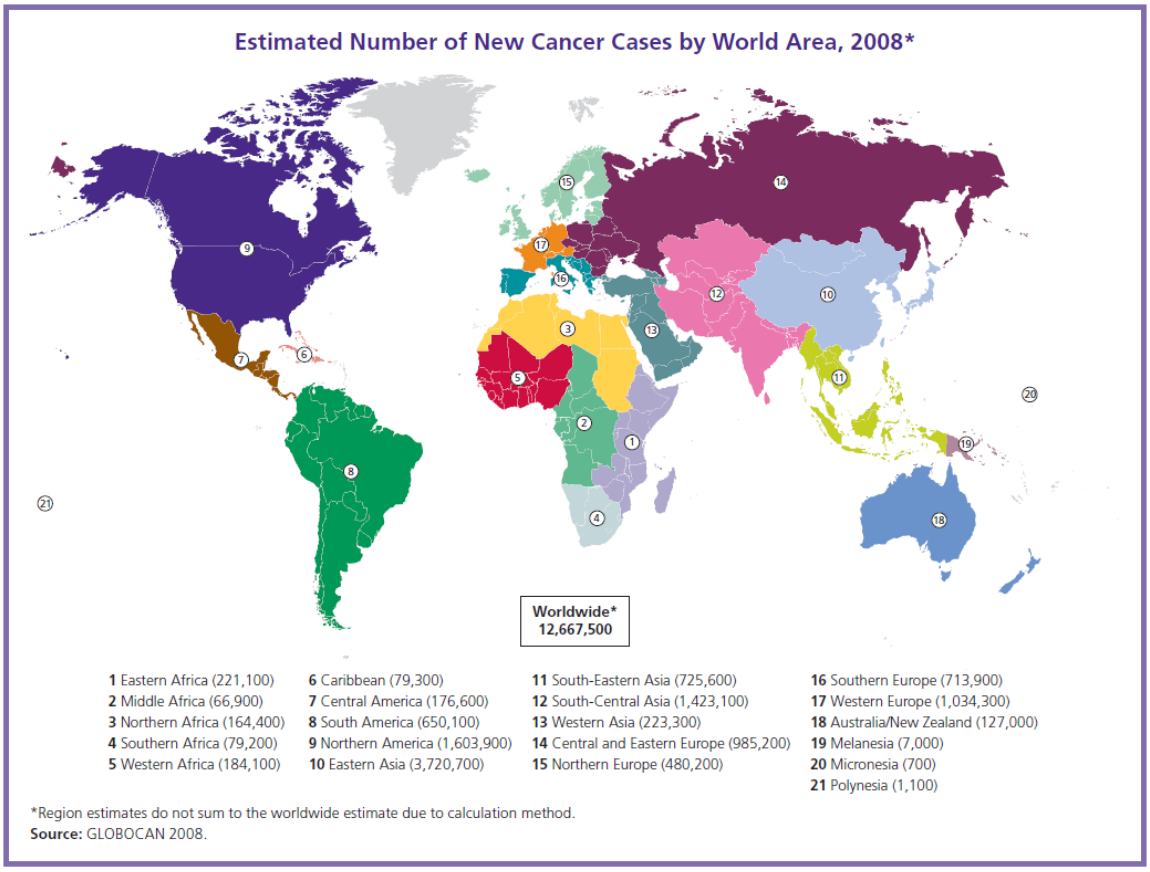

Figure 1.1. World cancer map showing the new cases as of year 2008 [2].

On the other hand, many treatment methods including surgery, chemotherapy, radiation therapy, immunotherapy and biologic therapy are applied to cure the disease or at

least slow down the tumor growth. Chemotherapy includes the use of drugs to eliminate cancer cells and constitutes the widely applied treatment among these methods. However, conventional chemotherapeutic drugs used in the treatment of cancer have undesirable toxicity to normal tissues, which lead to patient morbidity and mortality. Cancer drugs are poisonous and designed to attack cells with high proliferation rate, hence the cancer cells. Nevertheless, they also affect normal cells with high division potential. Furthermore, the nonspecific biodistribution of cancer drugs results in uptake by healthy cells causing cancer related negative side effects such as bone marrow suppression, inflamed mucous membranes, and hair loss. Lack of water solubility, short blood half-lives, rapid clearance and narrow therapeutic indices are the other important limitations of the chemotherapeutic drugs. Therefore, targeted drug delivery in which directing therapeutic agents to a particular cell type or tissue in a site-specific manner have gained a lot of attention in cancer research studies [3].

Recent decades have witnessed remarkable advancement in the construction of nanocarrier platforms to be used in targeted drug delivery systems. Using targeted drug delivery, it is aimed to carry a certain amount of the chemotherapeutic agent, for a prolonged period, to a particular cell type or tissue within the body. In other words, nanocarriers hit the target without damaging healthy tissues [4-5]. There is a vast range of nanoparticles available for drug delivery systems, recently used in cancer therapy such as liposomes, viral nanoparticles, carbon-based structures and polymeric nanoparticles as micelles and dendrimers (Figure 1.2) [6]. Among these chemotherapeutic drug delivery vehicles, polymer-based nanoparticles are being extensively investigated for their prospective use as drug carriers. Incorporating conventional low-molecular-weight (MW) drugs into high-MW water-soluble polymeric systems offers several advantages for cancer treatment. Drug can be passively accumulated in tumorous tissues via the enhanced permeability and retention (EPR) effect (Figure 1.3) [7-8]. Tumor vasculature system has a unique pathophysiologic character with respect to healthy cells. It has leaky structures which results in a selective increase of permeability to macromolecules in tumor environment [9]. Besides, limited lymphatic drainage prolongs the residence time of macromolecules in the interstitial space. As a result, enhancement of drug concentration in target tissue is observed compared to an equivalent dose of the drug given conventionally. Consequently, under favor of the EPR effect, systemic toxicity is decreased while

therapeutic efficacy is enhanced [10-11]**.** In addition to passive targeting, drug circulation time can be improved because of the higher hydrodynamic volume of polymeric system. It is known that larger molecules are eliminated more slowly from the renal filtration resulting in higher drug concentration in plasma [12]. Ultimately, by using nanoparticles such as polymer-based systems, respectable therapeutic advantages have gained due to higher drug accumulation in cancer cells, increased drug circulation time in the plasma and less toxicity in normal cells compared to conventional low molecular weight drugs [13].

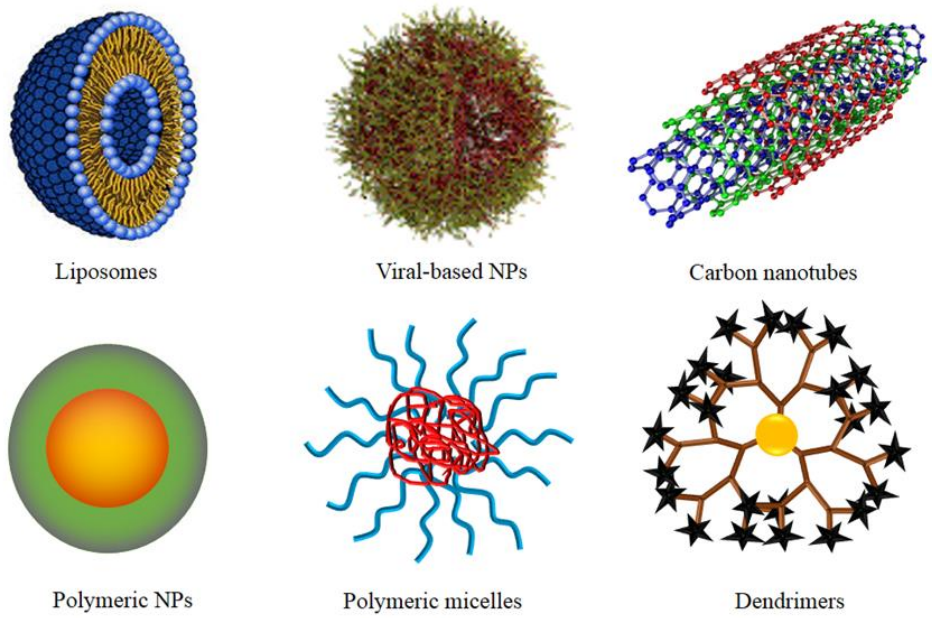

Figure 1.2. Types of nanoparticles used in assessment of drug delivery systems.

In recent years, polymeric micelles have gained considerable attention by enabling effective targeting of cytotoxic agents to solid tumors [14-16]. They are composed of amphiphilic macromolecules that have diverse hydrophilic and hydrophobic block domains [17]. Due to the large solubility difference between these segments, the macromolecules directly assemble into polymeric micelles in aqueous media and form a nano-sized core/shell structure (Figure 1.4). The hydrophobic core of micelle aids as storage for hydrophobic drugs, wherein hydrophilic shell provides steric barrier for the core and enables it to be water-soluble in aqueous environment. The core/shell architecture renders the polymeric micelles a remarkable drug delivery system in the field of drug targeting

owing to high drug loading capacity and narrow-size distribution. Common polymeric micelle sizes range from 10 to 100 nm to achieve higher accumulation of a drug at the tumor tissue. They also have a slow dissociation rate, thus prolonged retention times of the loaded drugs in the body [18].

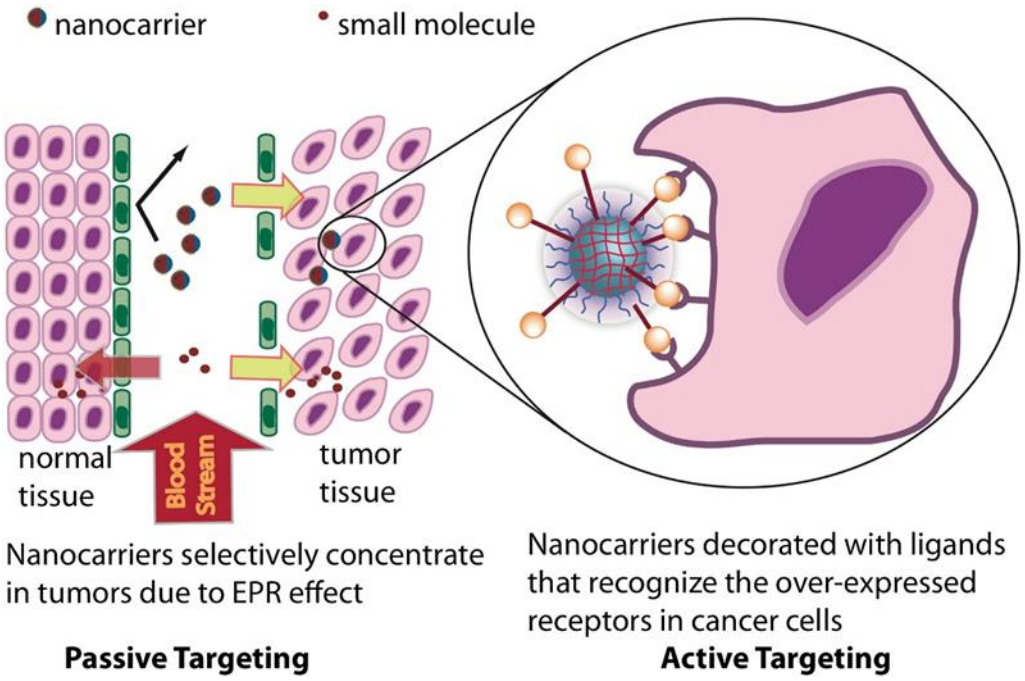

Figure 1.3. Passive targeting through the EPR effect and active targeting through ligand display [8].

In addition to all these, surface properties of polymeric micelles have a critical role in the distribution of hydrophobic drug in the body to achieve well-adjusted drug delivery with noteworthy efficacy. Reticuloendothelial systems (RES) in the body recognize the drug delivery agents, including polymeric micelles, and trigger non-specific uptake by RES elements as macrophages [19]. This is a great trouble, which results in short circulation of polymeric micelles in bloodstream, unless they have non-modulated surface properties [20]. Owing to these attractive features and advantages, polymeric micelles are considered as being efficient nanocarrier for drug delivery system.

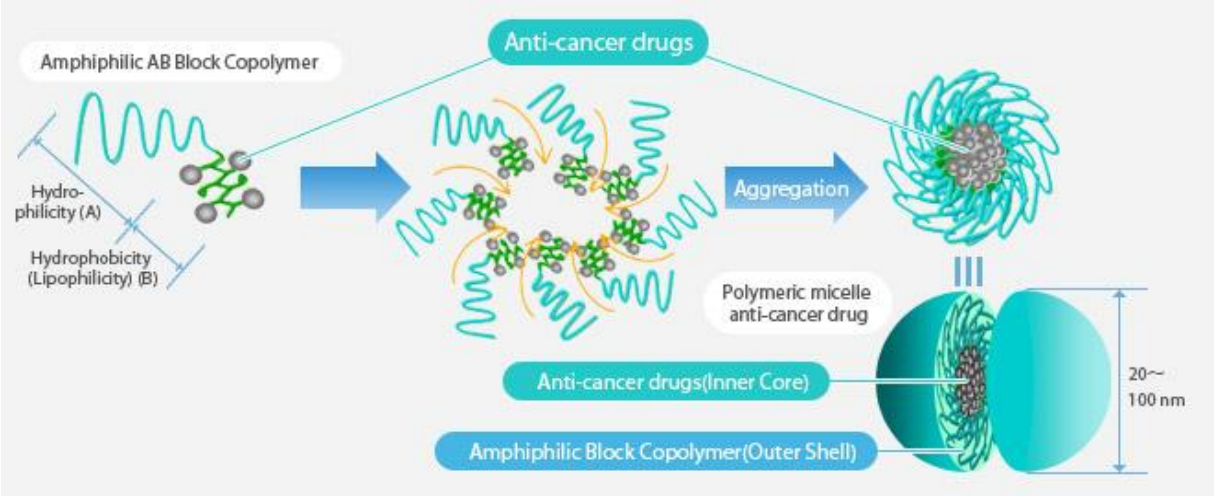

Figure 1.4. Self-assembly amphiphilic diblock copolymers in aqueous medium [21].

1.2. Composition and Structure of Polymeric Micelles

The distinctive property of a polymeric micelle is the core/shell structure. There are manifold self-assembled amphiphilic block copolymers to construct uniform micellar structures. However, the necessities in biocompatibility and biodegradability have narrowed down the option of applicable copolymers in clinical applications. In Table 1, there are names and structures of copolymers commonly used for drug delivery applications. The most commonly used hydrophilic segment is polyethylene glycol (PEG) that has the monomer subunit $–CH_2–CH_2–O–$ [22]. PEG is a non-toxic, completely water-soluble, non-immunogenic and biocompatible material. It is capable of forming hydrogen bonds with aqueous surroundings, thus it forms a shell around the hydrophobic micellar core and makes it water-soluble and sterically stable in aqueous systems. It has also demonstrated that PEG prevents protein adsorption and cellular adhesion. Hence, micelles are not recognized by the reticulo endothelial system (RES) cells, so they can circulate in the bloodstream for a longer time. In addition, the prolonged circulation time of micelles provides effective passive targeting of tumors via the EPR effect. To take these fabulous advantages, PEG is frequently used for hydrophilic segment of polymeric micelles.

Table 1.1. Commonly used block segments of copolymers used in micellar drug delivery [23].

Copolymers	Abbreviations	Repeating Unit Structure
Corona segment		
Poly(ethylene glycol)	PEG, PEO	
Poly(N-vinyl pyrrolidone)	PVP	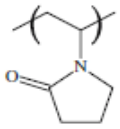
Poly(N-isopropyl acrylamide)	pNIPAM, NIPAM	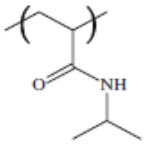
Core segment		
Polyethers		
Poly(propylene oxide)	PPO	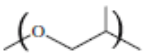
Polyesters		
Poly(L-lactide), Poly(D, L-lactide)	PLA, PDLLA*	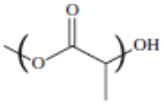
Poly(lactide-co-glycolide)	PLGA	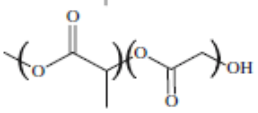
Poly(ε-caprolactone)	PCL	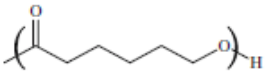
Poly(β-amino ester)		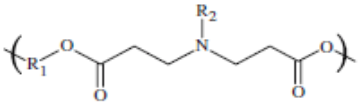
Polyamides		
Poly(L-histidine)	pHis	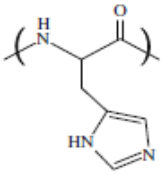
Poly(L-aspartic acid) derivatives	pAsp	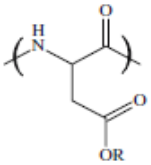
Poly(L-glutamic acid) derivatives	pGlu	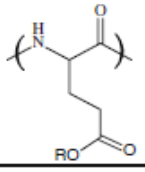

* Depending on stereochemistry

For the hydrophobic segments, several materials are synthesized such as polypeptides, polyethers and polyesters. However, the most commonly used hydrophobic blocks are comprised of polyesters. They are known as biodegradable materials due to undergoing hydrolytic and enzymatic cleavages.

1.3. Dendrimers

Dendrimers are novel synthetic polymeric materials. They are highly branched, spherical, monodispersed macromolecules, which have uniform size, shape and definite molecular weight (Figure 1.5). There are two main approaches to synthesize dendrimers which are divergent and convergent method.

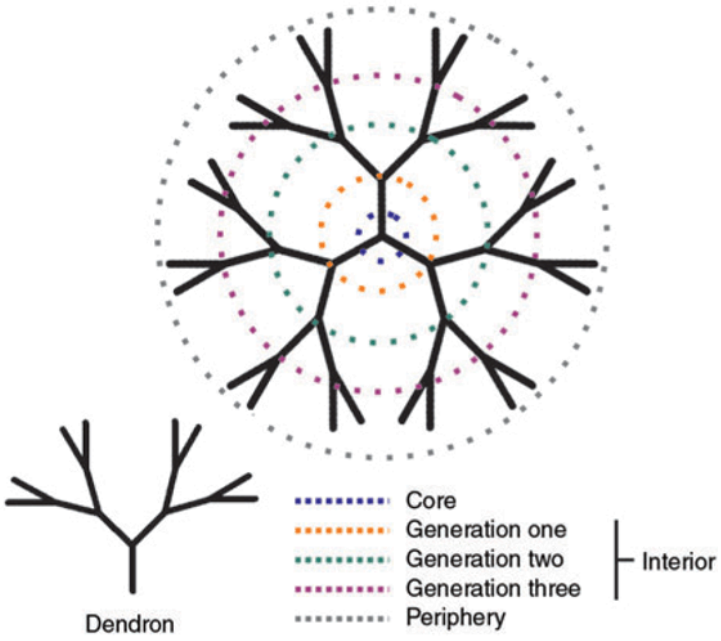

Figure 1.5. Structure of a dendrimer: increasing branching from a core [24].

In divergent method, dendrimer grows from inside (i.e. core) to outside. The multifunctional core reacts with monomers, which have one reactive, and two dormant groups. The obtained molecule gives the first generation dendrimer. Then, the periphery of the dendrimer is activated to react with more monomers. The dendrimer is built layer after layer in order to get several generations. In the convergent approach, dendrimer is synthesized starting from the periphery and construction goes into center giving dendritic

fragments called dendrons. Later, the built dendrons are attached to a multifunctional core molecule to give the final structure of dendrimer (Figure 1.6).

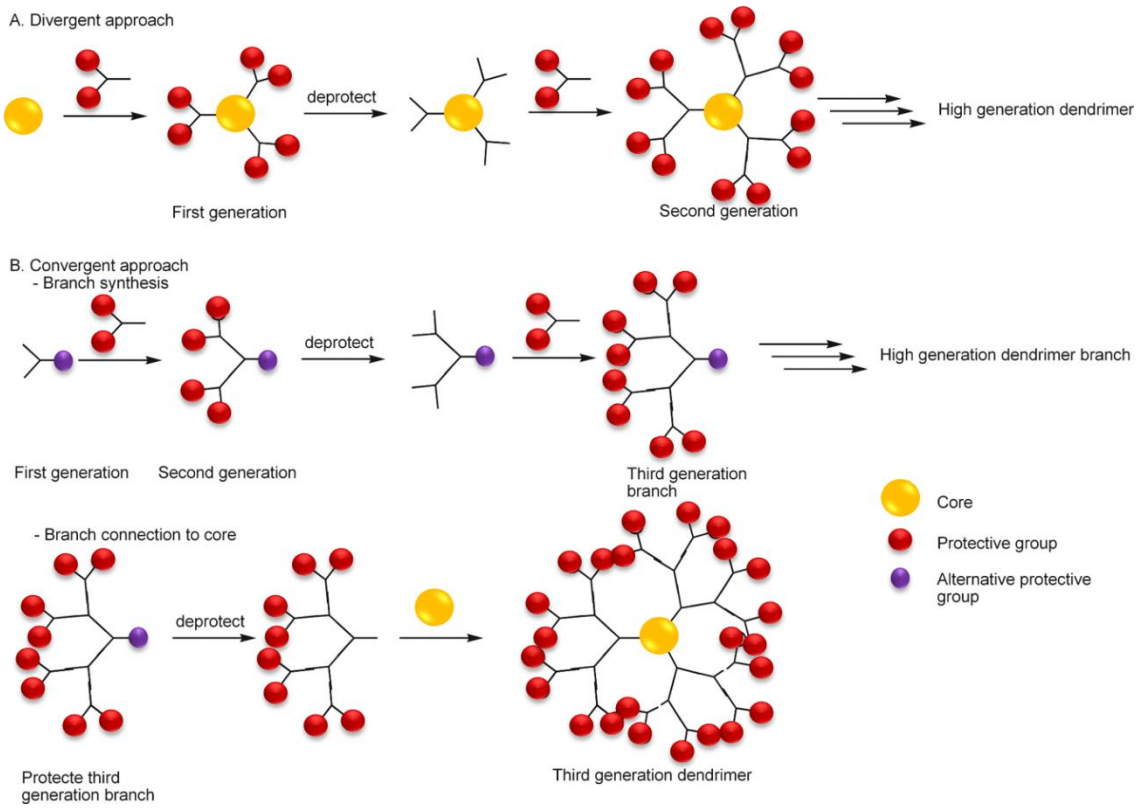

Figure 1.6. Synthesis of dendrimer by divergent and convergent methods [25].

Thanks to the stepwise synthetic processes, dendrimers have unique properties such as hyper-branched structure, monodisperse size or low polydispersity index, and precise number of peripheral groups. These features distinguish perfect-branched dendrimers from the more easily synthesized but less well-defined hyperbranched polymers [26].

Dendron is a part of a dendrimer that includes one type of functional group at the focal point and another at the periphery. It does not have a globular shape but has numerous functional groups depending on their generation number. Each branching unit from the focal point to the periphery determines the generation numbers of dendrons. Dendrons have mostly the same properties as opposed to dendrimers.

There are also several benefits for drug delivery applications arising from dendrimer architectures as compared with traditional linear polymers [27-28]. Dendrimers have perfectly design structures and contain a well-defined number of peripheral groups. Therefore, several drug molecules, targeting moieties, and solubilizing groups can be attached to the periphery of the dendrimers in controlled ratio. In addition, empty internal cavities are suitable for encapsulation of drug molecules and make them soluble. Furthermore, as dendrimers are generated in interactive multistep reactions, they have unique MW and narrow polydispersity index. For that reason, dendrimers show reproducible pharmacokinetic behavior when compared to most of linear polymers. Moreover, globular shape and branched structures of dendrimers affect their biological properties in contrast to random coil structure of linear polymers. Dendrimers cannot pass through small pores, such as glomerular filtration barrier. As a result, they may be eliminated more slowly as opposed linear polymers having same MW. In addition, they possess long circulation times; hence show the enhanced permeability and retention effect. All these properties make dendrimers attractive for biological and drug delivery applications. However, dendrimers with higher generations are hard to synthesize and due to the low reaction yields, pharmaceutically significant amount of dendrimer-based carriers are difficult to scale up. To overcome this obstacle, usually dendrimers are combined with polymers. This provides rapid growth in the hydrodynamic size of a dendrimer and increases drug loading capacity of linear of polymers.

1.4. Polymer Dendron Conjugates

Over the past several years, we have witnessed the utilization of polymer-dendron conjugates in both biopharmaceutical and materials research. Dendrons are attached to the polymers for the purpose of advancement of both their properties. Generally, dendrons are conjugated with polymers in order to increase their molecular weigth and solubility in the field of drug delivery. The conjugation occurs between end groups of the polymer and core or periphery of the dendrimer using coupling or addition reactions.

In 2013, Gu and She and their co-workers synthesized mPEGylated peptide dendron-doxorubicin conjugate as a candidate for drug delivery systems. The peptide dendron that has the multivalent functionality was PEGlylated from its tails. Then, the

dendritic framework was combined with the anticancer drug DOX via an acid-labile hydrozone linkage. The conjugate formed micelles in aqueous solution and showed a pH sensitive drug release feature due to the hydrozone bonds. They demonstrated that the functionalized peptide dendron-DOX based micelles effectively killed the cancer cells in vitro. Therefore, in this study, the polymer-dendron conjugate based micelles may be an effective drug delivery vehicle for cancer therapy (Figure 1.7) [29].

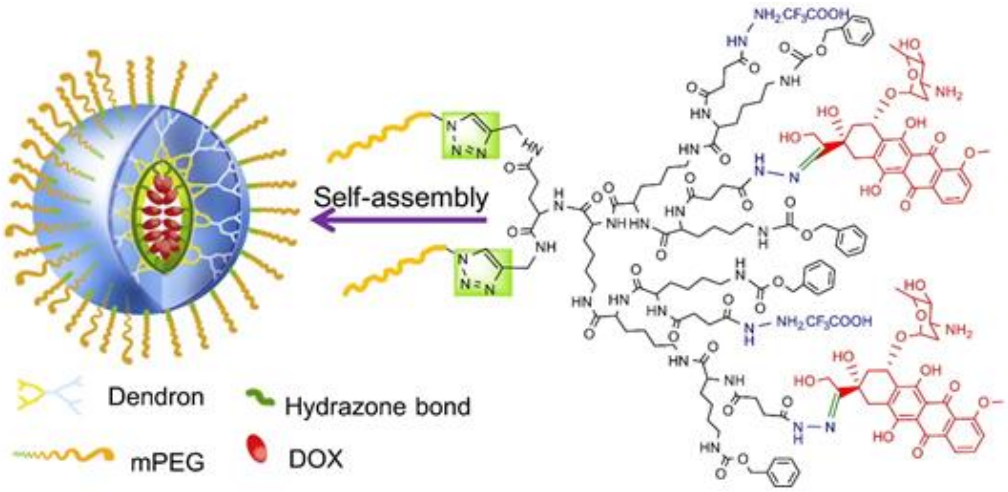

Figure 1.7. Formation of dendron-DOX conjugate-based micellar nanoparticles [29].

Sanyal and co-workers extended the methodology to prepare diblock and triblock dendron-polymer conjugates that contain biodegradable polyester dendron blocks and PEG polymer. The polymer –dendron conjugates were synthesized via Diels-Alder reaction by reacting maleimide end-functionalized PEG polymers with polyester dendrons bearing anthracene moiety at their focal point. The PEG polymer comprised a basis for water solubility of these block copolymers. The reported metal-free conjugation strategy is utilized to obtain multivalent linear PEG polymer (Figure 1.8) [30].

1.5. Micellar Constructs from Dendritic Macromolecules

As described above, polymeric micelles are amphiphilic block copolymers having nanascopic core/shell structures. They are used in various potential applications particularly for drug delivery purposes due to their inherent and modifiable properties. However, the molecular architecture of copolymer plays a crucial role in forming self-

assembled structure. By conjugating monodisperse dendrimer to narrow polydispersity polymer, the features of copolymer has been enhanced as high water solubility, low toxicity, biodegradability, tunable MWs and tunable drug loading capacities [31].

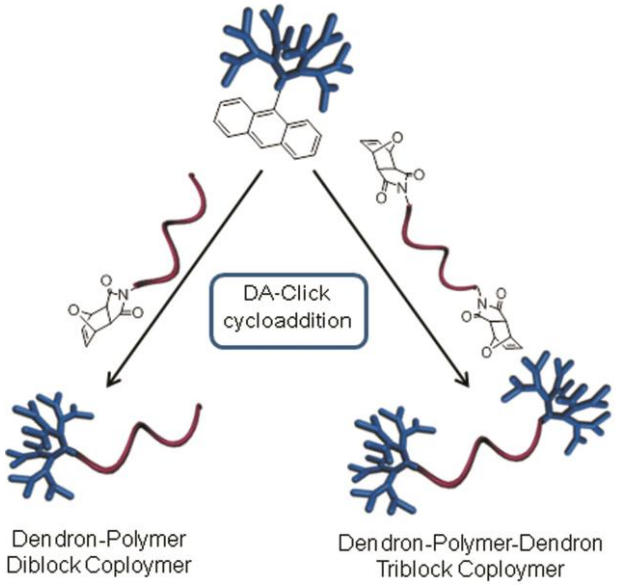

Figure 1.8. Synthesis of dendron-polymer-based block copolymers via the Diels-Alder reaction [30].

Recently, Kempe *et al*. reported the synthesis of a dendron-functionalized poly(2-ethyl-2-oxazoline) via one-pot cascade reaction. They synthesized alkyne-functionalized polymer and maleimide-substituted biodegradable dendron which contains acetal groups at the periphery. Then, they covalently linked these compounds with a bifunctional linker by the means of copper-catalyzed azide-alkyne cycloaddition (CuAAC) and the Diels–Alder cycloaddition. Finally, they did micelles with the resulting amphiphilic block copolymer and studied the aqueous solution behavior of the micelles in neutral and acidic pH. It is demonstrated that well-defined self-assembled micelles formed in neutral pH. However, due to the acid-labile protecting groups of the dendron, size of the micelles increased in acidic conditions, and formed hydrated loose aggregates. All together, the micellar construct from the polymer-dendron conjugates may be a promising candidate for drug delivery system (Figure 1.9) [32].

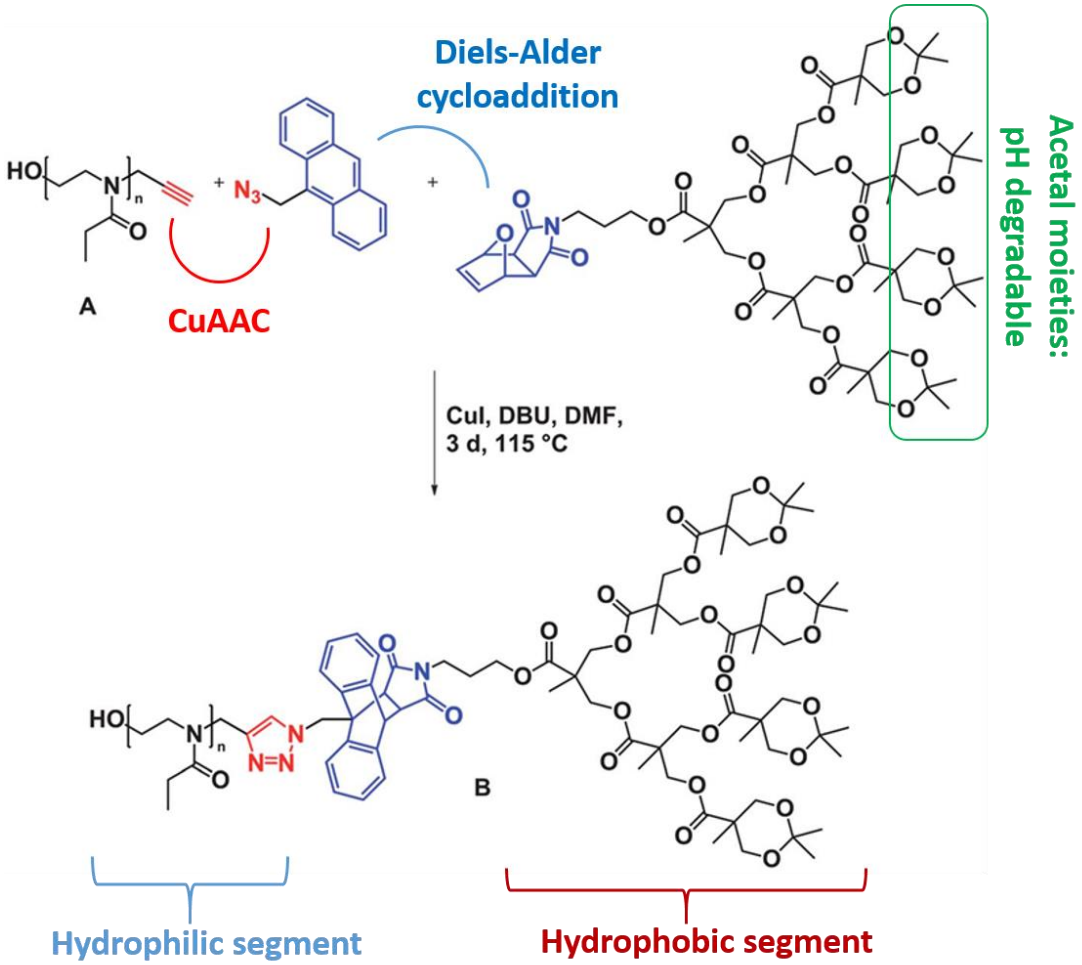

Figure 1.9. Synthesis of poly(2-ethyl-2-oxazoline)-block-G3 dendrimer (PtOx20bG3) by copper-catalyzed azide-akyne and Diels-Alder cycloadditions [32].

In 2012, Ambade and Gubta published a paper revealing a new approach for the synthesis of polymer-dendron conjugates. An amphiphilic block copolymer consists of a linear hydrophilic glycopeptide (GP) block was prepared and attached to a perfectly branched hydrophobic dendron using a amphipathic poly(ethylene glycol) (PEG) linker. They demonstrated that micellar aggregates and nanorods were obtained in aqueous solutions, wherein organogel was observed dimethylsulfoxide using varying polypeptide chain length and denron generation (Figure 1.10) [33].

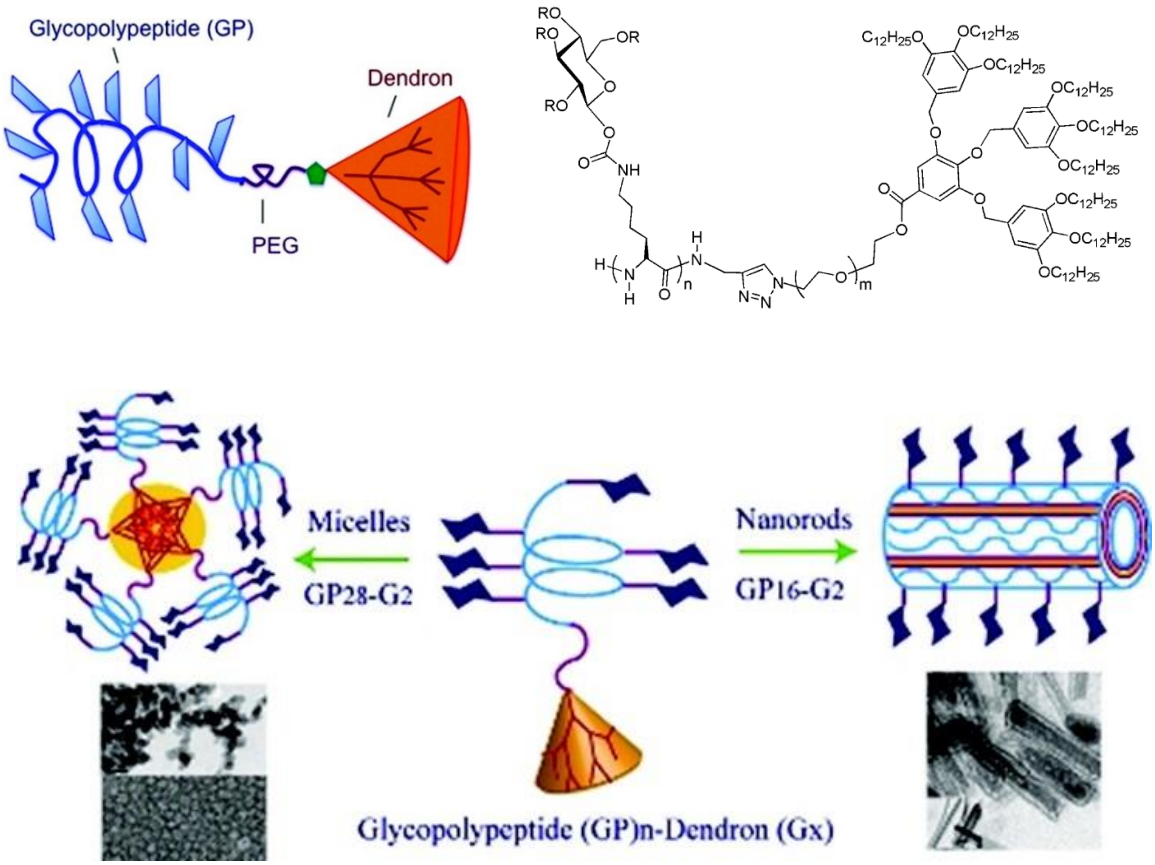

Figure 1.10. Glycopeptide-dendron conjugates, micelles and nanorods formation [33].

1.6. Increasing the Stability of Micelles

In spite of an exploding advancement in polymeric micelles such as improving drug water solubility, increasing drug accumulation at the tumor sites via the EPR effect, better drug bioavailability and diminished side effects, there are still some obstacles about in vivo stability [34-35].

Some polymeric micelles can lead to early drug release after intravenous administration because they can influence by many factors during blood circulation. However, micelles need to circulate long in the bloodstream in order to benefit from EPR effect, so that they can accumulate in the target tissue. In most circumstances, this problem is overcome using a PEG coating, which avoids opsonisation and recognition by reticulo-endothelial system cells [36-37]. Nevertheless, PEG corona of micelles may inhibit the

uptake of carriers by the target cells correspondingly [38]. It can be the explanation for some drug delivery systems, which do not permeate through cytosolic membranes spontaneously. However, accumulation of micelles in the tumor site can be obtained by coupling of a specific targeting group to the surface of the micelles. These targeting ligands can be peptides antibodies, antibody fragments and nanobodies which can be recognized and bind target cells (active targeting).

However, hydrophilic PEG shell can increase the thermodynamic stability of micelles in aqueous environment. The interactions of polymer chains between each other and with aqueous environment result in important forces such as Van der Waals, hydrogen bonding and dipole-dipole forces that increase the stability [39-40]. Increasing the surface density of PEG will force the polymers to form more rigid and extended, brush-like conformations. On the other hand, low molecular weight PEG and low surface density limit coverage properties of the micelle corona and the hydrophobic core and micelle destabilization can be affected from aqueous media [41-42].

Another reason for losing integrity of micelles is the low critical micelle concentration (CMC) of polymers. The block copolymers form micelles in water self-assembly when the concentration of the amphiphilic block copolymer reaches the critical micelle concentration (CMC). Critical micelle concentration is a phenomenon that is the lowest concentration of polymers to form micellar structures spontaneously. Below CMC, micelles are gradually disintegrated into their unimers in the bloodstream. They disassociate and cause non-targeted release of the drug. Low polymer concentrations leads insufficient numbers of chains to self-assemble and instead of assembling, the chains distribute throughout the solution. While the concentration of polymer increases, chains are getting closer at the interface. By increasing the concentration, both the bulk solution and interface start to be saturated with polymer chains until the CMC. Increasing concentration beyond this point will result in micelle formation in the bulk solution [43]. In addition, chemical structure of hydrophilic and hydrophobic blocks and the chain lengths affect the CMC value, hence micelle morphology [44].

1.7. Core Crosslinked Micelles

In order to improve stability of micelle, methodology of crosslinking can be applied to the core or shell of micelles. Important advancements due to the core-crosslinking strategy such, as high drug loading efficiency, greater stability against dilution, prolonged circulation time and enhanced drug accumulation at the tumor site was elaborated in many studies [45-47].

Available locations for crosslinking within diblock polymeric micelles are on the surface, throughout the shell layer, at the core-shell interface, within the core domain and at the core chain end. The domain of crosslinking is important because the obtained crosslinked polymeric micelles may have different physical and chemical properties depending on the location of crosslinking.

Core crosslinking strategy has been preferred more than shell crosslinking in order to get stable polymeric micellar systems. It has several advantages. For instance, the stealthiness of micelle is not damaged after crosslinking. In addition, by applying core crosslinking, micelle shell will be available to make use of many applications [48].

Zhiyuan Zhong and co-workers studied on the core crosslinkled pH-sensetive degradable micelles to get a promotive methodology to resolve the extracellular stability versus intracellular drug release dilemma. The micelles are prepared from diblock copolymer that contains photo-crosslinkable acryloyl and acid-labile acetal groups in the hydrophobic polycarbonate block for intracellular paclitaxel (PTX) release. This newclass of nanotherapeutics shows great promise in future cancer therapy (Figure 1.11) [49].

To minimize early drug release from carrier during blood circulation, Kit S. Lam and his co-workers developed reversible disulfide crosslinked micelles that can be triggered by thiols to release drug at the tumor tissues. First, thiolated linear-dendritic polymers (telodendrimers) was synthesized by introducing cysteines to the dendritic oligo-lysine backbone. The crosslinked micelles was achieved via oxidation of thiol groups on cysteines. It was used PTX as a hydrophobic cancer drug, and observed that the release of PTX from crosslinked micelles was considerably slower than that from noncrosslinked

micelles. Thus, release of PTX from crosslinked micelles can be gradually increased in a reducing environment. In addition, it was demonstrated that PTX loaded crosslinked micelles showed more effective release in nude mice bearing ovarian cancer xenografts than the equivalent dose PTX loaded noncrosslinked micelles and Taxol. Briefly, these core-crosslinked micelles can be a novel drug carrier for targeted cancer therapy (Figure 1.12) [50].

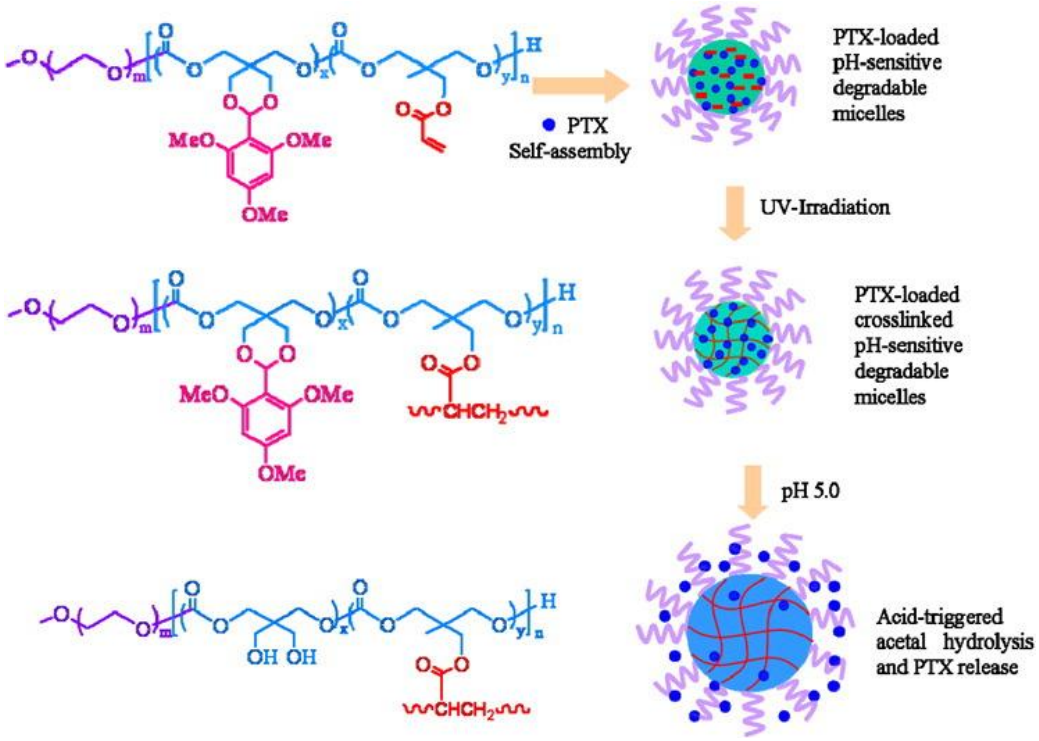

Figure 1.11. pH-sensitive degradable micelles based on PEG-b-p(TMBPEC-co-AC) block copolymer [49].

Figure 1.12. The disulfide crosslinked micelles formed by oxidization of thiolated dendron-polymer after self-assemble [50].

Kim, Park and their co-workers developed photo-crosslinked hyaluronic acid nanoparticles (c-HANP) by UV-triggered crosslinking of acrylate groups in the polymer backbone. By doing the chemical crosslinking inside the micelles, c-HANPs showed high stability in a physiological buffer and released the loaded drug, paclitaxel (PTX), in a continuous fashion. In addition, in vitro cellular uptake tests demonstrated that c-HANPs were rapidly taken up by the tumor cells via the receptor (CD44)-mediated endocytosis. Lastly, c-HANPs showed higher tumor-targeting ability than uncrosslinked micelles owing to having high stability, which enables their long blood circulation in the body (Figure 1.13) [51].

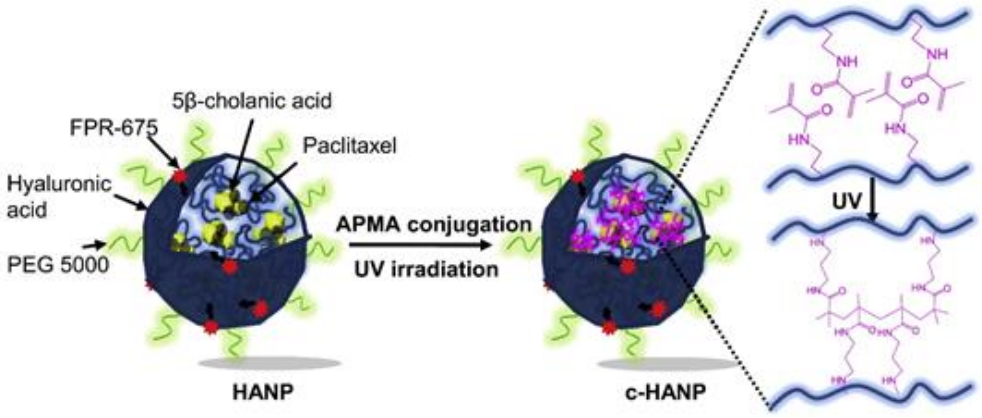

Figure 1.13. Preparation of photo-crosslinked hyaluronic acid nanoparticles [51].

1.8. Versatile Tools in Macromolecular Design: 'Click' Chemistry

'Click' reactions are known to be able to produce a variety of functional synthetic molecules and organic materials. There are various types of 'click' reactions such as the copper(I)-catalyzed 1,3-dipolar cycloaddition of azides and alkynes, nucleophilic ring-opening reactions and thiol-ene reactions. These reactions have several benefits including high yields, insensitivity to water or oxygen, regiospecificity and stereospecificity, orthogonality with other common organic synthesis reactions and mild, aqueous reaction conditions [52].

1.8.1. Copper (I) Catalyzed Azide-Alkyne [3+2] Cycloaddition

Huisgen [3+2] cycloaddition reaction is a well-known 'click' reaction which is occurred between azide and alkyne reactive groups in the precence of copper ions. It is widely used in the synthesis of well-defined macromolecules such as dendrimer synthesis [53], dendronized polymers [54] and biological studies [55]. In 1970, the reaction was firstly introduced by Rolf Huisgen without using water and catalyst, giving a mixture of 1,4 and 1,5-disubstituted triazoles at high temperature (Figure 1.14).

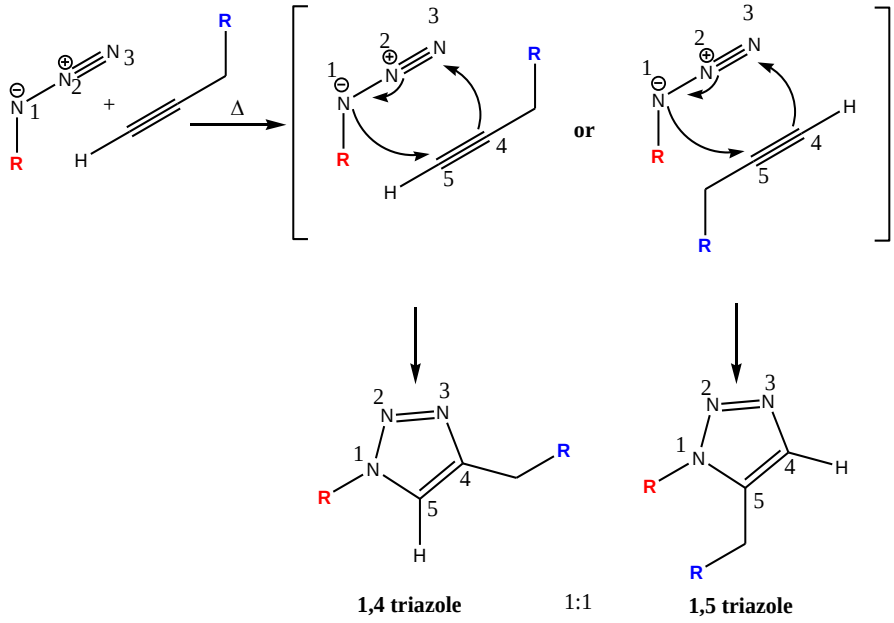

Figure 1.14. Azide-alkyne [3+2] cycloadditions.

Thirty two years later, Sharpless and Fokin [56] introduced a Cu (I) catalyst in Huisgen reaction which gives stereospecific, 1,4 heterocyclic product with high yield in either aqueous and organic solvents (Figure 1.15). By the help of Copper (I) catalyzed azide-alkyne [3+2] cycloaddition, dendrons are attached to polymers straightforwardly.

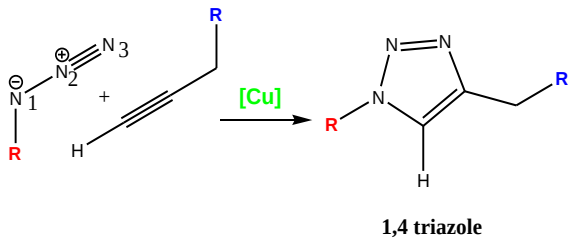

Figure 1.15. Copper catalyzed Huisgen reaction.

Sanyal group utilized functionalizable hydrogels to fabricate three-dimensional (3D) scaffolds that might find applications in biomedical purposes such as cell growth and tissue engineering. A biodegradable polyester dendron bearing alkyne group at its focal point was synthesized and successfully conjugated to linear PEG diazide via Huisgen type 'click' reaction. The peripheral groups of dendrons were thereafter functionalized with alkyne groups in order to crosslink the dendron-polymer-dendron conjugate with a hydrophilic crosslinker via the 'click' reaction in a controlled manner (Figure 1.16) [57].

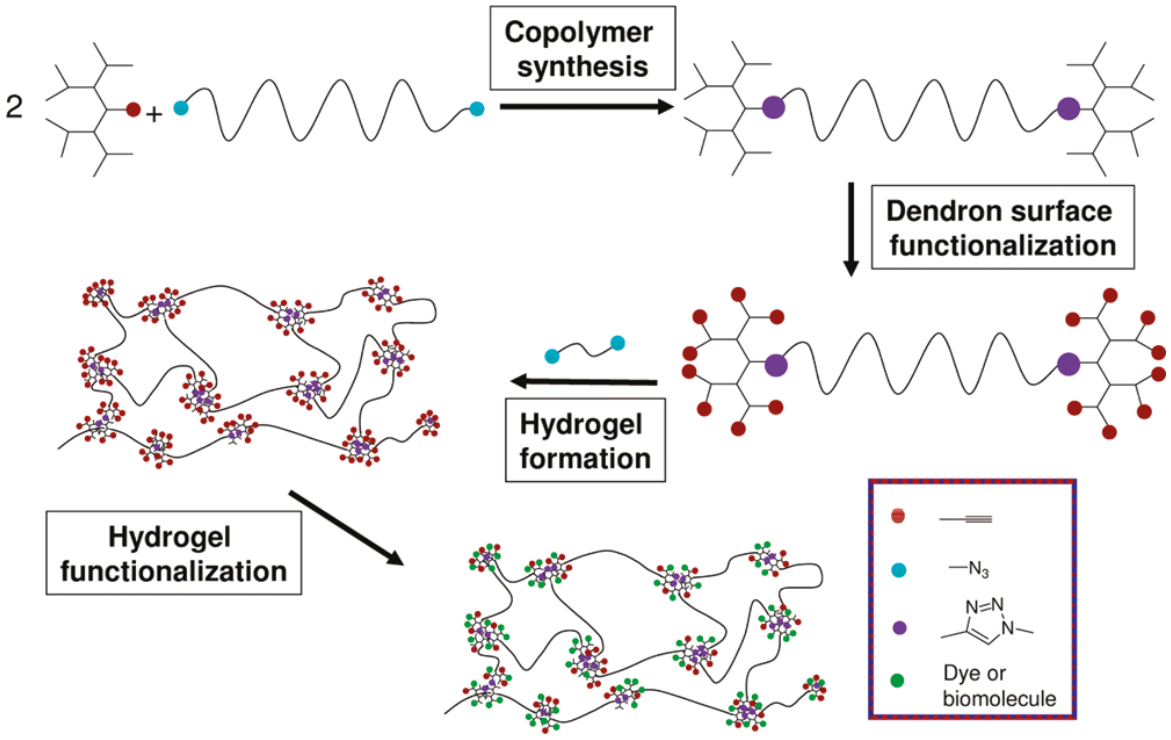

Figure 1.16. Synthesis of functionalized hydrogels using dendron-polymer-dendron conjugates [57].

In another study, Fre´chet group reported the synthesis of dendronized linear polymers via 'grafting to' approach. Azide containing dendrons at the focal point were conjugated with the pendant alkynes on the poly(vinylacetylene) with the help of CuAAC catalyzed 'click' reaction (Figure 1.17) [58].

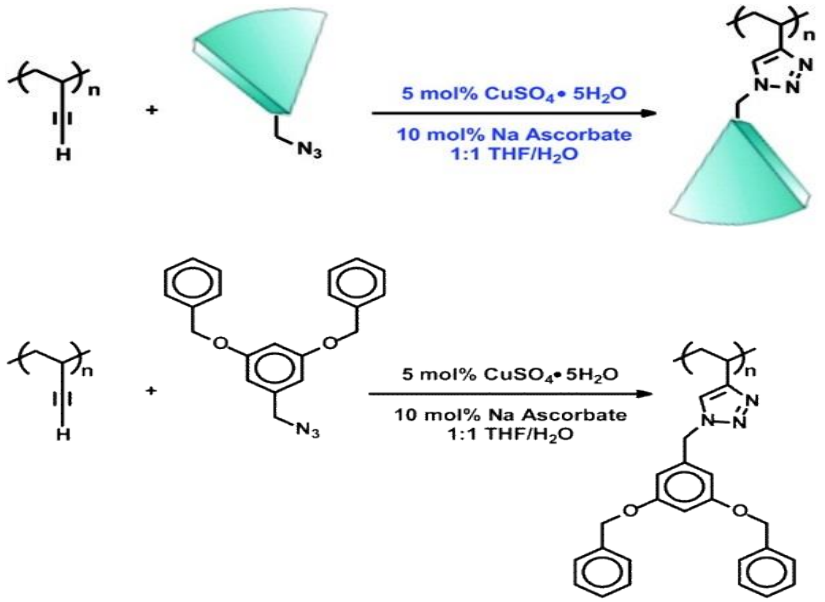

Figure 1.17. First-generation dendronized linear polymer synthesis achieved by "click chemistry" [58].

1.8.2. Thiol-ene Click Reaction

Thiol-ene Click Reaction is one of the popular click reactions owing to have easy synthetic strategies and clearly defined reaction mechanism. It is involves the addition of sulphur hydrogen bond across a double bond by either a free radical or ionic mechanism (Figure 1.18). There are so many advantages in thiol-ene click reaction which make it smart, simplistic and versatile process. To begin with, the reaction can proceed under different conditions comprising by a radical pathway or catalytic processes mediated by acids, bases, nucleophiles and in the tiny amount of catalyst. Furthermore, a large variety of enes and thiols serve as suitable reactants. Lastly, thiol-ene click reactions are generally extremely extremely fast that reactions can be completed within minutes even at ambient conditions. The reactions is also tolerant to the oxygen and moisture [59].

The thiol-ene reaction has recently attracted researchers to be used in many applications including the fabrication of coatings, optical and sensing devices, biomedical and bioorganic modification fields.

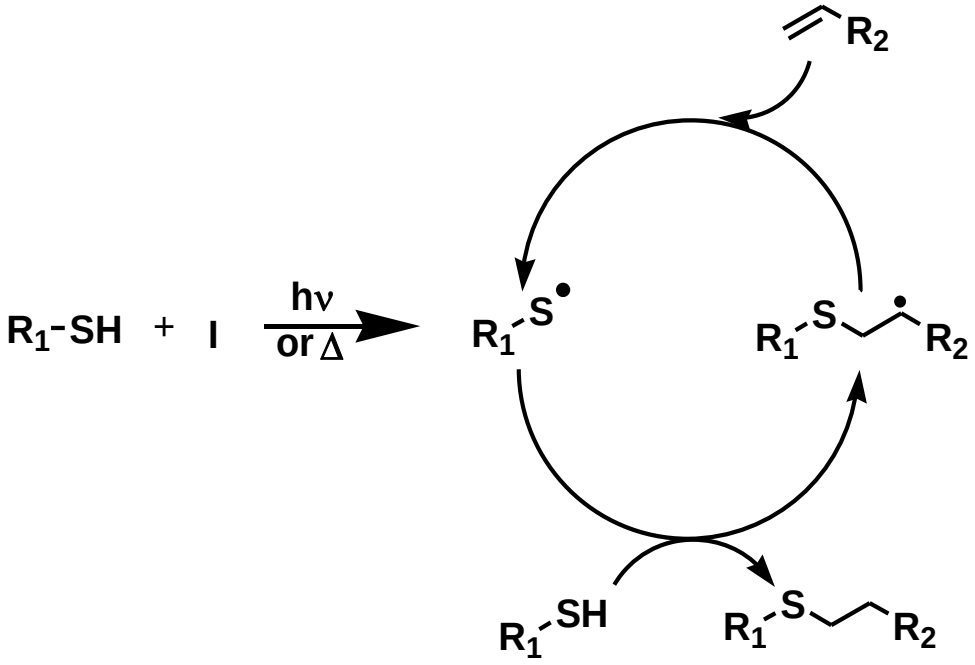

Figure 1.18. Thiol-ene 'click' reaction mechanism.

Eva Harth and co-workers synthesized crosslinked polyester nanoparticles in selected nanoscale size dimensions via ‘click’ chemistries, such as the alkyne-azide reaction and the thiol-ene coupling reaction. In order to crosslink linear polyester, firstly, pendant alkyne groups of polymer reacted with bisazides in the presence of copper(I) bromide. Than, to compare the azide-alkyne chemistry, the thiol-ene ‘click’ reaction was carried out between alkene moieties of polymer and dithiols without precense of any catalyst or initiator. It has been demonstrated that both azide-alkyne and thiol-ene click chemistries were equally efficient in the performance of a crosslinking reaction in a control manner resulting in well-defined spherical particles [60].

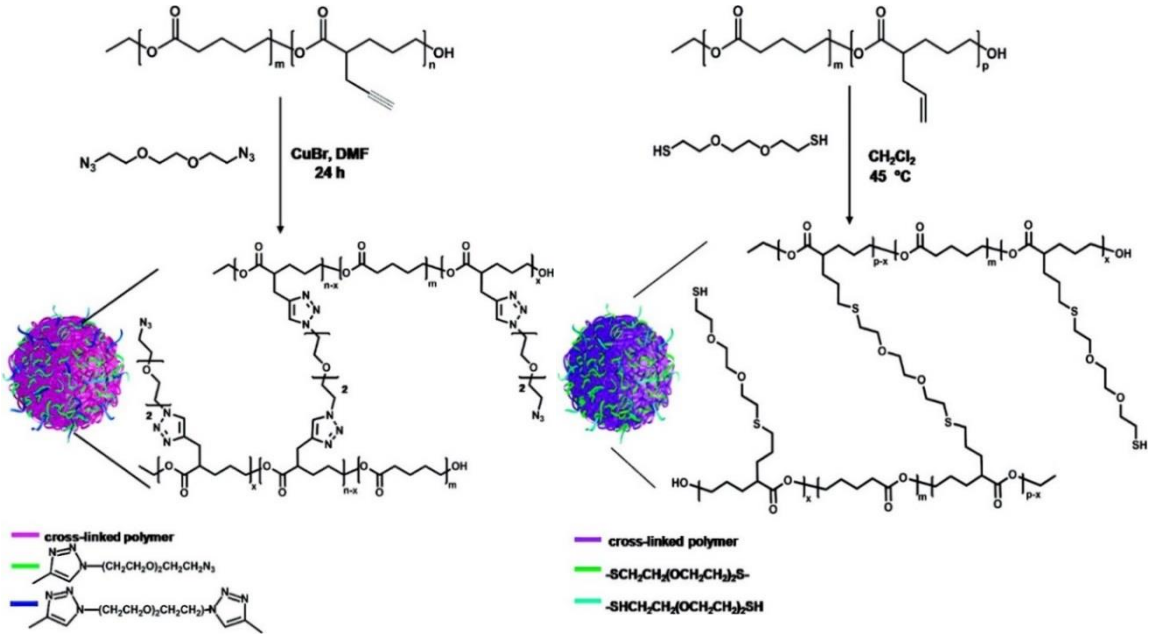

Figure 1.19. Crosslinked nanoparticles via azide-alkyne and thiol-ene click chemistry [60].

2. AIM OF THE STUDY

The nanoscopic length scale, high loading capacity, long circulation in the blood stream and enhanced accumulation in solid tumors makes micellar drug carriers excellent candidates as drug delivery vehicles. The aqueous stabilities of these polymeric micelles are very crucial to achieve controlled release of the drugs. Recently, a growing interest has been dedicated to produce core crosslinked micelles to benefit from their increased stabilities and prolonged drug release profiles. In this study, we have demonstrated the synthesis of core crosslinked polymeric micelles from amphiphilic polymer-dendron conjugates in a modular fashion using 'click' chemistry. An alkene functionalized biodegradable polyester dendron was used as a building block to constitute the hydrophobic part of the micelle. On the other hand, biocompatible, water-soluble and non-immunogenic p(PEGMA)-based polymer was utilized to form the hydrophilic segment of the conjugate. Three different polymers were synthesized that were varied by chain lengths and they were used to further conjugation with dendron. Micelle formation studies were performed with three diffrent polymer-dendron conjugates in aqueous solution. Effect of different hydrophilic chain leghts were investigated in terms of size and stability. Efficient crosslinking of peripheral alkene units using thiol-ene click chemistry provided stable polymeric micelles.

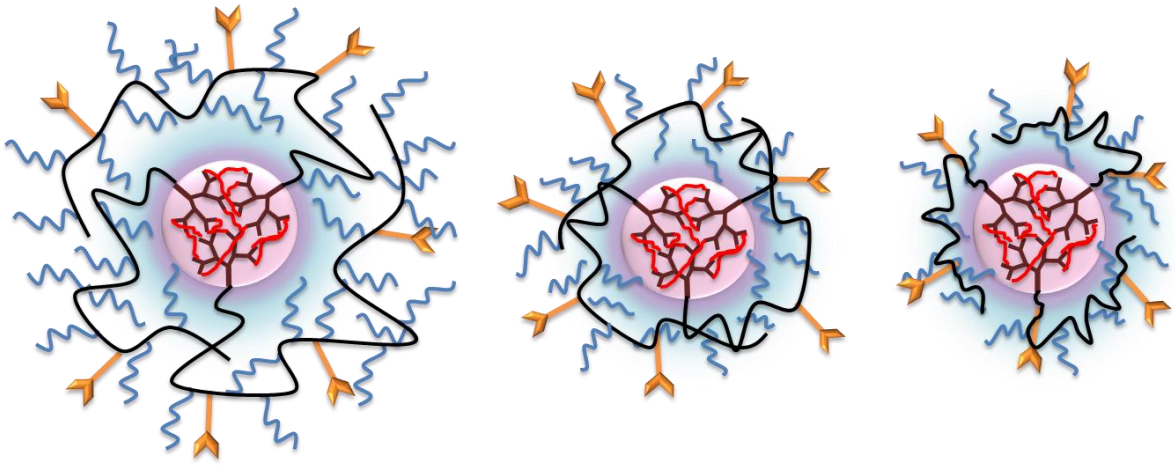

Figure 2.1. Micelles assembled from three different polymer-dendron conjugates that have different hydrophilic chain lengths.

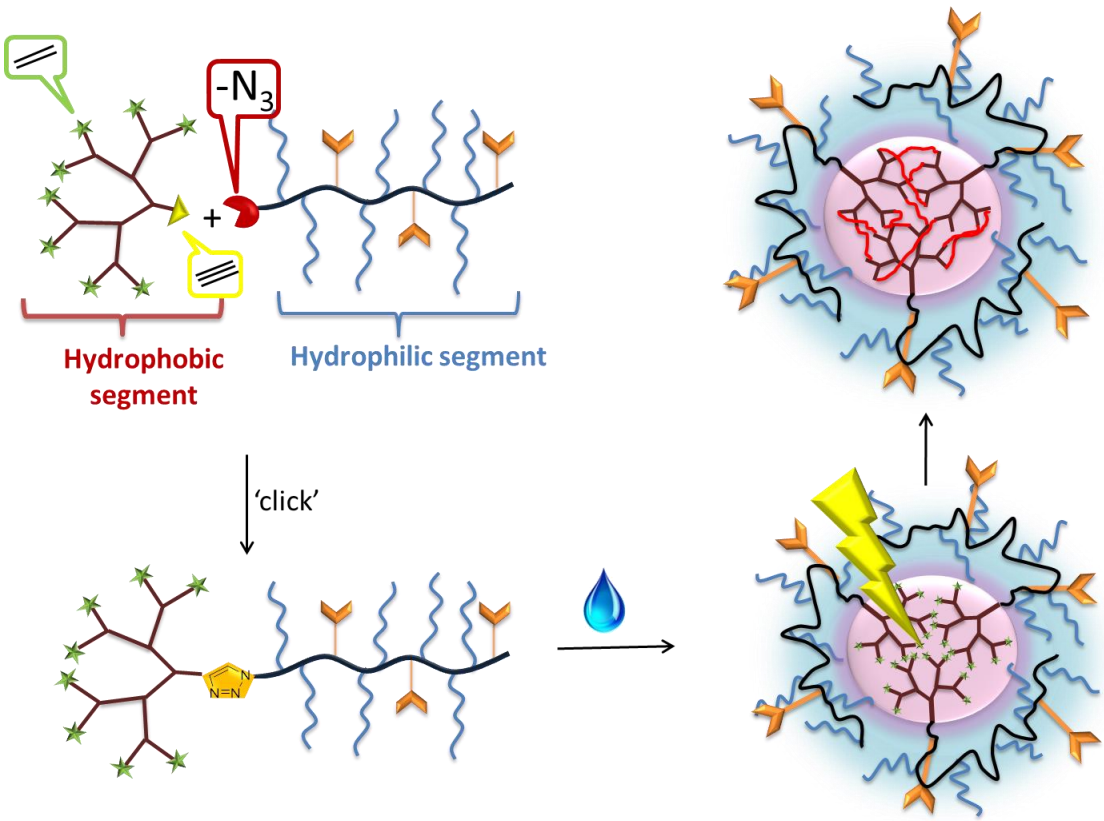

Figure 2.2. General representation of amphiphilic block copolymers.

3. RESULTS AND DISCUSSION

3.1. Synthesis of Polymer-Dendron Conjugates via Click Chemistry

For the design of polymer-dendron conjugate, two main building blocks were utilized; alkyne-functionalized third generation bis-MPA dendron (G3 dendron) and azide-functionalized copolymer of PEGMA (Poly(ethylene glycol) methyl ether methacrylate) and NHSMA (N-hydroxysuccinimide methacrylate). Both components were covalently coupled via copper catalyzed Huisgen type 'click' reaction (Figure 3.1).

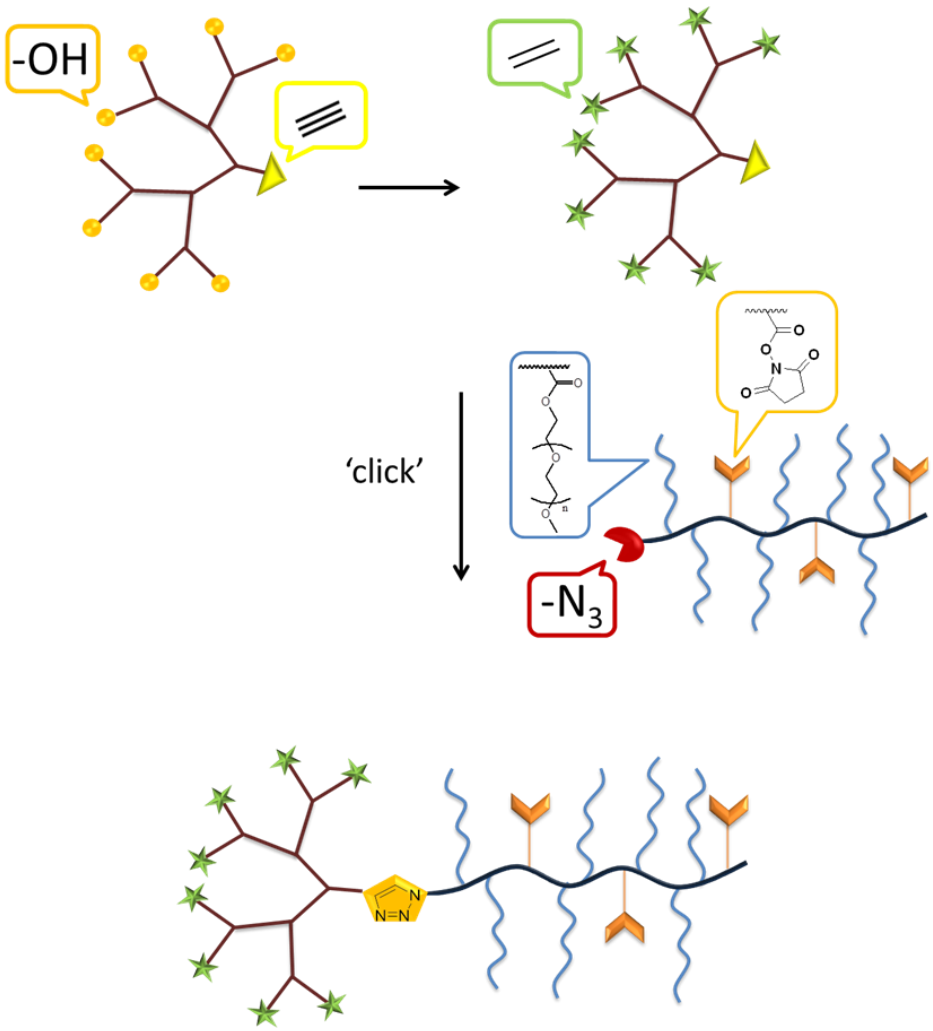

Figure 3.1. Schematic representation of formation of amphiphilic polymer-dendron conjugates.

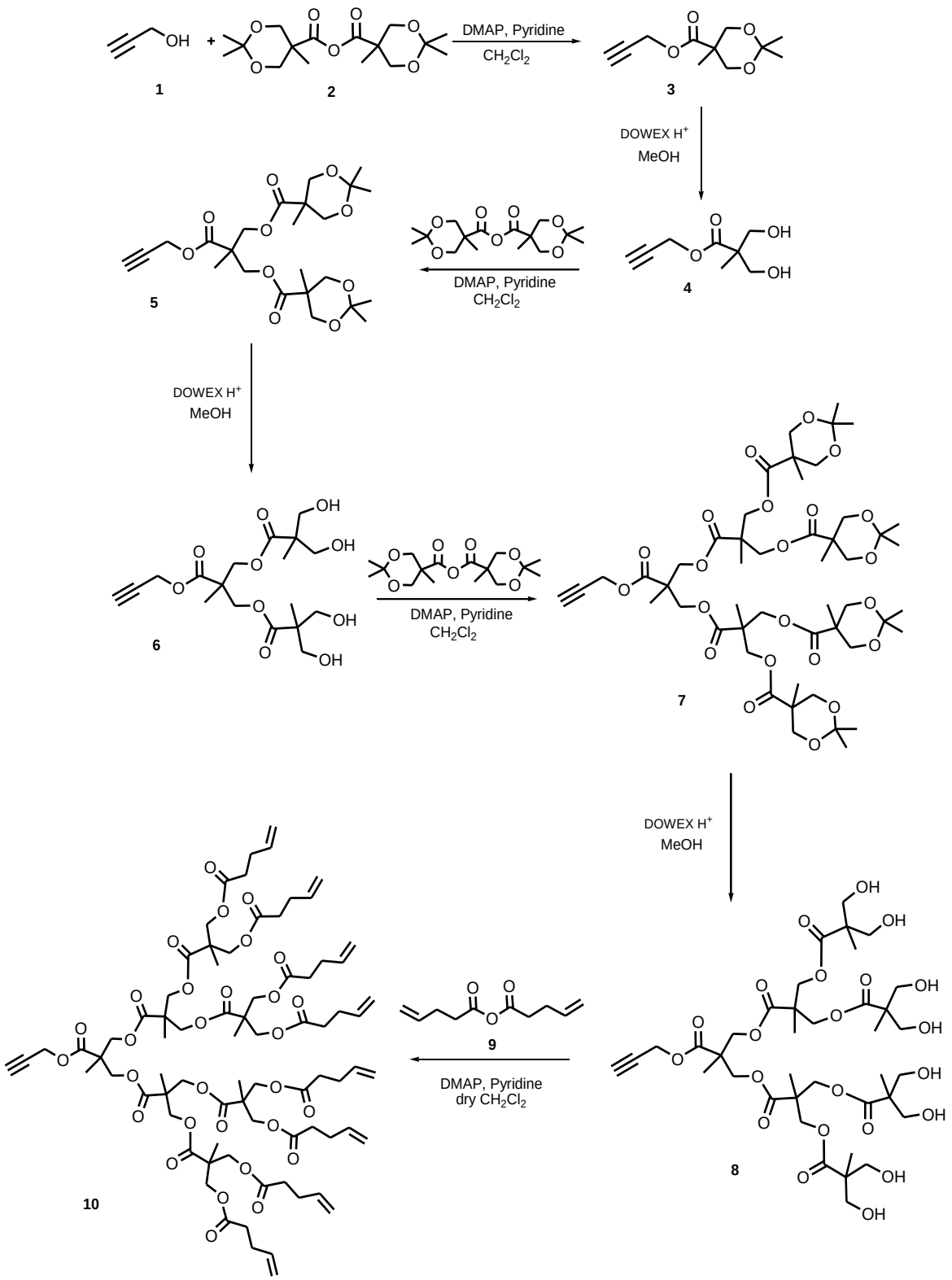

Figure 3.2. General scheme of alkene functionalized dendron synthesis.

For the hydrophobic part of the micelle, aliphatic polyester dendrons with alkyne unit at the focal point was synthesized. The polyester dendron is biodegradable due to

hydrolysable ester bonds on its structure. The third-generation polyester dendron was prepared using a well-established divergent synthesis strategy in our group [61]. The growth of the dendron was started from the alkyne core towards the periphery (Figure 3.2). The dendrimer backbone was based on 2,2-bis(hydroxymethyl) propionic acid (bis-MPA) as a biocompatible building block. In order to install the alkyne functionality at the core, an alkyne group containing alcohol **1** was used. The first generation dendron was synthesized via reacting propargyl alcohol with anhydride **2**. Then, the acetonide protecting unit was removed by acidic DOWEX-H resin. The resulting product **4** gave the G1 dendron bearing alkyne unit at the core. The alcohol groups at the periphery were further utilized for dendrimer growth. The G2 (**6**) and G3 (**8**) generation dendrons were synthesized in the same manner using anhydride acylation and acetonide protection sequences. Finally, G3 dendron with alcohol surface groups (**8**) was obtained and subsequently used for end group modification to install peripheral alkene units.

The hydroxyl end groups of the G3 dendron was functionalized with alkene groups using 4-pentanoic anhydride (**9**) in the presence of DMAP and pyridine in dry CH_2Cl_2. To check the conversion efficiency of hydroxyl groups to alkene moieties, the product **10** was characterized by FT-IR and ^{1}H NMR spectroscopy. All FT-IR and ^{1}H NMR characterizations are included in Appendix and are in agreemnet with previous products [61].

G3 dendron bearing alkene units at the peripery was also characterized by MALDI-TOF for the analysis of molecular composition (Figure 3.3). It was revealed that molecular weight distribution was in agreement with the real composition. The G3 dendron has the molecular weigth 1524 g/mole. However, it was seen 1547 g/mole which was the sodium adduct of the dendron (M+23). The dendron was analyzed using 9-nitro antracene (9-NA) as the matrix and sodium cloride to improve the ionization of the polymer.

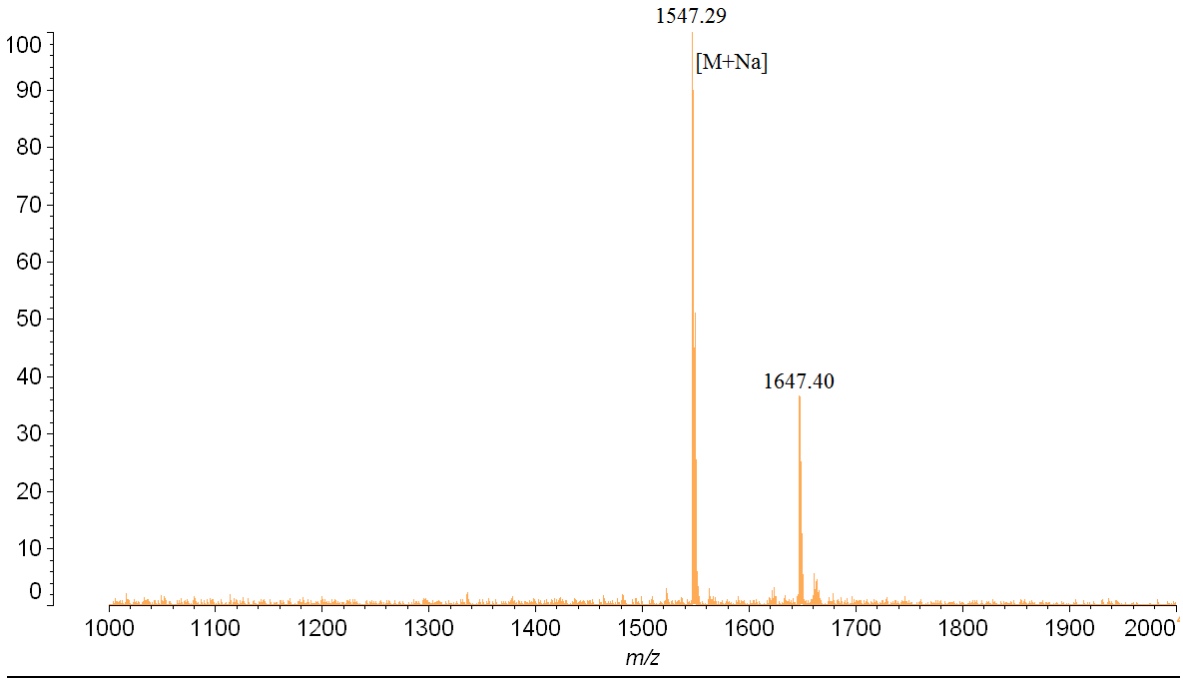

Figure 3.3. MALDI-TOF spectrum of 10.

For the hydrophilic part of the amphiphilic copolymer, p(PEGMA) is preferred. It is water-soluble, biocompatible and non-immunogenic. The reason of why p(PEGMA) is preferred instead of linear PEG is that it can be possible to introduce another methacrylate based functional monomer during polymerization. As a result, desired functional groups can be incorporated to copolymer chains that would allow post-polymerization modification. In this study, copolymers of PEGMA and **N-hydroxysuccinimide methyl methacrylate** (NHSMA) monomers were synthesized. NHSMA is a methacrylate-based monomer, which contains succinimide ester group. It includes activated carboxylic acid unit that reacts with amines efficiently. Thus, proteins from amino termini or other polypeptides containing amino group at their side chains can be easily attached to the polymeric platforms carrying NHS-activated carbonyl groups. Ultimately, it is possible to decorate polymers with desired peptides or any amine containing groups serving for an intended use.

For the synthesis of NHSMA monomer (**13**), N-hydroxysuccinimide (**11**) was reacted with methacryloyl chloride (**12**) in the presence of triethylamine (Figure 3.4). The monomer was purified by re-crystallization method and obtained with high yield.

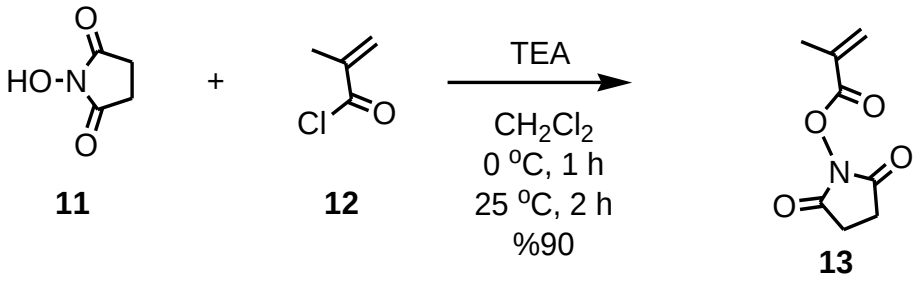

Figure 3.4. NHSMA monomer synthesis.

The polymers were synthesized via Atom Transfer Radical Polymerization (ATRP), which is one of the most commonly employed controlled/living radical polymerization techniques. ATRP method allows the synthesis of polymers with desired molecular weights and low polydispersity indices. In polymerization, a transition metal is used as catalyst and an alkyl halide serves as the initiator. Generally, copper salts are preferred for polymerization of various kinds of monomers. The most commonly used initiator is 2-bromoisobutyryl bromide (**16**). In this study, the initiator was functionalized with an azide group in order to install the azide unit at the polymer chain ends that allow [3+2] Huisgen 'click' functionalization with alkyne containing dendron.

The azide-functionalized initiator was obtained after two-step reactions (Figure 3.5) similar to literature [62]. Firstly, 6-chloro-hexan-1-ol (**14**) reacted with sodium azide to obtain 6-azido-hexan-1-ol (**15**). Then, hydroxyl group of this alcohol was reacted with 2-bromoisobutyryl bromide (**16**) in the presence of Et_3N to give the azido ATRP initiator (**17**). Products **15** and **17** were characterized by FT-IR and ^1H NMR spectroscopies and aggrement with previous synthesis [61].

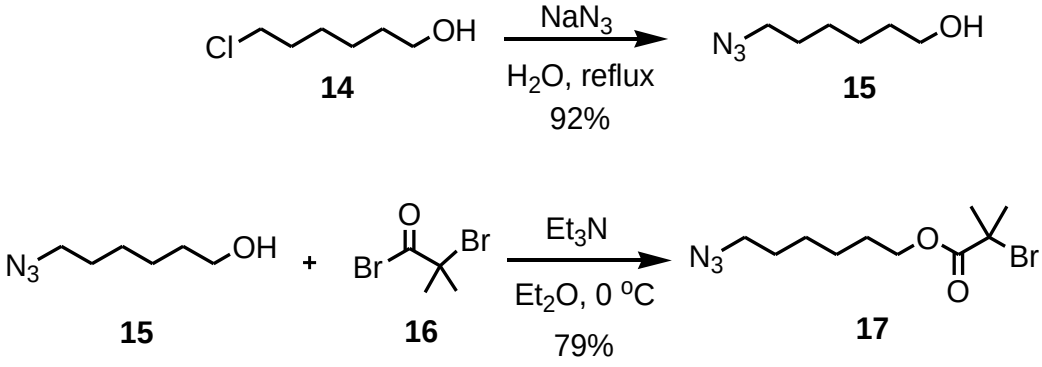

Figure 3.5. Synthesis of azide-functionalized initiator.

For the copolymer synthesis, commercially available PEGMA (M_n=300 g/mole) (**18**) and NHSMA monomer **13** were used. The reactions were carried out with the ATRP initiator **17** and the polymerizations were performed using different ratios of the initiator. The polymerization reactions were conducted in anisole under varying temperatures (Figure 3.6). As indicated in Table 3.1, copolymers with desired molecular weights were synthesized with relatively low polydispersity indices (PDI). The obtained polymers **19** carrying azide functionality at the end were used for further conjugation to a polyester dendron carrying alkyne group at focal point. Three different copolymers were chosen with different molecular weights; approximately 3 kDa (**P4**), 7 kDa (**P12**), 10 kDa (P10) for conjugation with G3 dendron **10**.

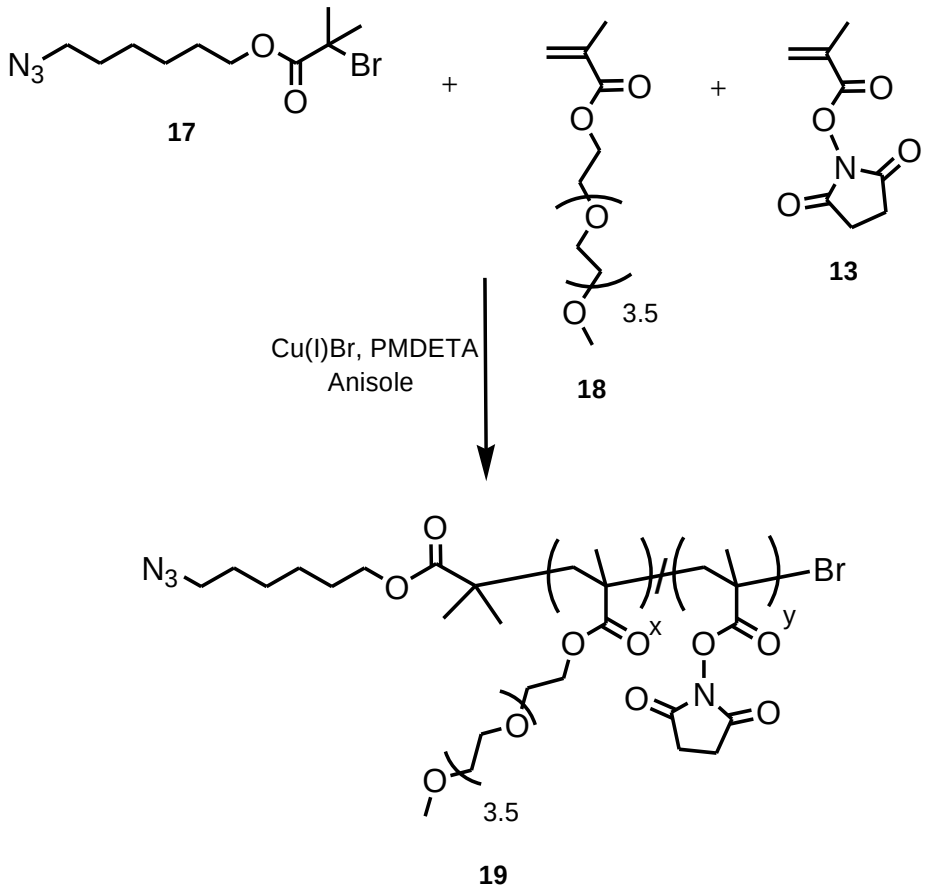

Figure 3.6. Synthesis of p(PEGMA)-b-p(NHSMA) block copolymer.

As seen in Table 3.1, molecular weigth of polymer increased as decreasing the ratio of initiator. The amount of solvent was effective on polydispersity indices. Generally,

small solvent amounts resulted in high M_w/M_n value. Also, high solvent amount decreased the molecular weigth of polymer and lowered the polymerization yield.

P4, **P10** and **P12** were compared in GPC traces (Figure 3.7). P10 has the higher hydrodynamic volume, so came in GPC traces earlier. This indicated that it had the higher molecular weigth. PDI values and molecular weights of polymers were reported in the polymerization Table 3.1.

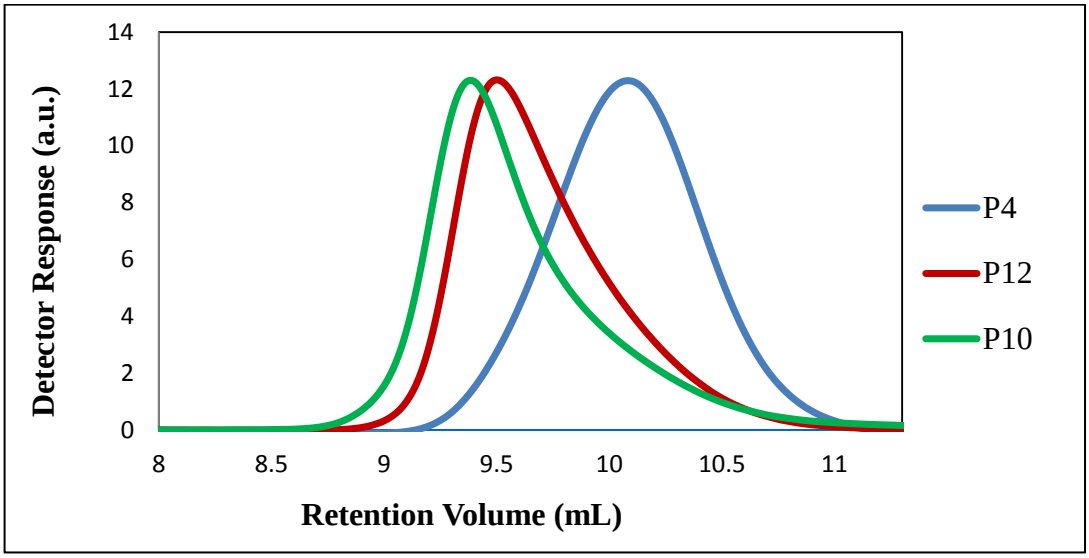

Figure 3.7. GPC traces of polymers P4, P12 and P10.

^{1}H NMR spectrum of copolymer P4 is shown in Figure 3.8. H_a protons of polymer was at 3.27 ppm as a triplet with an integration value of two protons. H_p protons of PEGMA methoxy group is at 3.37 ppm as a singlet. Finally, H_n protons of NHSMA methylene group appeared at 2.80 ppm as a broad singlet. From the integration values, molecular weight of the polymer was calculated as 3.264 g/mole. To calculate the molecular weigth of polymer, integration value of H_p protons was divided by three due to the 3H on methoxy group and the resulting value was multiplied with molecular weight of PEGMA. The same procedure was applied for H_n. The 3.60 ppm was divided by four, and the result was multiplied with the molecular weigth of NHMA. Lastly, the two results and the molecular weight of azido initiator were summed up to give the Mw of polymer.

Table 3.1. Conditions and results of polymerization reactions.[a]

No	Co-polymer	$[M_1+M_2]_o/[I]_o$	Solvent (mL)	Temp. (^oC)	Yield (%)	Feed ratio		Obtained ratio		$M_{n,\ theo.}$[b] g/mole	$M_{n,\ NMR}$[c] g/mole	$M_{n,\ GPC}$[d] g/mole	M_w/M_n[d]
1	P1	3.3	6	40	55	10	90	6	94	821	3.1K	5.8K	1.30
2	P2	5	6	40	54	10	90	-	-	1072	-	5.9K	1.30
3	P3	6.7	6	40	58	10	90	-	-	1411	-	6.5K	1.34
4	P4	10	6	40	54	10	90	10	90	1853	3.3K	8.7K	1.21
5	P5	20	6	40	56	10	90	-	-	3496	-	9.8K	1.46
6	P6	30	8	40	52	10	90	-	-	4784	-	13.5K	1.76
7	P7	30	16	40	43	10	90	-	-	4021	-	8.9K	1,50
8	P8	30	16	85	35	10	90	-	-	3359	-	9.4K	1.28
9	P9	40	8	40	58	10	90	-	-	7029	-	11.2K	1.61
10	P10	40	8	85	73	10	90	13	87	8941	10.1K	13.3K	1.29
11	P11	50	8	85	56	10	90	14	86	8423	9.2K	15K	1.29
12	P12	50	12	85	34	10	90	14	86	5197	7.3K	11.1K	1.25
13	P13	50	16	85	29	10	90	-	-	4405	-	10K	1.23

a. $[I]_o$:[CuBr]:[L] = 1:1:2; time: 30 min.; solvent: anisole.

b. Theoretical molecular weight was calculated according to: $M_{n(teo)} = ([M]_o/[I]_o)$ x conversion x 288.32 + 292.17. Where 288.32 and 292.17 are the average molecular weight of monomers (183.16 x 10% + 300 x 90% = 288.32, $M_{w,\ NHSMA}$= 183.16; $M_{w,\ PEGMA}$= 300) and initiator respectively.

c. Calculated from ^{1}H NMR.

d. Determined from size exclusion chromatography (SEC) calibrated with PMMA standards in THF as eluent.

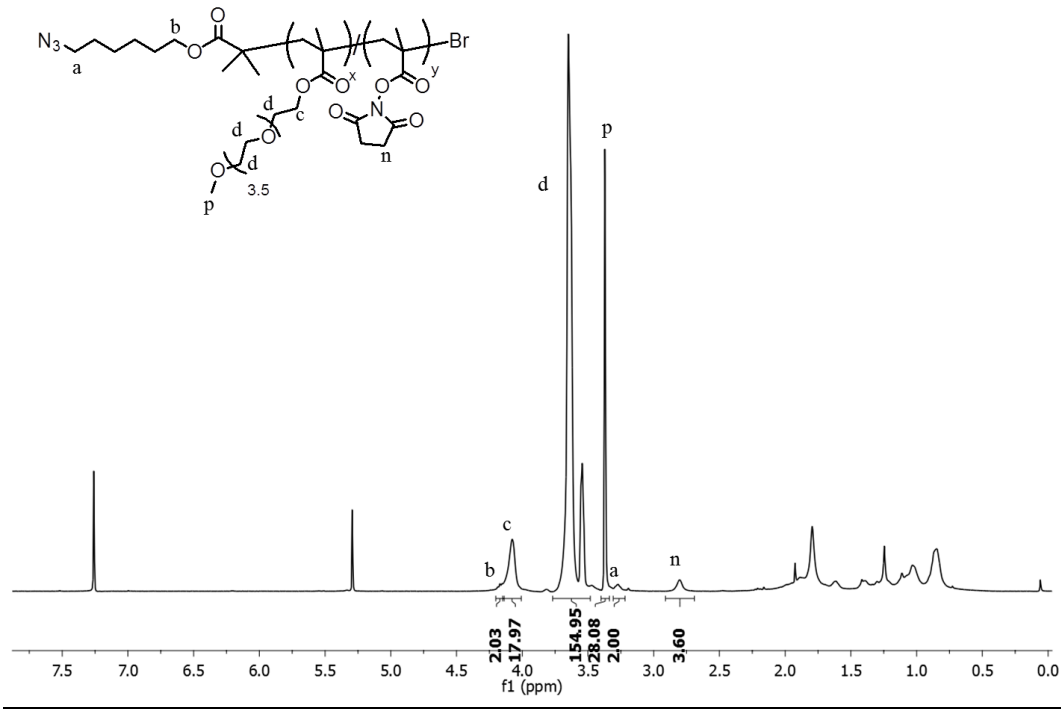

Figure 3.8. ^{1}H NMR spectrum of P4 polymer (Mwt=3.3 kDa).

Obtained biocompatible copolymer bearing azide group at the end and biodegradable polyester G3 dendron with alkyne group at its focal point were conjugated successfully via [3+2] Huisgen type 'click' reaction (Figure 3.9). The reaction took place at 40 ^{o}C in THF in the precence of Cu(I)Br. Three different copolymers with varying molecular weights were used for conjugation as shown in Table 3.2.

Table 3.2. Polymer-dendron conjugates.

Copolymer	**Conjugate**	**$Mn^{a}_{conjugate}$**	**$M_w/M_{n\ conjugate}$**	**Yield**
P4	C1	10.7 kDa	1.26	55%
P12	C2	14.1 kDa	1.23	58%
P10	C3	16.2 kDa	1.24	62%

a. Determined from size exclusion chromotography (SEC) calibrated with PMMA standards in THF as eluent.

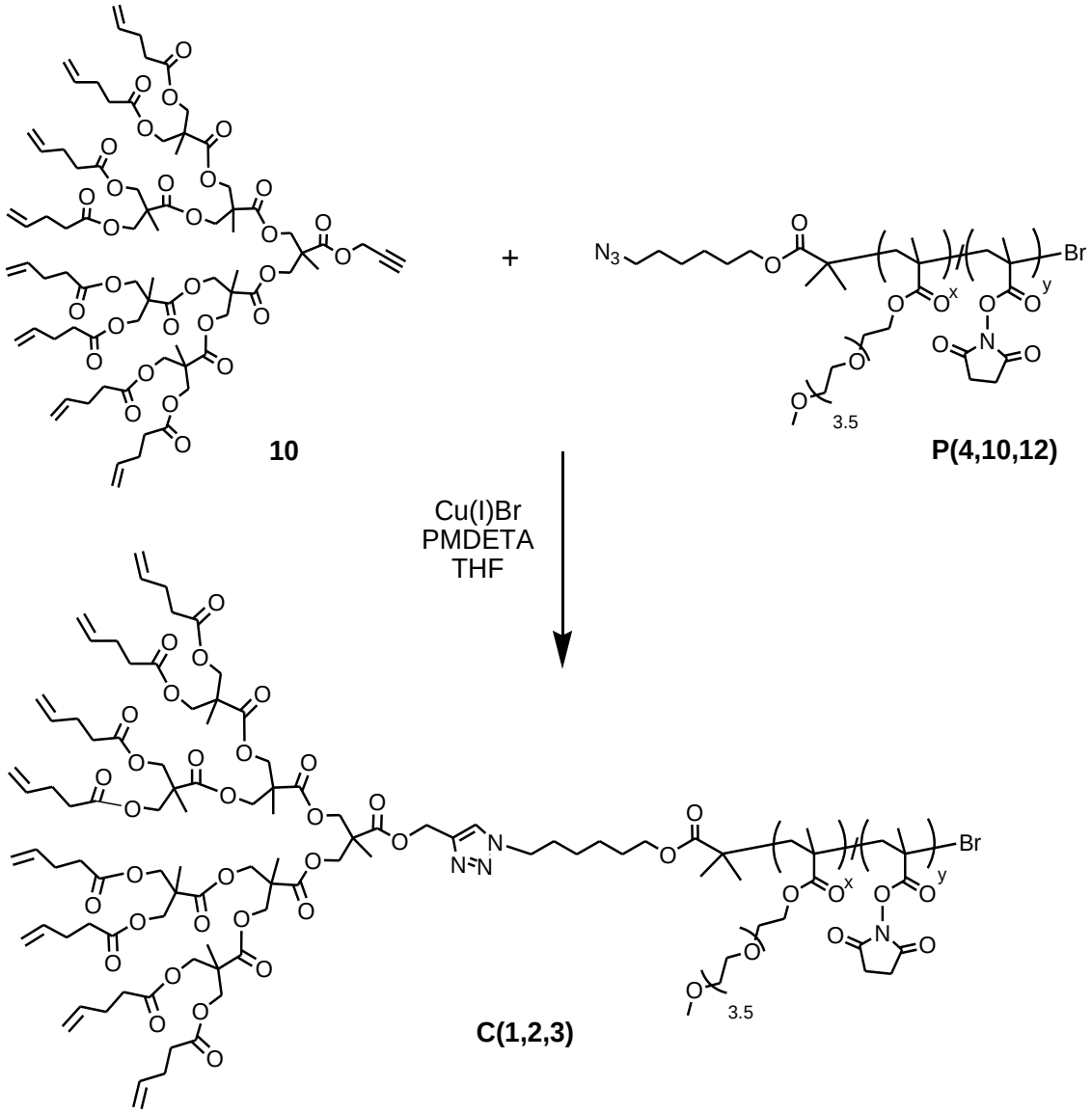

Figure 3.9. Synthesis of polymer-dendron conjugate.

The increase in hydrodynamic volume of polymer-dendron conjugate (C1) was monitored by the evolution of GPC traces **G3$_{alkene}$** and **P4**. The molecular weigth increase of **C1** upon attachment of dendron to polymer was evident from GPC traces (Figure 3.10).

Polymer – dendron conjugate were also characterized via ^{1}H NMR analysis (Figure 3.11). After the 'click' reaction with the formation of the triazole ring, a new aromatic proton formation was expected. The triazole proton H_d appeared at 7.68 ppm. The proton of the alkyne core of the dendron H_b at 2.52 ppm disappeared. The methylene proton H_c shifted from 4.72 to 5.22 ppm. Finally, H_a proton of polymer near the azide group shifted to downfield region.

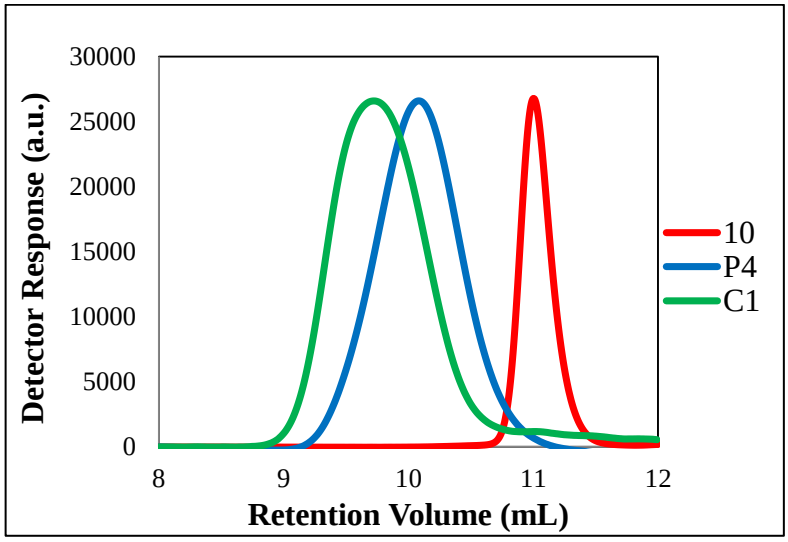

Figure 3.10. Comparison of GPC traces of 10, P4 and C1.

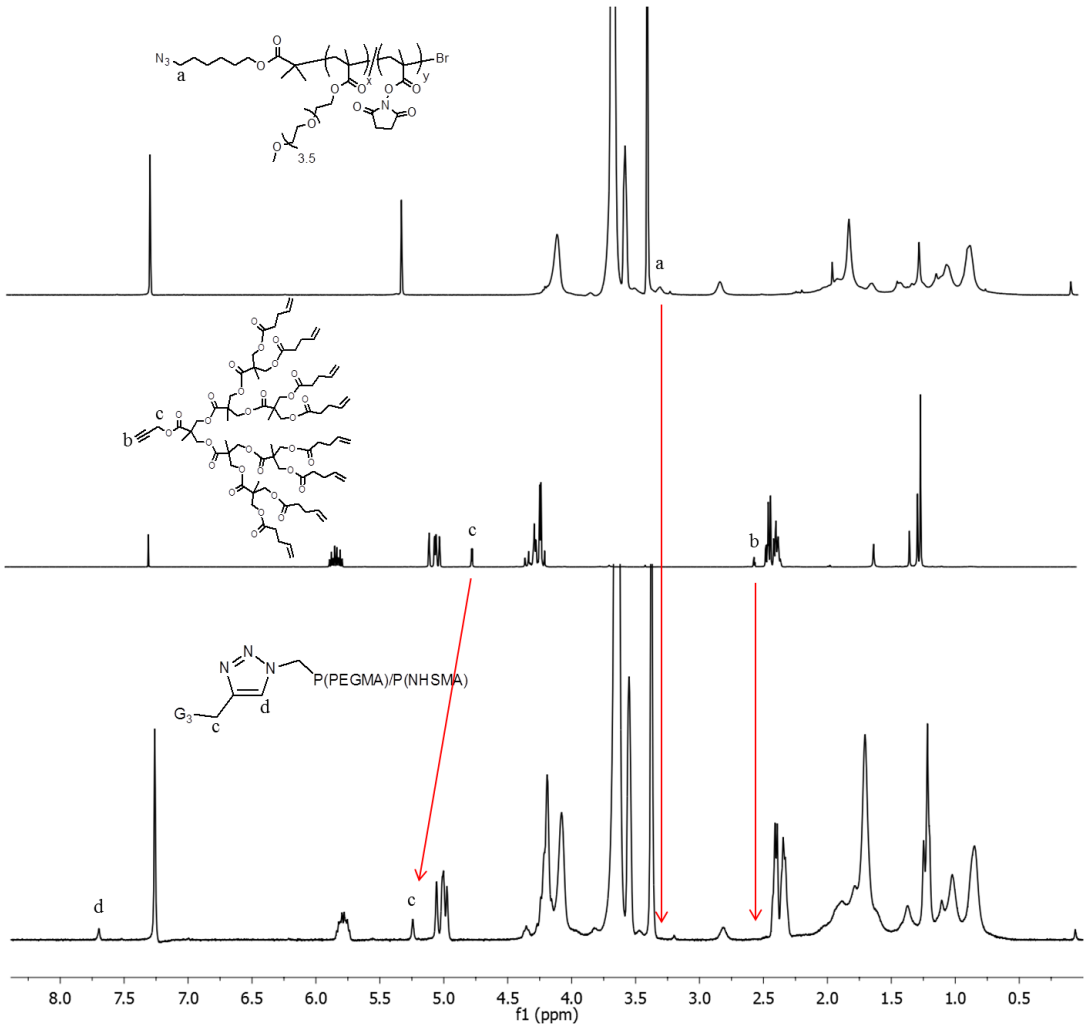

Figure 3.11. Comparison of ^{1}H NMR spectra of 10, P4 and C1.

3.2. Micelle Formation from Polymer-Dendron Conjugates

The polymer-dendron conjugates are composed of amphiphilic macromolecules that have diverse hydrophilic and hydrophobic block domains. Due to the solubility difference between these blocks, the macromolecules have a tendency of assembling into polymeric micelles in aqueous media. In order to study the aquous solution behavior of the macromolecular construct, the conjugates were dissolved in water and micelle formation was accounted using different techniques.

3.2.1. Critical Micelle Concentration (CMC) Measurement

The critical micelle concentration means the minimum concentration of copolymer that is required to form micellar structures in water via self-assembly. The CMC value may give an opinion about the thermodynamic stability of the micelles. It is known that below CMC, polymeric micelles are gradually disintegrated into their unimers which will in the release of their cargo. However, the micelles having lower CMC values do not dissociate easily and they will be more stable in aqueous environment.

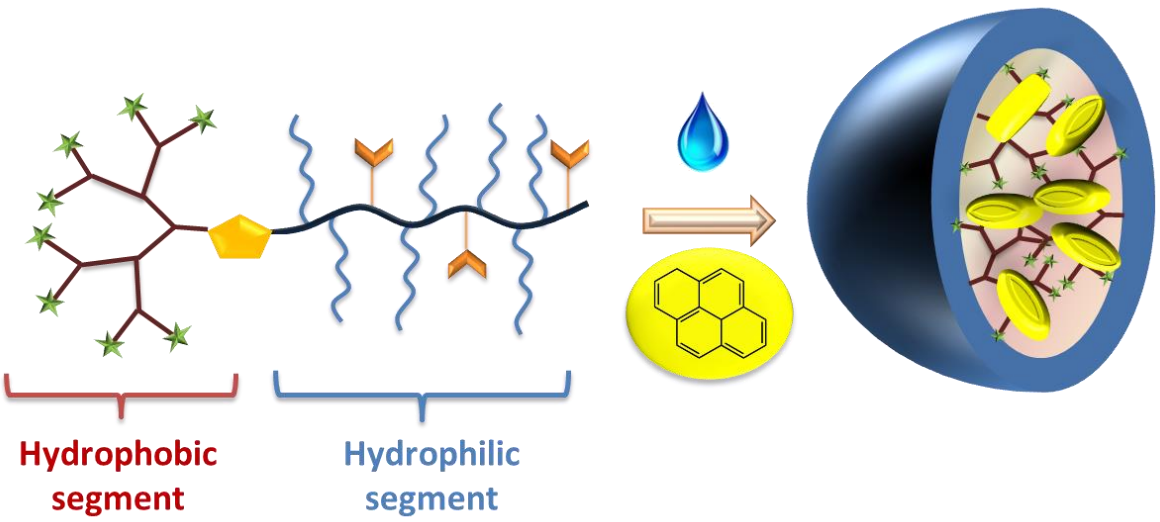

Figure 3.12. Schematic representation of polymer-dendron conjugate and pyrene loaded self-assembled micellar structure.

To prepare micelles from the polymer-dendron conjugates and measure their critical micelle concentrations, pyrene probe method was used. Pyrene is a hydrophobic fluorescence dye. It is commonly used to determine CMC values.

To study our micelles formation in an aqueous environment, the conjugates were dissolved in an organic solvent such as tetrahydrofuran (THF), and transferred into vials to have different concentrations ranging from 10^{-5} M to 10^{-9} M. After evaporation of THF, pyrene solution (10 µL, $1.8x10^{-4}$ M) in acetone was added to all the vials. Acetone was also removed under *vacuo*. Afterward, all samples were dissolved in 3 mL MilliQ water (pH 7), and micelle formations were triggered with sonication for 1 h, at 70 ^{o}C. Finally, fluorescent signal arising from pyrene in micellar solutions having different copolymer concentrations were measured by fluorescence spectrometer.

Pyrene exhibits a number of characteristic intensity bands between 300-360 in the fluorescence spectrum. The excitation spectra of micelles obtained from conjugates C**1**, **C2** and **C3** are given in Figure 3.13. It is indicated that as the concentration of conjugates increased, the intensity of pyrene in the spectrum increased, too. In addition, the maximum intensity peak shifted to 338 nm from 334 nm after a certain point.

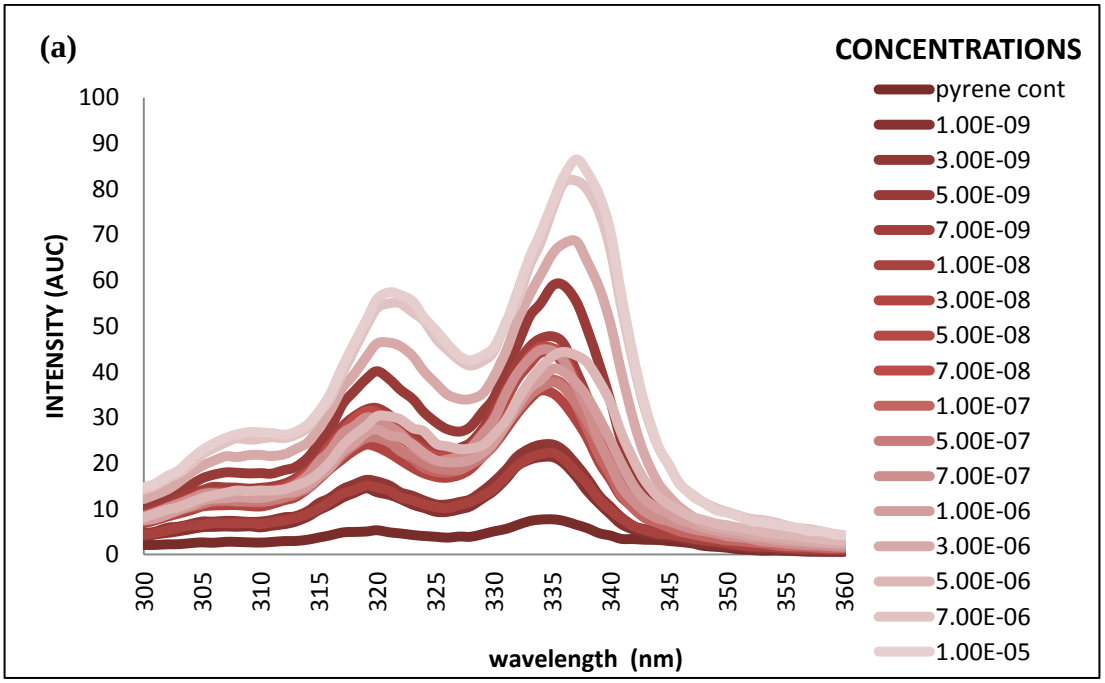

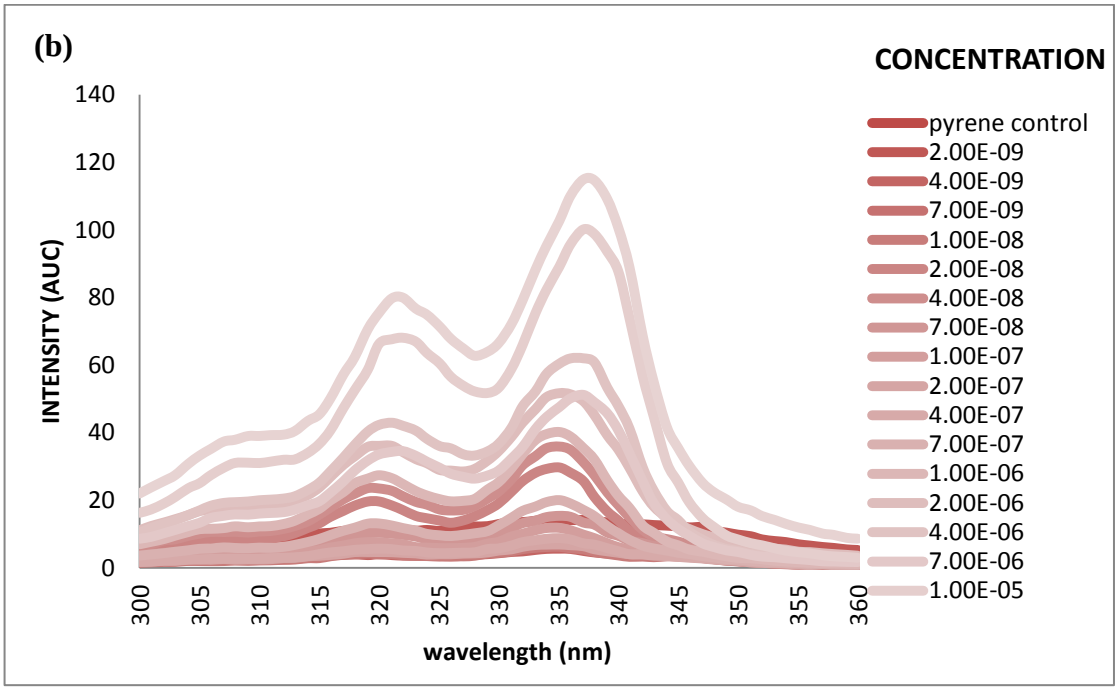

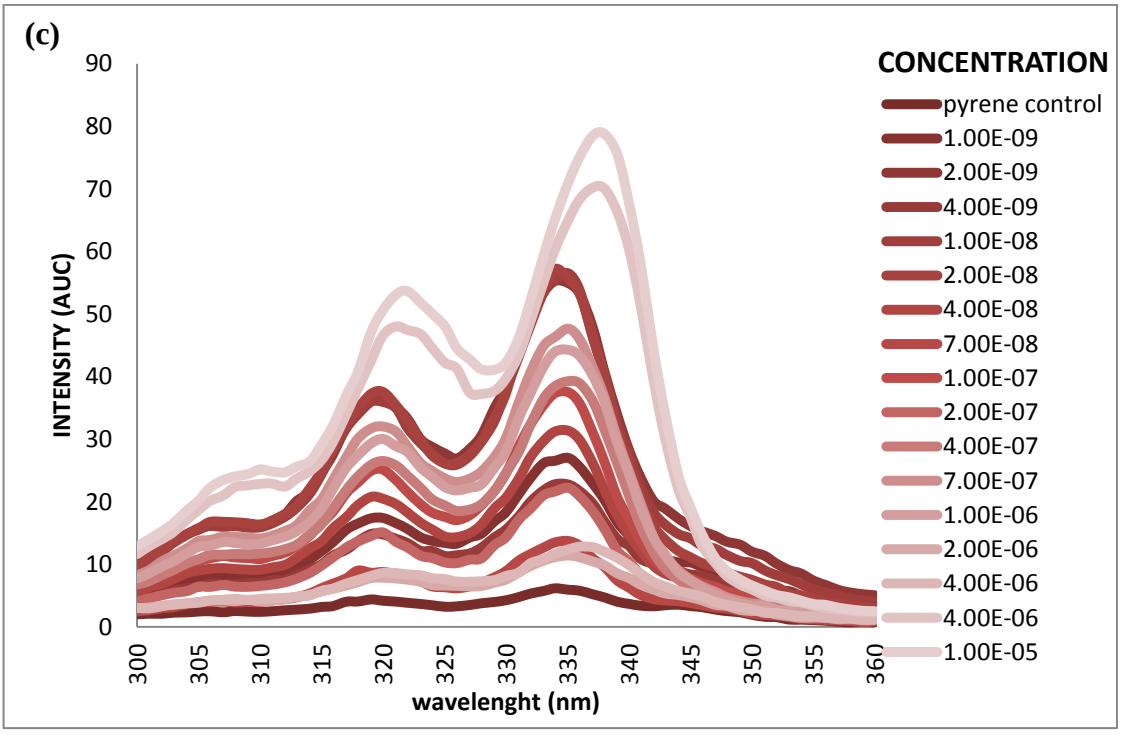

Figure 3.13. Excitation spectra of pyrene loaded (a) C1, (b) C2 and (c) C3 copolymers.

From fluorescence spectrum, it is easy to draw CMC graph. Pyrene shows different characteristic intensity bands in the excitation graph according to the environment that it is found. In an aqueous solution, maximum intensity of pyrene is 334 nm (I_1). However, when pyrene is in an organic media, the intensity is shifted to the higher nm (I_3). This number is generally in between 337-338 nm. To obtain the CMC graph, it is benefited from the ratio of I_3/ I_1. This ratio is fixed for certain concentrations, which demonstrates that pyrene is still in aqueous environment. However, after a certain concentration (intercept point of trendlines in Figure 3.14), this value is starting to increase. This indicates that pyrene is located in less polar environment. In other words, micelle formation has been started in aqueous solution, so pyrene prefers to go in the hydrophobic core of the micelles. As can be seen in Figure 3.14, the intercept points give the CMC values.

Three different micelles were formed from three different copolymers, namely **C1**, **C2** and **C3**. The CMC values did not differ from each other significantly. These results indicate that stability of micelles did not change as increasing the size of the hydrophilic portion of copolymer.

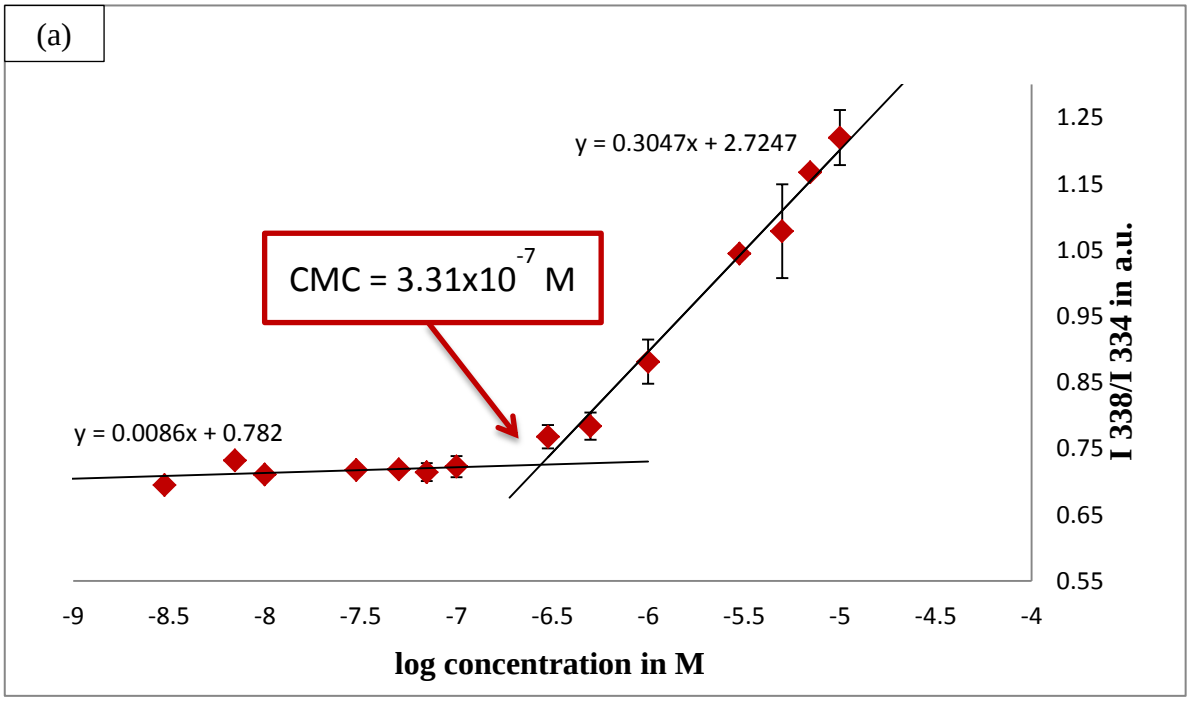

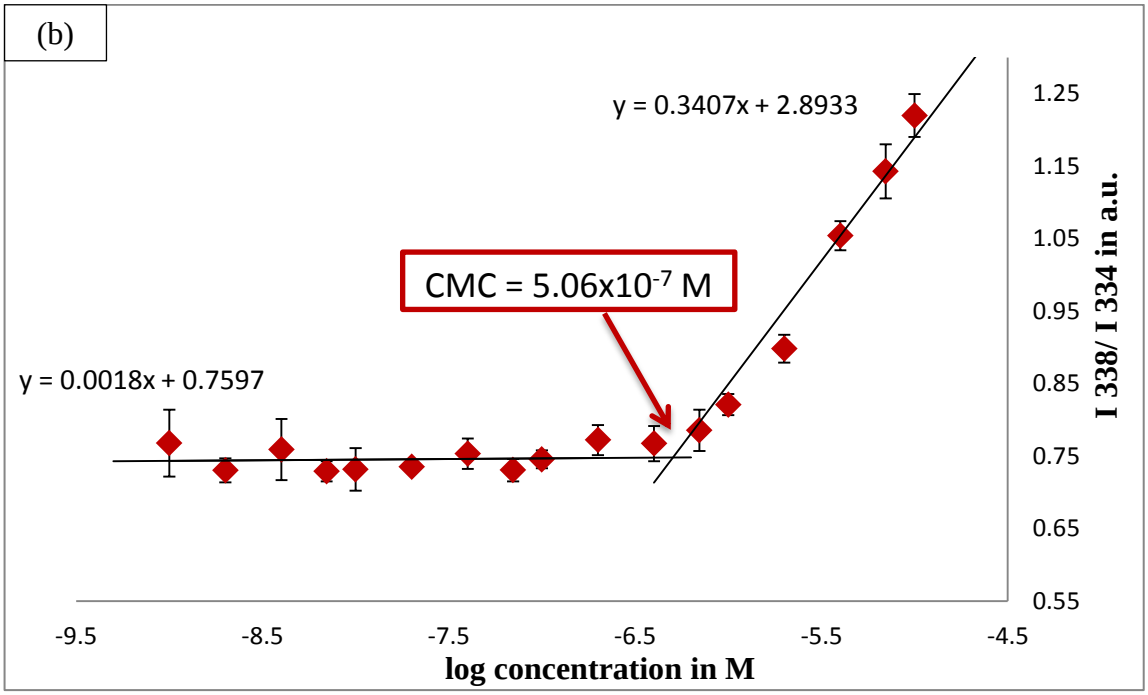

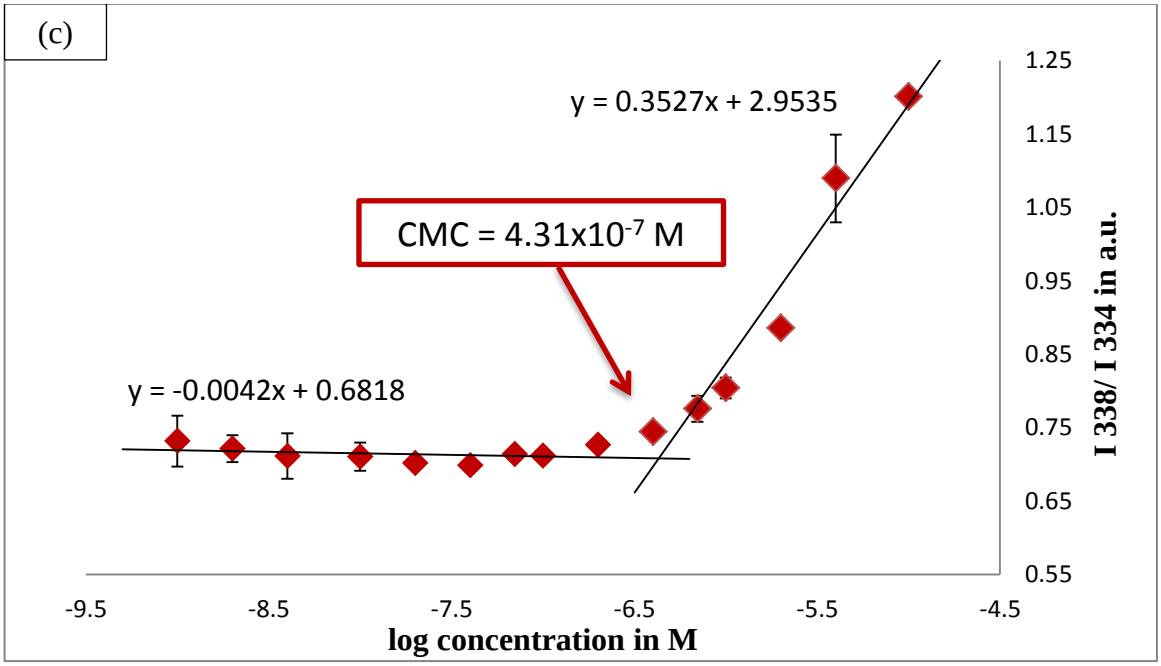

Figure 3.14. Log C vs I_{338} / I_{334} graph of micelles assembled from (a) C1, (b) C2 and (c) C3.

3.3. Stability of Micelles

Stability of micelles plays an important role for the micellar drug delivery systems. Micelles should be stable enough against dilution and they can be able to circulate in the blood stream for sufficient time in order to reach and accumulate the tumor tissue. If the macromolecules do not have the feature of stability, they result in early drug release which lead to undesired side effects to healthy tissues. In this research, core crosslinking strategies were applied to further stabilize the micelles. Then, core cross-linked micelles were compared with non-cross-linked ones and the size differences were observed via dynamic light scattering (DLS) instrument.

3.3.1. Core Crosslinking of Micelles

After demermination of the CMC of the micelles, core crosslinking method has been applied in order to stabilize the system. For this, the hydrophobic crosslinker (tetrathiol, **20**) and photoinitiator (DMPA, **21**) were used (Figure 3.15). These reagents reacted with the periphery of dendron via UV irradiation at 335 nm and the core of the micelles were crosslinked by means of thiol-ene 'click' chemistry (Figure 3.16).

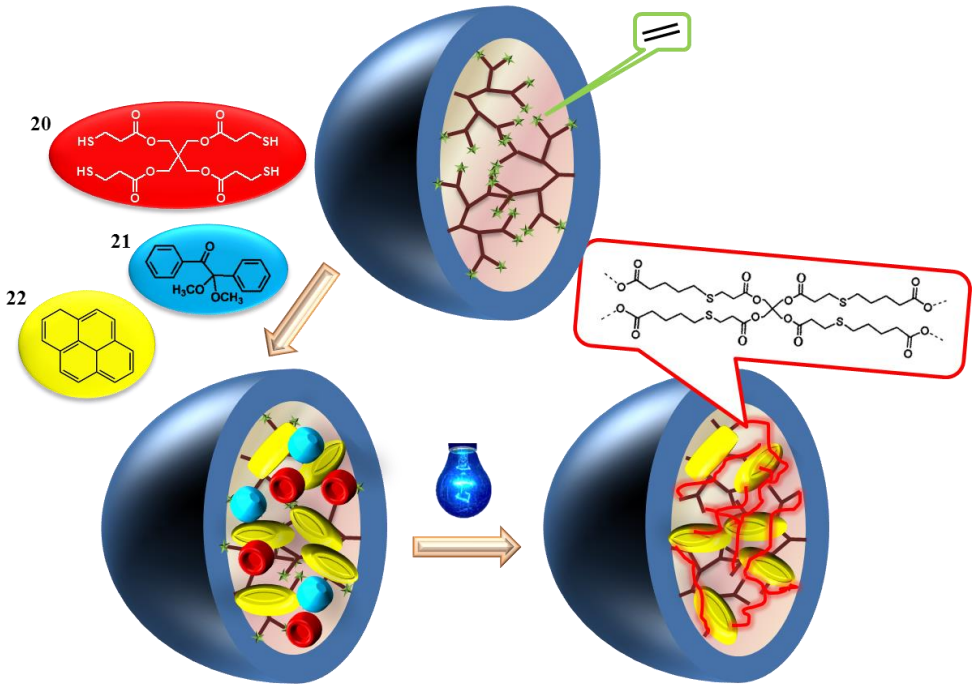

Figure 3.15. Schematic representation of core crosslinking.

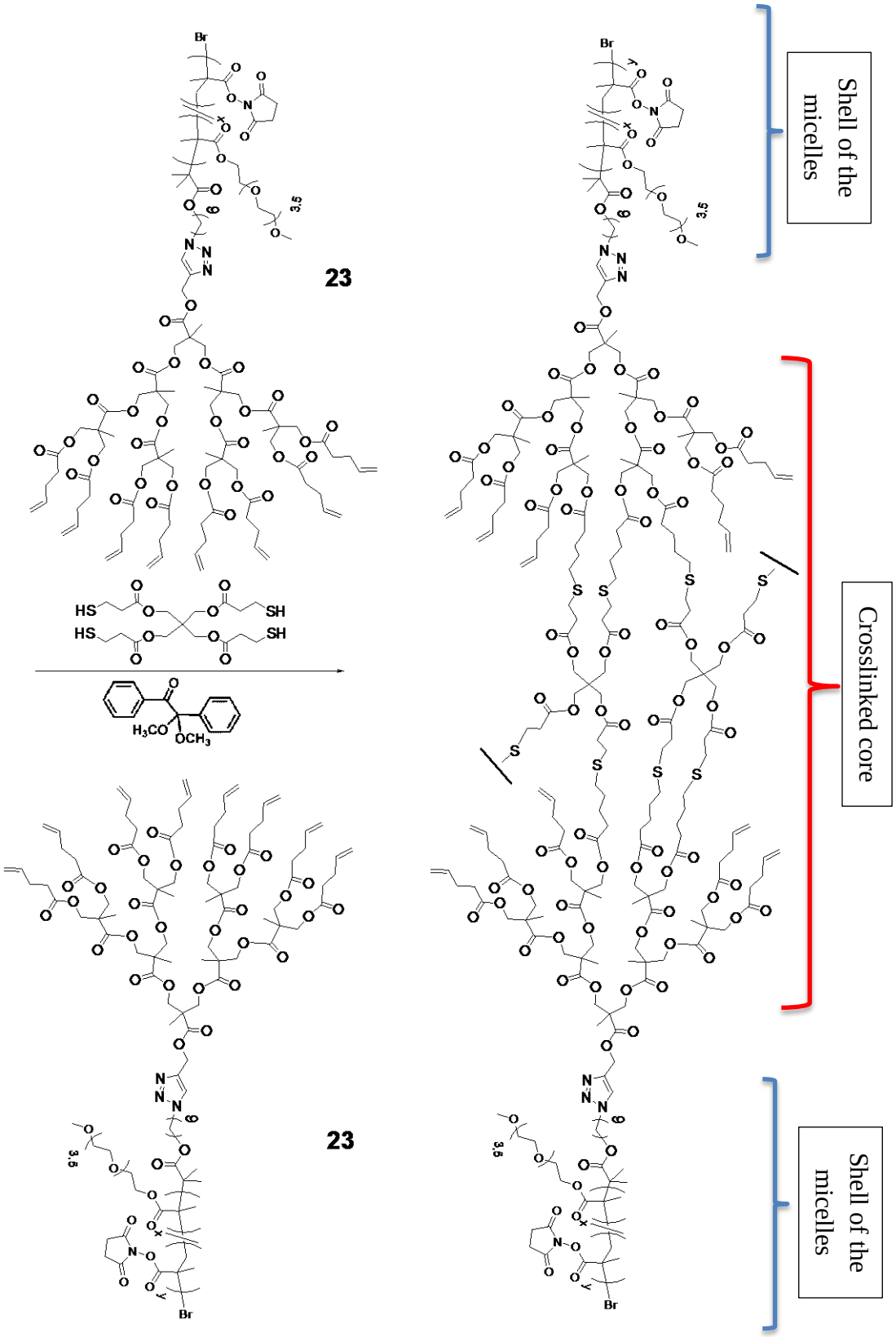

Figure 3.16. Core crosslinking of micelles via thiol-ene ‘click’ chemistry.

3.4. Dynamic Ligth Scattering Measurements

The size of micelles has an important role for tageted drug delivery. The ideal micelle size should be between 10 to 100 nm in order to prevent rapid clearence by the reticuloendothelial system (RES).

The sizes and stabilities of both noncrosslinked and crosslinked micelles were studied using DLS. Twelve different micelles were prepared from the three conjugates. They were classified according to their crosslinking and whether they have pyrene as a cargo, namely empty non-crosslinked, pyrene loaded non-crosslinked, empty crosslinked and pyrene loaded crosslinked micelles. The measurements were performed at a concentration of 10^{-5}M which is above the CMC concentrations of all micelles. The polydispersity of micellar structures was shown in number vs. diameter graph (Figure 3.18). All the copolymer formed monodisperse micellar with diameter below 100. The size distribution of micelles obtained from the three conjugate did not change considerably.

The diameter of non-crosslinked micelles were in the range of 60-80 nm. After applying core crosslinking, the diameter reduced to 20-30 nm. In addition, pyrene loaded non-crosslinked micelles had smaller sizes as compared to empty ones. The reason may be the hydrophobic interaction between pyrene and G3 dendron. However, there was no change in diameter for crosslinked micelles due to the pyrene loading. DLS measurements data are shown in Appendix and summarized in the Table 3.3 and in Figure 3.17.

Table 3.3. Micellar sizes obtained from DLS measurements.

No	Copolymer	Non-crosslinked empty	Non-crosslinked pyrene loaded	Crosslinked empty	Crosslinked pyrene loaded
1	C1	77±8 nm	53±4 nm	29±5 nm	29±6 nm
2	C2	64±15 nm	58±4 nm	25±4 nm	25±3 nm
3	C3	61±6 nm	59±3 nm	25±5 nm	23±5 nm

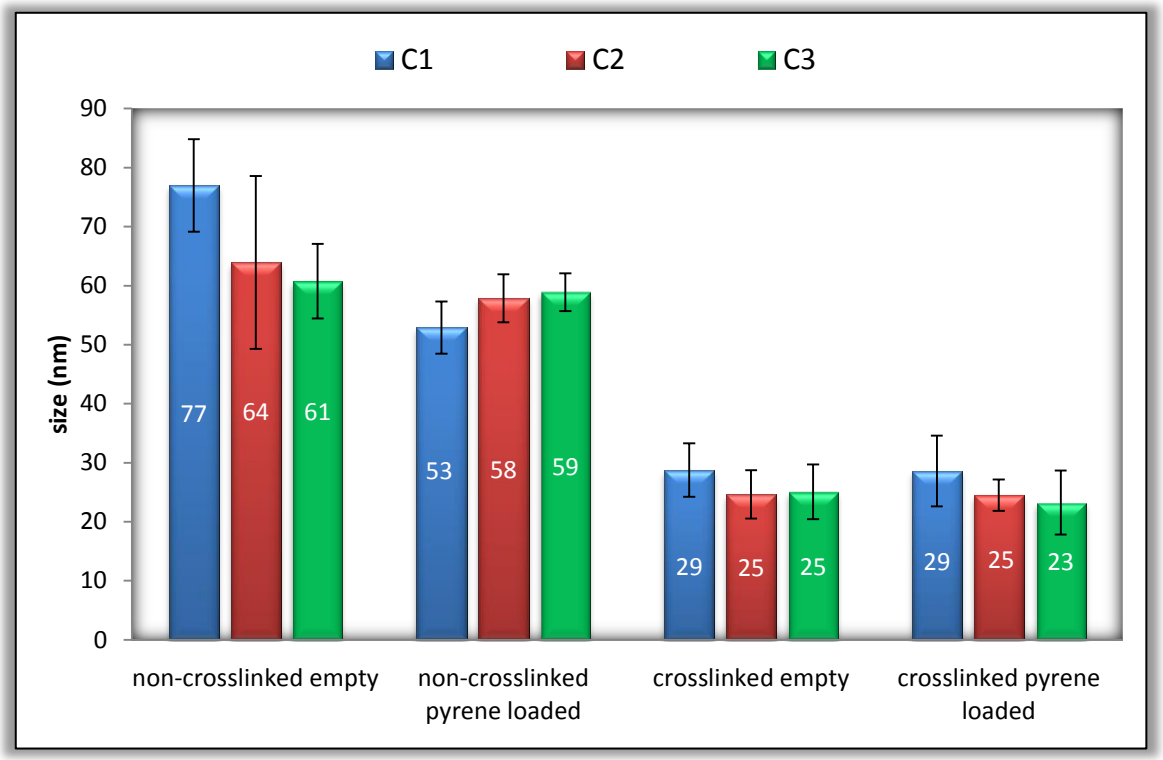

Figure 3. 17. Comparison of micellar sizes obtained from DLS measurements.

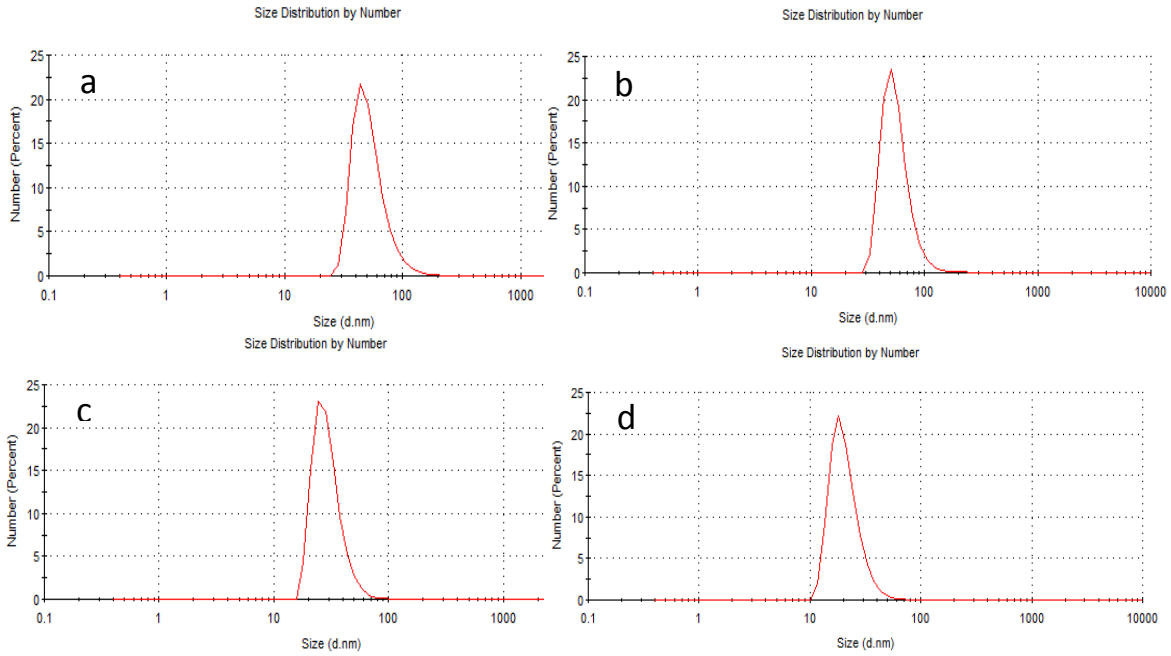

Figure 3.18. Size distribution of (a) non-crosslinked empty, (b) non-crosslinked pyrene loaded, (c) crosslinked empty, (d) crosslinked pyrene loaded micelles assembled from C2 in water.

In order to confirm the stability of core-crosslinked micelles, THF was added to all micelles. THF is a good solvent both blocks of the copolymer. Non-crosslinked micelles completely disassociated into their unimers (free block copolymers) upon addition of THF. (Figure 3.19a). However, crosslinked micelles just swelled (Figure 3.20). These results confirmed that micelles were successfully crosslinked by UV irradiation. As a control, polymer-dendron conjugate was dissolved in THF, nearly the same size distribution was found (Figure 3.19b).

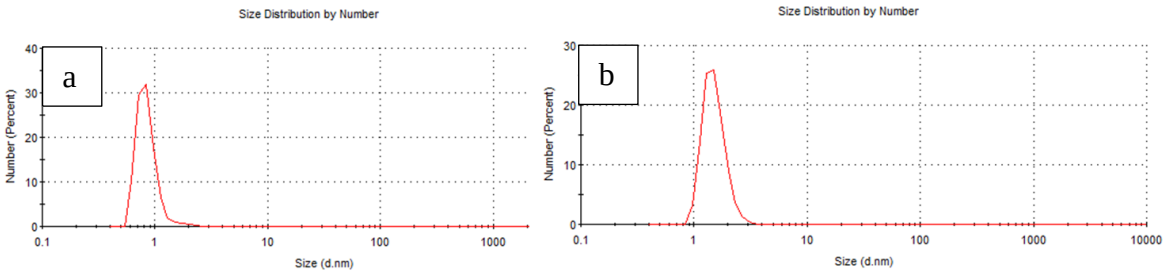

Figure 3.19. DLS image of (a) non-crosslinked micelles after THF addition (0.85 nm), (b) polymer-dendron conjugate

Figure 3.20 demostrates the sizes of crosslinked micelles after addtion of THF. The results show that crosslinked empty micelles swelled more in THF than the crosslinked pyrene loaded micelles did.

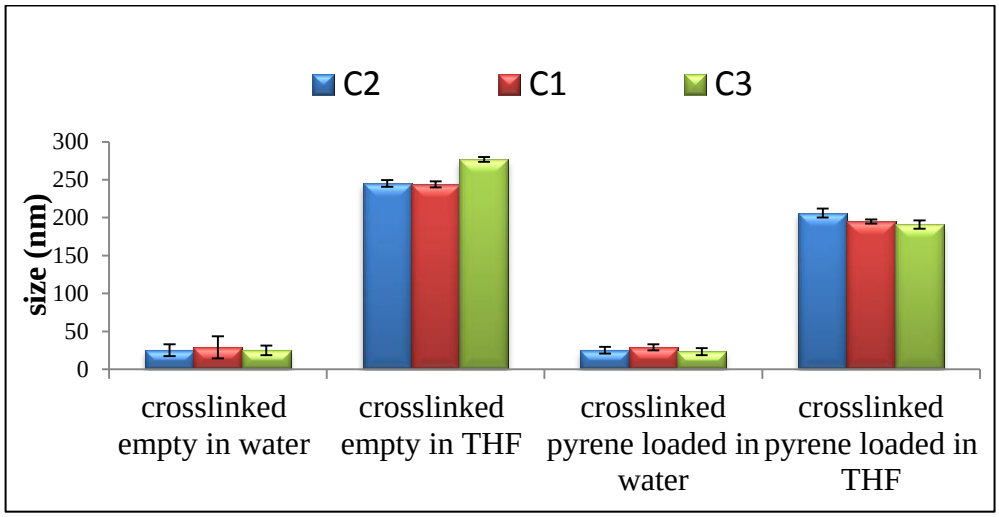

Figure 3. 20. Comparison of micellar sizes after addition of THF. The size numbers were obtained from DLS measurements.

4. EXPERIMENTAL

4.1. General Methods and Materials

2,2-Bis(hydroxymethyl) propionic acid (BMPA), Dowex X50WX2, Propargyl Alcohol, 4-pentenoic anhydride were purchased from Alfa Aesar. Pentaerythritol tetrakis(2-mercaptopropionate) was purchased from Aldrich and DMPA (2,2-Dimethoxy-2-phenylacetophenone) from Acros. All solvents were purchased from Merck and used as obtained without further purification unless otherwise noted. Azide functionalized initiator and dendron 10 were synthesized according to literature procedures [62]. The initiator, dendron and polymer characterizations involved ^{1}H NMR spectroscopy (Varian 400 MHz) and Fourier transform infrared (ATR-FT-IR) spectroscopy (Thermo Fisher Scientific Inc. Nicolet 380). MALDI-tof of dendron was characterized by Axima Performance instrument (Shimadzu Biotech) Micelle formations were characterized using Fluorescence spectroscopy (Cary Eclipse) and Zetasizer Nano particle analyser series (Malvern). The molecular weights of the polymers were estimated by GPC analysis using a Shimadzu PSS-SDV (length/ID 8 × 300 mm, 10 mm particle size) mixed-C column caliberated with polystyrene standards (1–150 kDa) using a refractive-index detector. Tetrahydrofuran (THF) was used as eluent at a flow rate of 1 mL min^{-1} at 30 °C. UVP Black-Ra B-100AP/R High Intensity UV lamp (100 Watt / 365 nm) was used for crosslinking experiments.

4.2. Synthesis of Polyester Dendron

The first, second and third-generation polyester dendrons were prepared using a well-established divergent synthesis strategy [63]. The growth of the dendron was started from the alkyne core towards the periphery (Figure 4.1). The dendrimer backbone was based on 2,2-bis(hydroxymethyl) propionic acid (bis-MPA) as a biocompatible building block. In order to install the alkyne functionality at the core, an alkyne group containing alcohol (**1**) was used. The first generation dendron was synthesized via reacting propargyl alcohol with anhydride **2**. Then, the acetonide protecting unit was removed by acidic

DOWEX-H resin. The resulting product **4** gave the G1 dendron bearing alkyne unit at the core. The alcohol groups at the periphery were further utilized for dendrimer growth. The second and third generation dendrons were synthesized in the same manner using anhydride acylation and acetonide deprotection sequences.

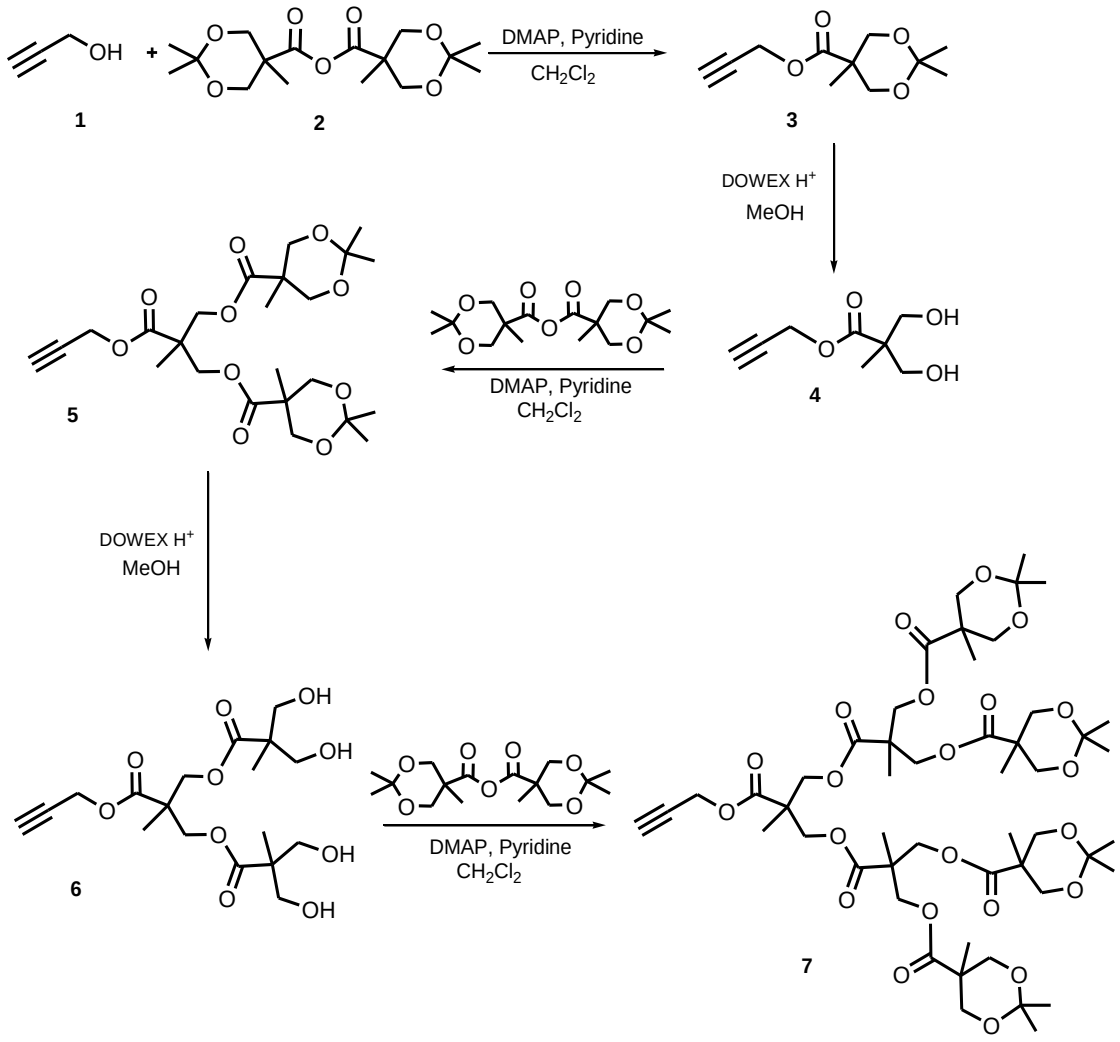

Figure 4.1. Synthesis of alkyne core functionalized deprotected and protected G1, G2 and G3 dendron with acetal groups at the periphery.

4.2.1. Synthesis of Third Generation Polyester Dendron

To obtain third generation dendron bearing alkyne group at the focal point, compound **7** (1 g, 0.90 mmol) was dissolved in MeOH (40 mL). Dowex H^+ resin (1.00 g), washed with MeOH (5 x 30 mL), was added to this solution. The resulting mixture was stirred at 40 ^oC until the compound **7** was not observed via TLC. After the reaction was completed, the resin was filtered off and MeOH was evaporated under *vacuo*. The crude product was purified by recrystallization from CH_2Cl_2 and the product **8** was obtained as white solid yielding (0.82 g, 97%). ^1H NMR (CD_3OD, δ, ppm) 4.77 (s, 2H), 4.33 - 4.22 (m, 12H), 3.66 (d, 8H, *J* = 12.0 Hz), 3.58 (d, 8H, *J* = 12.0 Hz), 2.97 (s, 1H), 1.30 (s, 3H), 1.28 (s, 6H), 1.12 (s, 12H). FTIR (cm^{-1}): 3305.5, 1727.7.

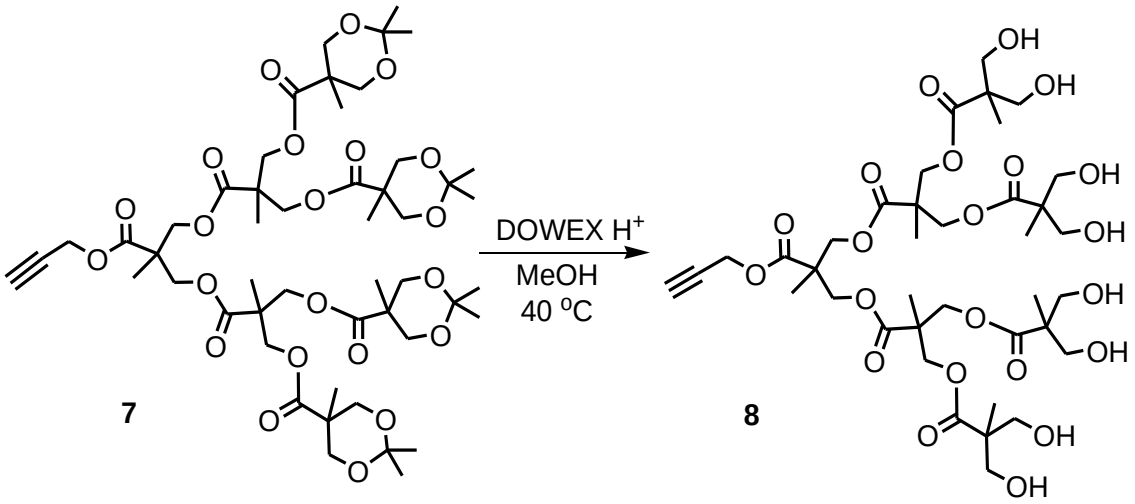

Figure 4.2. Synthesis of alkyne functionalized deprotected G3 dendron.

4.2.2. Peripheral Functionalization of Generation 3 Dendron

In order to functionalize the hydroxyl end groups of **8** with alkene groups, compound **8** (0.0974, 0.122 mmol) and DMAP (0.015g, 0.122 mmol) were added to a round bottom flask and purged with N_2 for two minutes. Then, dry CH_2Cl_2 (1.3 mL) was added as a solvent. Finally, pyridine (0.109 mL, 1.347 mmol) and 4-pentenoic anhydride (0.246 mL, 1.347 mmol, **9**) were added to the solution under N_2, respectively. The reaction was stirred for 24 h. Water (0.109 mL) was added to the reaction flask and stirred for 2 h. Reaction mixture was diluted with CH_2Cl_2 (3 mL) and then extracted with 1M $NaHSO_4$ solution (3 x 3 mL), 10% Na_2CO_3 solution (3 x 3 mL) and with brine solution (1 x 3 mL). Organic layer was dried over anhydrous Na_2SO_4. Pure product **10** was obtained as 0.147 g (86% yield). ^{1}H NMR ($CDCl_3$, δ, ppm) δ 5.84 – 5.74 (m, 8H) , 5.07 – 4.98 (m, 16H), 4.73 (d, 2H, J = 2.4 Hz), 4.31 – 4.16 (m, 28H), 2.52 (t, 1H, J = 2.4 Hz), 2.43 – 2.39 (m, 16H), 2.37 – 2.32 (m, 16H), 1.31 (s, 3H), 1.24 (s, 6H), 1.22 (s, 12H). FTIR (cm^{-1}): 3079.04, 2980.7, 1727.7, 1641.4. Maldi-tof (9-NA, NaCl): 1547 g/mole.

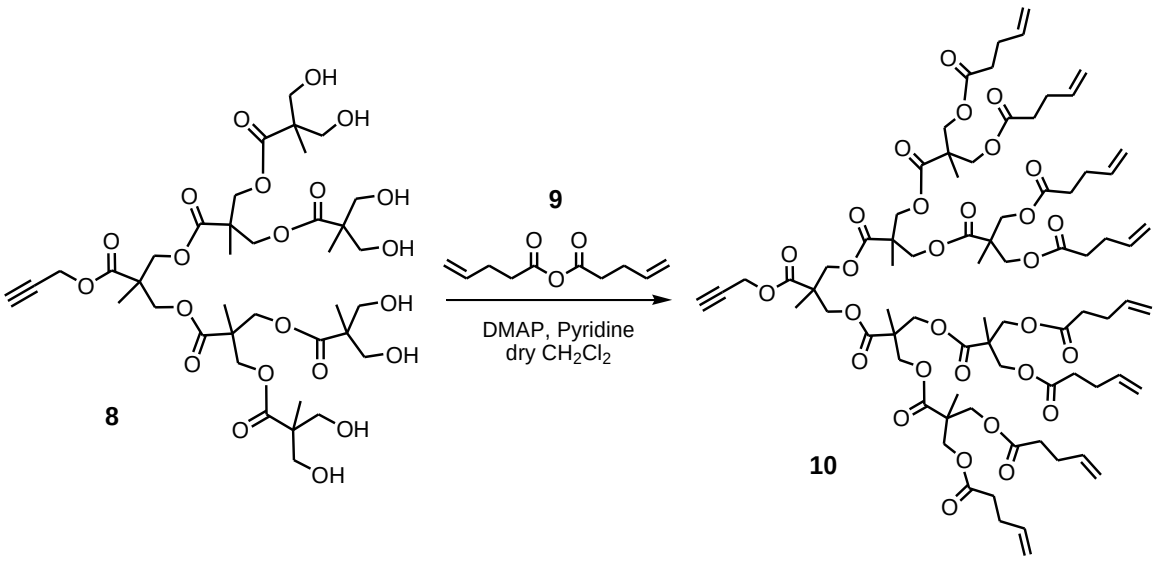

Figure 4.3. Functionalization of periphery of G3 dendron.

4.3. Synthesis of Polymer

4.3.1. Synthesis of Azido Initiator

4.3.1.1. Synthesis of 6-Azido-hexan-1-ol (**14**).

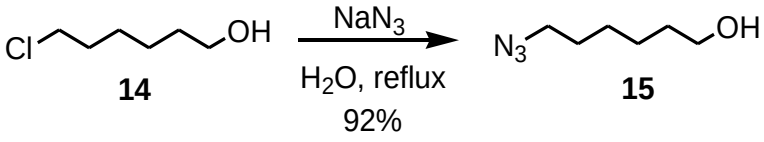

Figure 4.4. First step of azido initiator synthesis.

Sodium azide (1.3 g, 20.5 mmol) were dissolved in distilled water (8 mL) and 6-chloro 1-hexanol (**14**, 1 mL, 7.5 mmol) was added to this solution. The reaction was heated under reflux for 20 h, then cooled to ambient temperature . The product was extracted with EtOAc (3 x 15 mL). Then, the combined extracts were washed with brine, dried over anhydrous Na_2SO_4 and concentrated to yield 1.02 g (95 %) of **15** as transparent liquid. ^{1}H NMR ($CDCl_3$, δ, ppm) δ 3.64 (t, 2H, J = 6.4 Hz) , 3.27 (t, 2H, J = 6.8 Hz), 1.64 – 1.55 (m, 4H), 1.41 – 1.39 (m, 4H). FTIR (cm^{-1}); 3326.2, 2094.5.

4.3.1.2. Synthesis of 2-Bromo-2-methyl-propionic acid 6-azido-hexyl ester (**17**).

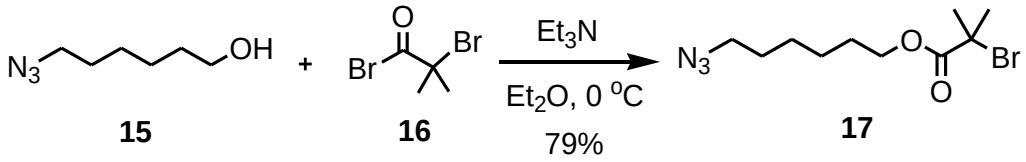

Figure 4.5. Synthesis of azido initiator.

Compound **15 (**1.02 g, 7.13 mmol) and triethylamine (1.03 mL, 7.13 mmol) were added to a round bottom flask and dissolved in Et_2O (25 mL). The solution was cooled to 0 ^oC and 2-bromo-2-methyl propionyl bromide (**16**, 0.97 mL, 7.84 mmol) was added slowly via syringe. The reaction was stirred at 0 ^oC for 1 h, then for 12 h at room temperature. The resulting white suspension was filtered through sintered glass and the obtained yellowish-orange solution was washed with saturated $NaHCO_3$ solution (2 x 50 mL) and dried over Na_2SO_4. After filtration, the solvent was removed under *vacuo*, the residue was purified by flash chromatography with 100% hexane to give **17** (1.81 g, 87 %) as colourless oil. ^1H NMR ($CDCl_3$, δ, ppm) 4.18 (t, 2H, J = 6 Hz), 3.27 (t, 2H, J = 6.8 Hz), 1.93 (s, 6.4H), 1.73 – 1.67 (m, 2H), 1.65 – 1.58 (m, 2H), 1.44 – 1.42 (m, 4H). FTIR (cm^{-1}); 1731.96.

4.3.2. Synthesis of NHSMA Monomer

N–hydroxy succinimide (2.54 g, 20.11 mmol), triethylamine (3.37 mL, 24.17 mmol) and CH_2Cl_2 (130 mL) was added to a reaction flask at 0 ^oC. Then, methacryloyl chloride (2 mL, 20.66 mmol) was added slowly to the solution (0.1 mL each 5 min). Reaction was stirred at room temperature for 2 h. The resulting product was extracted with distilled water (2 x 50 mL) and concentrated under *vacuo*. The resulting residue was recrystallized in EtOAc (10 mL) : Hexane (20 mL) mixture. The solid obtained after filtration, yielded 3.41 g (90 %) of the white crystals.

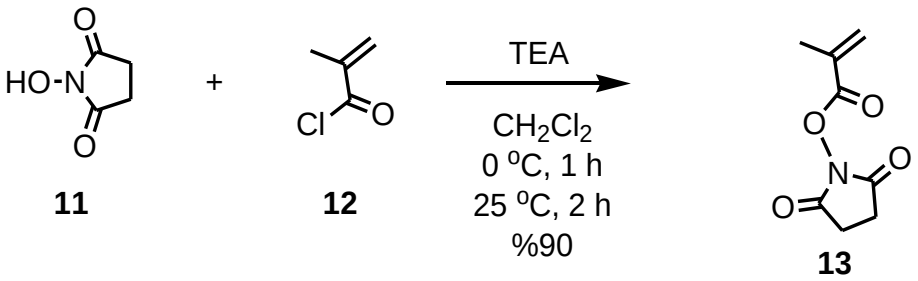

11 **12** **13**

Figure 4.6. Sythesis of NHSMA monomer.

4.3.3. Synthesis of p(PEGMA)-b-p(NHSMA) Block Copolymer

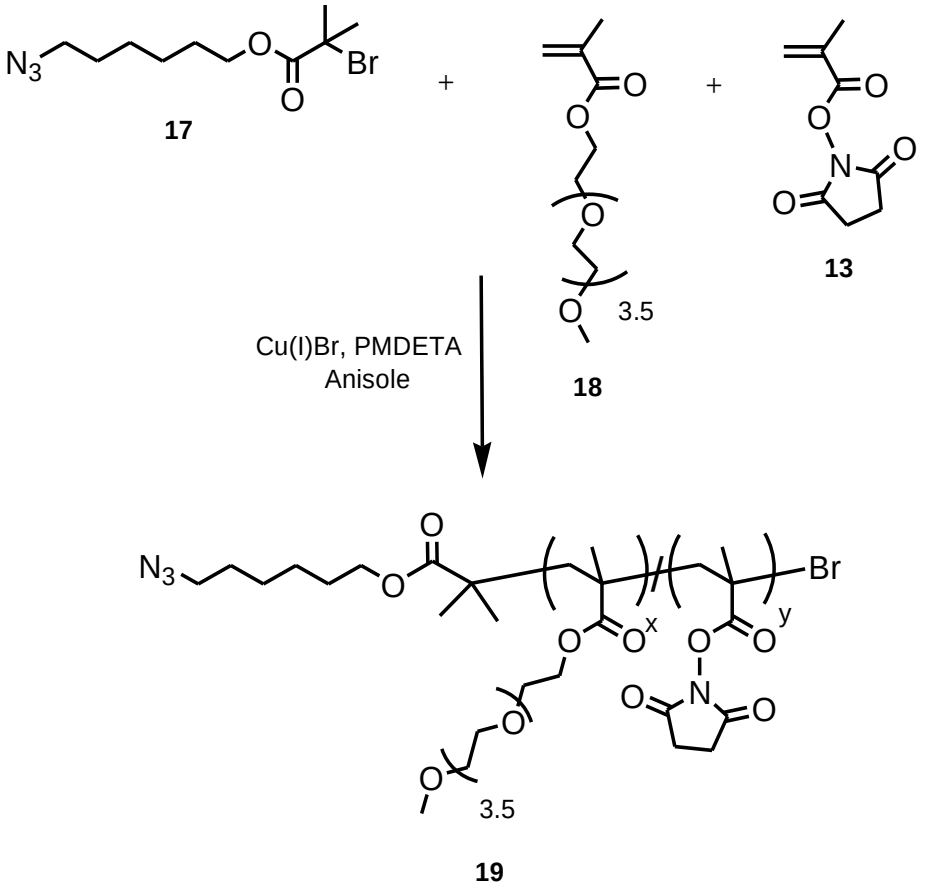

Figure 4.7. Synthesis of p(PEGMA)-b-p(NHSMA) block copolymer.

4.3.3.1. Synthesis of Copolymer 4.

Copper (I) bromide (0.112 g, 0.78 mmol) was weighed into a dry 10 mL reaction flask equipped with a stir-bar. The flask was sealed and purged with N_2 for 1 min. In a vial, N,N,N′,N″,N″-Pentamethyldiethylenetriamine (PMDETA) (330 µL, 0.27 mmol) and 3 mL anisole were added, sealed and purged with N_2 for 10 min. Then, the solution was transferred into the flask via syringe, the mixture was stirred under N_2 until the copper dissolved and formed complex with PMDETA. In a separate vial, PEGMA (**18**, 2 mL, 7 mmol), NHSMA (**13**, 0.142 g, 0.78 mmol) and anisole (3 mL) were added, sealed and purged under N_2 for 10 min. Then, this solution was transferred into the first flask. The reaction flask was immersed into the oil bath, allowed to stir at 40 ^{o}C. To the reaction

mixture which was stirring vigorously, liquid azido initiator (149 µL, 0.78 mmol, **17**) was added as quickly as possible. The reaction was stirred at 40 ^{o}C for 30 min. The starting material ratio was [PEGMA]:[NHSMA]:[PMDETA]:[Cu(I)Br]:[In], 9:1:2:1:1. After the polymerization was completed, anisole was evaporated. For purification, minimum amount of CH_2Cl_2 was added to crude mixture and precipitated by dropping into cold Et_2O. The mixture was kept in the fridge for more precipitation. After decantation of ether, the ppt was dissolved with MeOH: CH_2Cl_2 (1:10) mixture and passed through silica gel to remove copper catalyst. For further purification product was precipitated 2 times in cold Et_2O. Finally, purified product was dried under *vacuo*. ^{1}H NMR ($CDCl_3$, δ, ppm) 4.08 (bs), 4.19-4.13 (m, 19H), 3.65-3.54 (m, 19H), 3.37 (s, 30H), 3.27 (t, 2H), 2.80 (s, 4H). FTIR (cm^{-1}); 2097.01, 1726.02.

4.3.3.2. Synthesis of Copolymer 10.

Copper (I) bromide (0.028 g, 0.195 mmol) was weighed into a dry 10 mL reaction flask equipped with a stir-bar. The flask was sealed and purged with N_2 for 1 min. In a vial, N,N,N′,N″,N″-Pentamethyldiethylenetriamine (PMDETA) (81 µL, 0.390 mmol) and 4 mL anisole were added, sealed and purged with N_2 for 10 min. Then, the solution was transferred into the flask via syringe, the mixture was stirred under N_2 until the copper dissolved and formed complex with PMDETA. In a separate vial, PEGMA (**18**, 2 mL, 7.023 mmol), NHSMA (**13**, 0.142 g, 0.78 mmol) and anisole (4 mL) were added and purged with N_2 for 10 min. This solution was transferred into the first flask. Then, the reaction flask was immersed into the oil bath, allowed to stir at 85 ^{o}C and purged was closed. To the reaction mixture which was stirring vigorously, liquid azido initiator (37.5 µL, 0.195 mmol, **17**) was added as quickly as possible. The reaction was stirred at 85 ^{o}C for 30 min. The starting ratio was [PEGMA]:[NHSMA]:[PMDETA]:[Cu(I)Br]:[In], 36:4:2:1:1. After the polymerization was completed, anisole was evaporated. For purification, minimum amount of CH_2Cl_2 was added to crude mixture and precipitated by dropping into cold Et_2O. The mixture was kept in the fridge for more precipitation. After decantation of ether, the ppt was dissoled in MeOH: CH_2Cl_2 (1:10) mixture and passed through silica gel to remove copper catalyst. For further purification product was precipitated 2 times in cold Et_2O. Finally, purified product was dried under *vacuo*. ^{1}H

NMR ($CDCl_3$, δ, ppm) 4.08 (bs, 68H), 3.66-3.55 (m, 490H), 3.38 (s, 90H), 3.28 (t, 2H), 2.81 (s, 19H). FTIR (cm^{-1}); 2101.49, 1727.55.

4.3.3.3. Synthesis of Copolymer 12.

Copper (I) bromide (0.0223 g, 0.156 mmol) was weighed into a dry 10 mL reaction flask equipped with a stir-bar. The flask was sealed and purged with N_2 for 1 min. In a vial, N,N,N′,N″,N″-Pentamethyldiethylenetriamine (PMDETA) (65 µL, 0.312 mmol) and 6 mL anisole were added, sealed and purged with N_2 for 10 min. Then, the solution was transferred into the flask via syringe, the mixture was stirred under N_2 until the copper dissolved and formed complex with PMDETA. In a separate vial, PEGMA (**18**, 2 mL, 7.023 mmol), NHSMA (**13**, 0.142 g, 0.78 mmol) and anisole (6 mL) were added and purged under N_2 for 10 min. Then, this solution was transferred into the first flask. The reaction flask was immersed into the oil bath, allowed to stir at 85 ^oC. To the reaction mixture which was stirring vigorously, liquid azido initiator (30 µL, 0.156 mmol, **17**) was added as quickly as possible. The reaction was stirred at 85 ^oC for 30 min. The starting material was [PEGMA]:[NHSMA]:[PMDETA]:[Cu(I)Br]:[In], 45:5:2:1:1. After the polymerization was completed, anisole was evaporated. For purification, minimum amount of CH_2Cl_2 was added to crude mixture and precipitated by dropping into cold Et_2O. The mixture was kept in the fridge for more precipitation. After decantation of ether, the ppt was dissoled in MeOH: CH_2Cl_2 (1:10) mixture and passed through silica gel to remove copper catalyst. For further purification product was precipitated 2 times in cold Et_2O. Finally, purified product was dried under *vacuo*. ^1H NMR ($CDCl_3$, δ, ppm) 4.09 (bs, 45H), 3.66-3.55 (m, 349H), 3.38 (s, 64H), 3.28 (t, 2H), 2.81 (s, 13H). FTIR (cm^{-1}); 2098.27, 1727.80.

4.4. Synthesis of Polymer-Dendron Conjugates

4.4.1. Synthesis of Conjugate 1

In a 25 mL reaction flask, Cu(I)Br (0.0074 mg, 0.0516 mmol), PMDETA (11 µL, 0.0516 mmol) were dissolved in dry THF (2 mL) and purged with N_2. Dendron (**10**, 0.157 mg, 0.1031 mmol) and copolymer **P4** (0.4 mg, 0.0688 mmol) were taken into a vial,

dissolved in dry THF (5 mL) and purged with N_2. Then, the mixture was transferred into the reaction flask and stirred at 40 ^oC for 96 h. The crude product was dissolved in more THF and filtered through Al_2O_3 column to remove copper salts. The solvent was concentrated under *vacuo* and the desired product was precipitated 3 times in cold Et_2O. Precipitate was dissolved in THF and dried under vacuo yielding 55% of product. ^1H NMR ($CDCl_3$, δ, ppm) 7.69 (s, 1H), 5.83-5.73 (m, 8H), 5.23 (s, 2H), 5.04-4.96 (m, 16H), 4.34 (t, 2H, J = 8 Hz), 4.26-4.15 (m, 38H), 4.07 (bs, 32H), 3.64-3.54 (m, 279H), 3.36 (s, 51H), 2.80 (s, 3H). FTIR (cm^{-1}); 1728.69, 1641.53.

4.4.2. Synthesis of Conjugate 2

In a 25 mL reaction flask, Cu(I)Br (0.006 mg, 0.043 mmol), PMDETA (9 μL, 0.043 mmol) were dissolved in dry THF (2 mL) and purged with N_2. Dendron (**10**, 0.131 mg, 0.086 mmol) and copolymer **P12** (0.4 mg, 0.057 mmol) were taken into a vial, dissolved in dry THF (5 mL) and purged with N_2. Then, the mixture was transferred into the reaction flask and stirred at 40 ^oC for 96 h. The crude product was dissolved in more THF and filtered through Al_2O_3 column to remove copper salts. The solvent was concentrated under *vacuo* and the desired product was precipitated 3 times in cold Et_2O. Precipitate was dissolved in THF and dried under vacuo yielding 58% of product. ^1H NMR ($CDCl_3$, δ, ppm) 7.68 (s, 1H), 5.84-5.74 (m, 8H), 5.25 (s, 2H), 5.06-4.98 (m, 16H), 4.35 (t, 3H, J = 8 Hz), 4.28-4.09 (m, 155H), 3.65-3.55 (m, 863H) 3.38 (s, 158H), 2.81 (s, 33H), 2.43-2.33 (m, 42H). FTIR (cm^{-1}); 1728.30, 1642.11.

4.4.3. Synthesis of Conjugate 3

In a 25 mL reaction flask, Cu(I)Br (0.0044 mg, 0.0306 mmol), PMDETA (6.4 μL, 0.0306 mmol) were dissolved in dry THF (2 mL) and purged with N_2. Dendron (**10**, 0.093 mg, 0.0612 mmol) and copolymer **P10** (0.4 mg, 0.0408 mmol) were taken into a vial, dissolved in dry THF (5 mL) and purged with N_2. Then, the mixture was transferred into the RBF and stirred at 40 ^oC for 96 h. The crude product was dissolved in more THF and filtered through Al_2O_3 column to remove copper salts. The solvent was concentrated under *vacuo* and the desired product was precipitated 3 times in cold Et_2O. Precipitate was

dissolved in THF and dried under vacuo yielding 62% of product. ^{1}H NMR ($CDCl_3$, δ, ppm) 7.63 (s, 1H), 5.77-5.68 (m, 8H), 5.18 (s, 2H), 5.00-4.92 (m, 16H), 4.32-4.27 (m, 3H), 4.13-4.02 (m, 162H), 3.59-3-49 (m, 1034 H), 3.31 (s, 188H), 2.75 (s, 30H), 2.36-2.27 (m, 41H). FTIR (cm^{-1}); 1728.11, 1641.60.

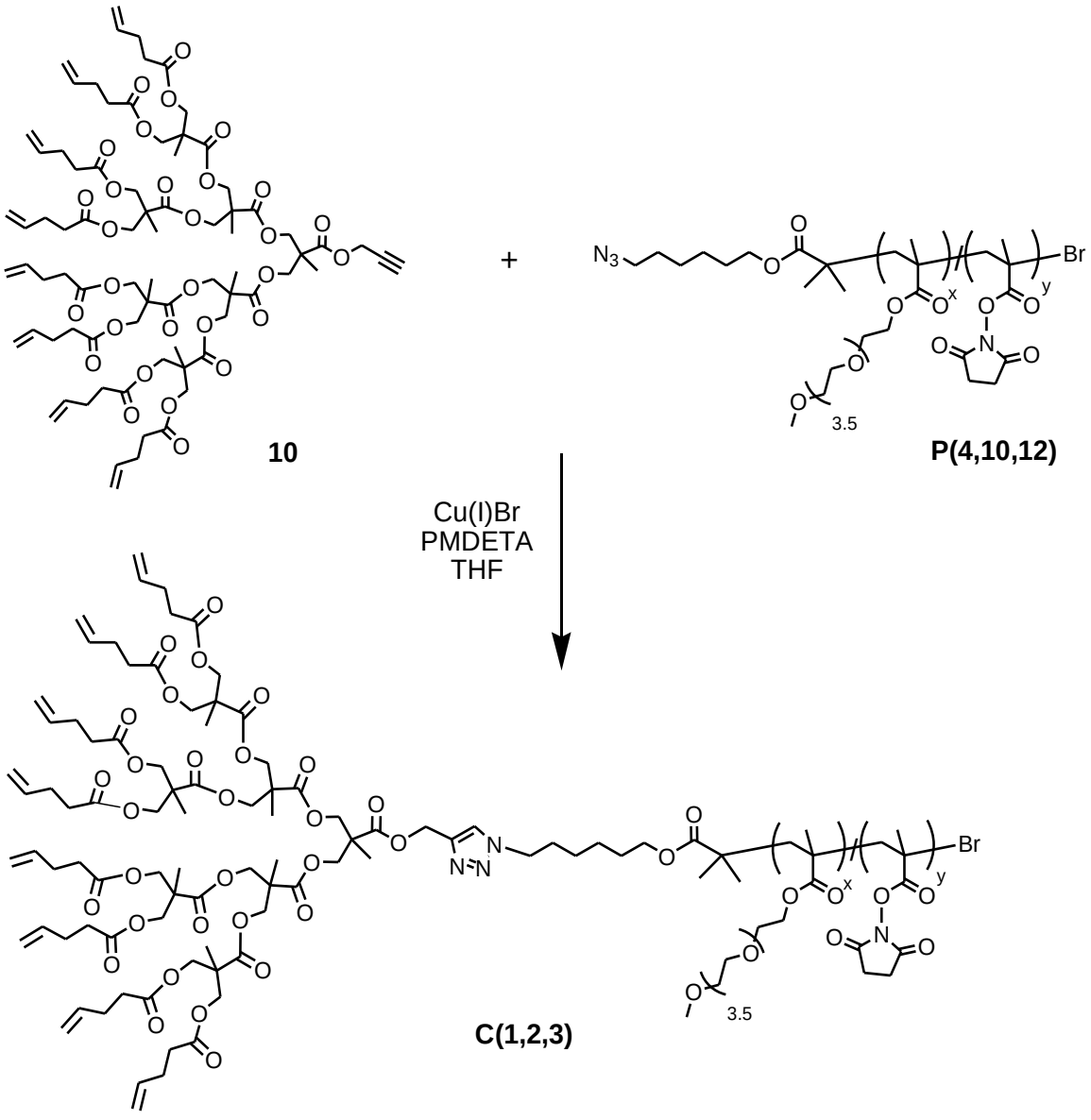

Figure 4.8. Synthesis of polymer-dendron conjugate.

4.5. Micelle Formation from Polymer-Dendron Conjugates and Measurements

Critical micelle concentrations for three different copolymers were determined at neutral pH by using fluorescent probe technique. Pyrene was used as the probe for the micellar encapsulation. It exhibited number of characteristic intensity bands between 300-360 in the fluorescence spectrum. So, data was collected at 300-360 nm range using 5 nm width. To study the micelle formations of each conjugates in an aqueous environment, the conjugates were dissolved in an organic solvent such as tetrahydrofuran (THF). Then, conjugates having concentrations ranging from 10^{-5} M to 10^{-9} M were transferred into vials. To evaporate the organic solvent, all vials were put in desicator under high *vacuo* for 2 hours. Then, pyrene stock solution (10 μL, $1.8x10^{-4}$ M) in acetone was added to all vials, and again they were placed in desicator to remove acetone. Blank pyrene sample without copolymer for each set of measurements was also prepared as a control and fluoresence data was checked to be sure that all acetone solution was evaporated. Afterward, all samples were dissolved in 3 mL MilliQ water (pH=7), and micelle formations were triggered with sonication for 1 h at 70 ^{o}C.

4.5.1. Fluorescence Measurements

Fluorescence signal arising from pyrene in micellar solutions having different concentrations were measured by fluorescence spectrometer. From the excitation spectra of the micelles, CMC graphs were drawn and CMC values were calculated from these graphs.

Table 4.1. CMC values of conjugate C1, C2 and C3.

No	Conjugate	CMC (M)
1	C1	3.31×10^{-7} M
2	C2	5.06×10^{-7} M
3	C3	4.31×10^{-7} M

4.6. Core Crosslinking Experiments

Stock solutions were prepared from polymer-dendron conjugate, tetrathiol and photoinitiator as 1 mg in 1 mL THF. Polymer – dendron conjugate ($3x10^{-5}$ mmol) from stock solution was addded into a vial, the solvent was evaporated under *vacuo* at least 3 hour. Then, into the vial, pentaerythritol tetrakis(3-mercaptopropionate) (tetrathiol, 30 µL, $6x10^{-5}$ mmol) and 2,2-Dimethoxy-2-phenylacetophenone (photoinitiator, DMPA, 7 µL, $3x10^{-5}$ mmol) transferred. For core crosslinked pyrene loaded micelles, pyrene (10 µL, $1.8x10^{-4}$ M) was added in the vial, too. The solvent was evaporated, again. 3 mL of Milli-Q water was added, the solution was sonicated for 1 h at 70 ^{o}C. It was left for overnigth. Then, the resulting solution was crosslinkedby applying UV irradiation (365 nm) for 30 min.

4.7. Dynamic Light Scattering (DLS) Measurements

In order to measure the effective diameter and the size distribution of micelles, dynamic ligth scattering instrument was used. The size distribution was determined using number vs diameter graphs which show the number of micelles at certain diameter. Four different micelles, namely empty non-crosslinked, pyrene loaded non-crosslinked, empty crosslinked and pyrene loaded crosslinked micelles, were prepared from the three conjugates by using using Milli-Q water . Each micelle concentration was 10^{-5} M which was higher than the respective CMC values. They were formed using sonication method as described above.

Table 4.2. Micellar sizes obtained from DLS measurements.

No	Copolymer	Non-crosslinked empty	Non-crosslinked pyrene loaded	Crosslinked empty	Crosslinked pyrene loaded
1	C1	77±8 nm	53±4 nm	29±5 nm	29±6 nm
2	C2	64±15 nm	58±4 nm	25±4 nm	25±3 nm
3	C3	61±6 nm	59±3 nm	25±5 nm	23±5 nm

The DLS measurements were also done in THF in order to check the stability of non-crosslinked and crosslinked micelles. For this study, to 1 mL micelle solution in water, 0.1 mL THF was as added and sonicated. Then, the size was monitored. It was seen that micelle size became bigger due to swelling. So, THF volume was optimized, and size changes were observed for crosslinked micelle At a certain THF volume (0.7 mL), the micelle stopped the swelling.

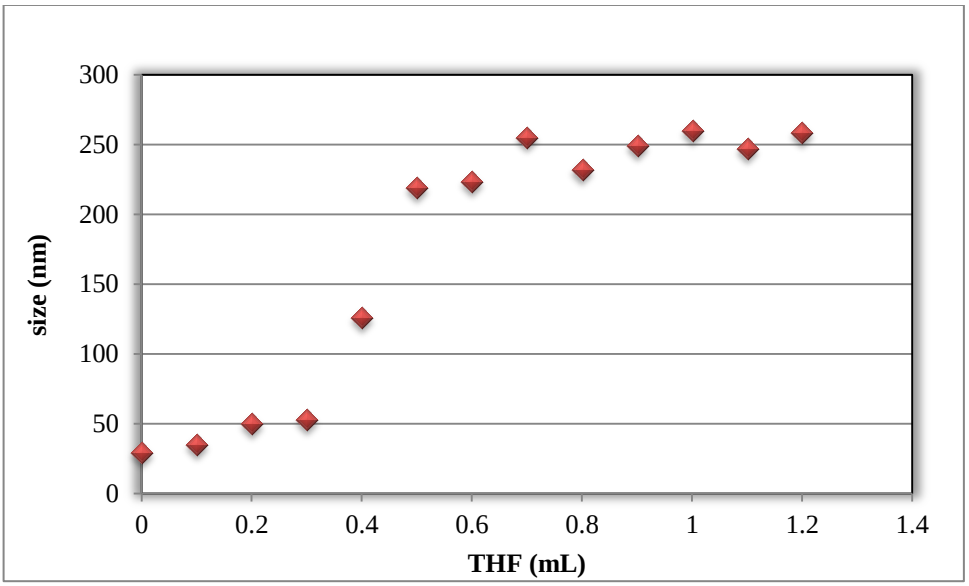

Figure 4.9. Swelling of crosslinked micelles with THF addition.

5. CONCLUSION

In this thesis project, we synthesized core crosslinked polymeric micelles from amphiphilic linear polymer-dendron conjugates in a modular fashion using [3+2] Huisgen type ‘click’ chemistry. The hydrophobic portion is biodegradable polyester dondron which contains alkyne unit at the focal point and alkene units at the periphery. Poly (PEGMA)-based azide group bearing copolymer constitutes the hydrophilic portion and the copolymer contains activated carboxylic acid units on the backbone. By changing the length of hydrophilic part, different copolymers were obtained and used for furher conjugation with dendron. These conjugates were self-assembled in aqueous media to form micellar structures. Available functional groups of dendrons on the hydrophobic core were crosslinked with a tetrathiol successfully via thiol-ene chemistry in order to get stable micellar constructs. Pyrene was used as a probe and was loaded successfully into both core crosslinked and noncrosslinked micelles. We have focused on the size and stability of these micelles using fluorescence and dynamic light scattering spectroscopies.

From the fluorescence studies, critical micelle concentrations of each micellar structures assembled from three different polymer-dendron conjugates were calculated. It can be seen that, as increasing the chain length of polymer part, CMC values do not significantly differ from each other. Therefore, the stability of micelles does not change while playing the size of hydrophilic segment of polymer-dendron conjugates. In addition, the size and stability of both noncrosslinked and crosslinked micelles were studied using DLS. Four different micelles were prepared from the three conjugates, seperately. They were classified according to empty non crosslinked, pyrene loaded non crosslinked, empty crosslinked and pyrene loaded crosslinked micelles. DLS measurements revealed that after applying core crosslinking, the sizes of micelles reduced. In addition, pyrene loaded non-crosslinked micelles had smaller sizes as compared to empty ones. The reason may be the hydrophobic interaction between pyrene and G3 dendron. However, the decrease was smaller in the case of crosslinked micelles as expected. The size distribution of micelles obtained from the three conjugate did not change considerably also, as in the case of CMC.

APPENDIX A: SPECTROSCOPY DATA

^{1}H NMR, FT-IR spectra and GPC data of the synthesized products are included.

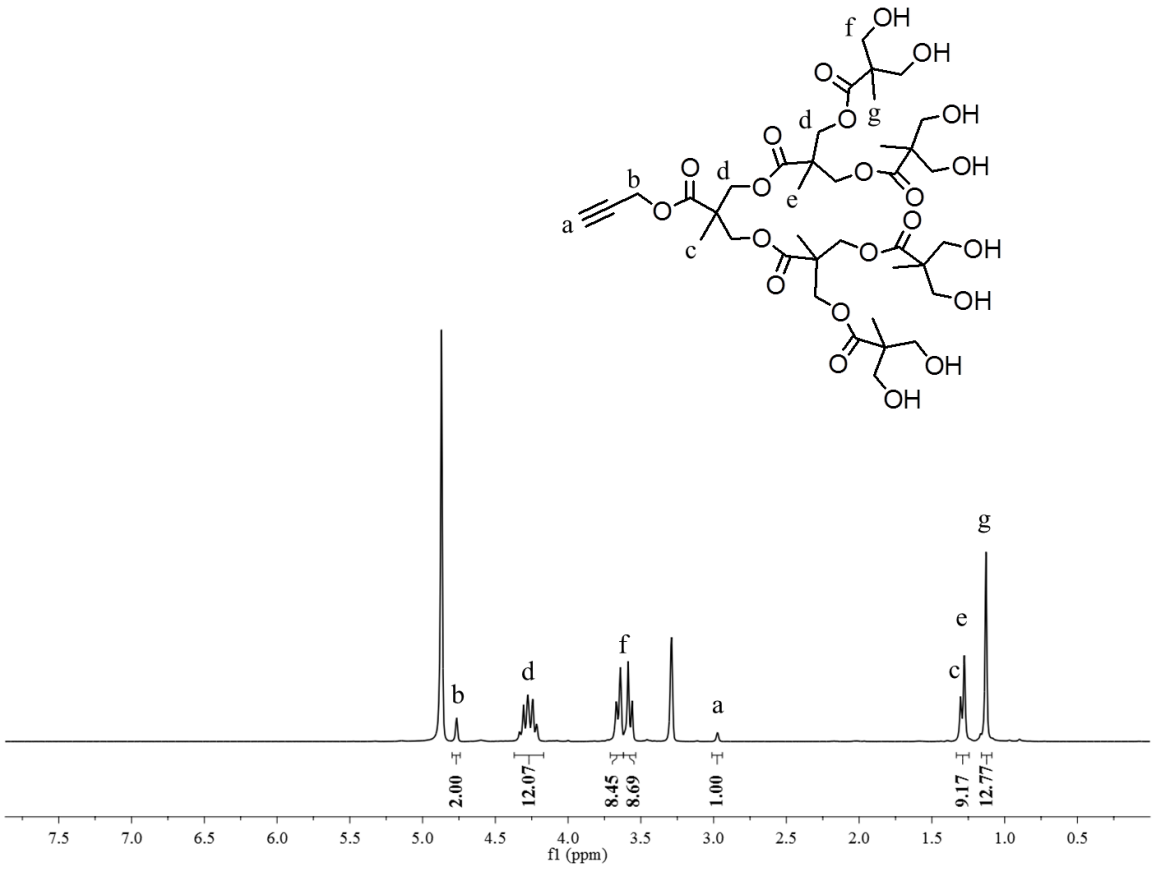

Figure A.1. ^{1}H NMR spectrum of product 8.

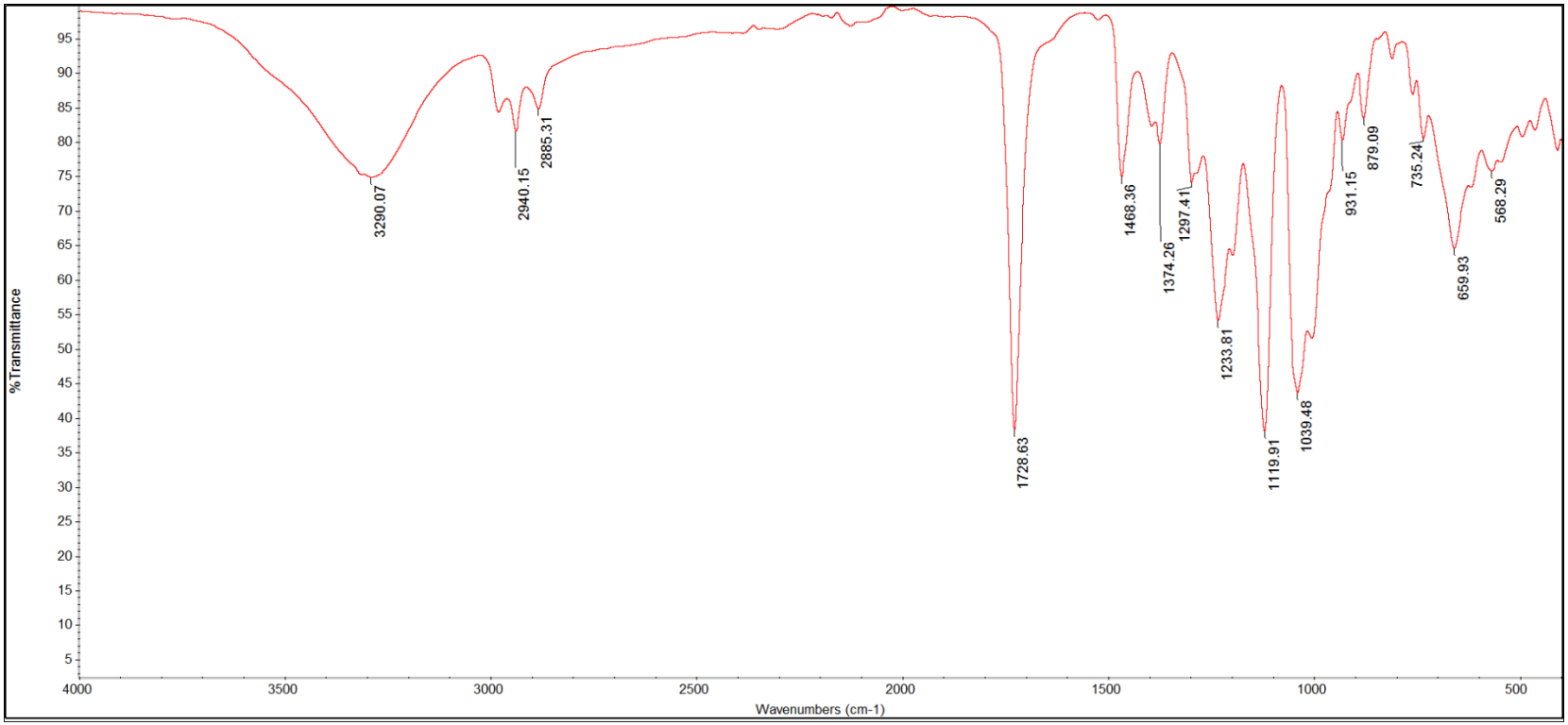

Figure A.2. FT-IR spectrum of 8.

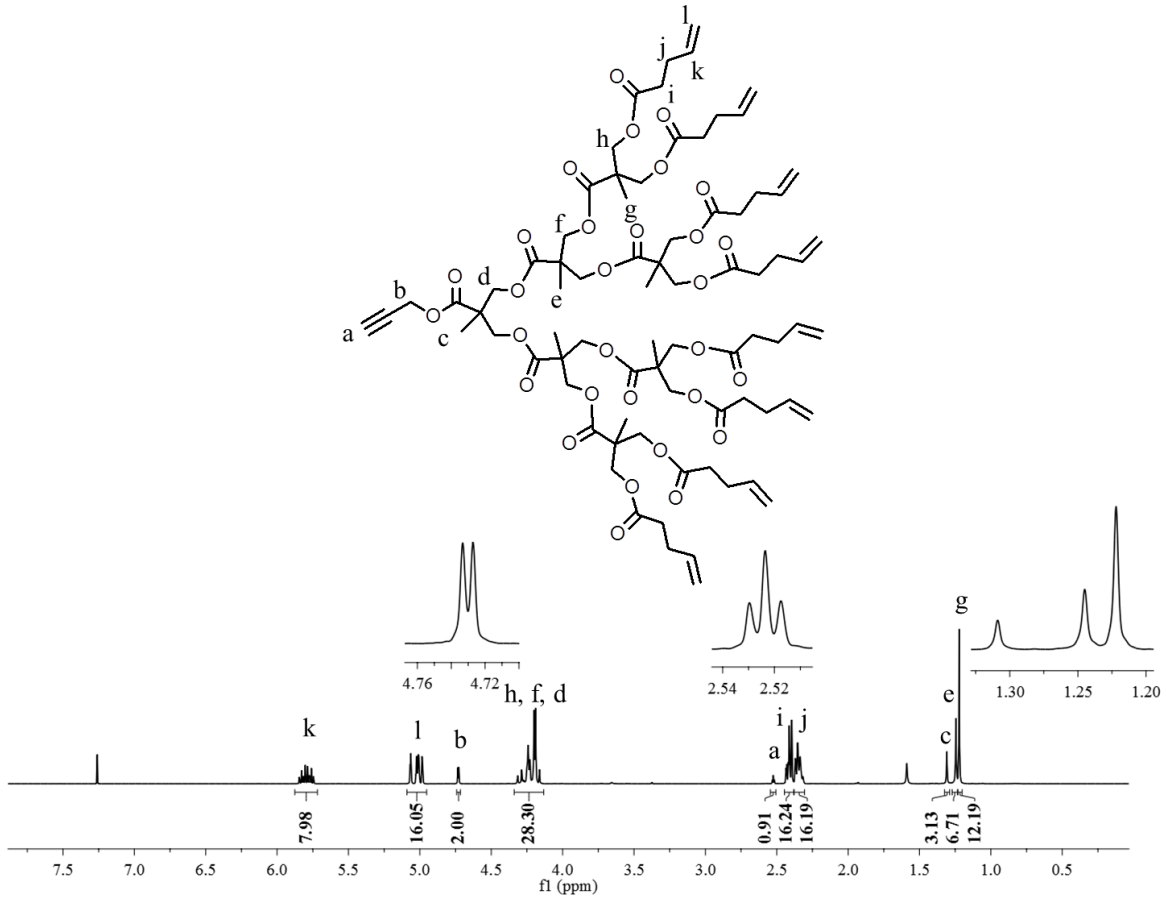

Figure A.3. ^{1}H NMR spectrum of product 10.

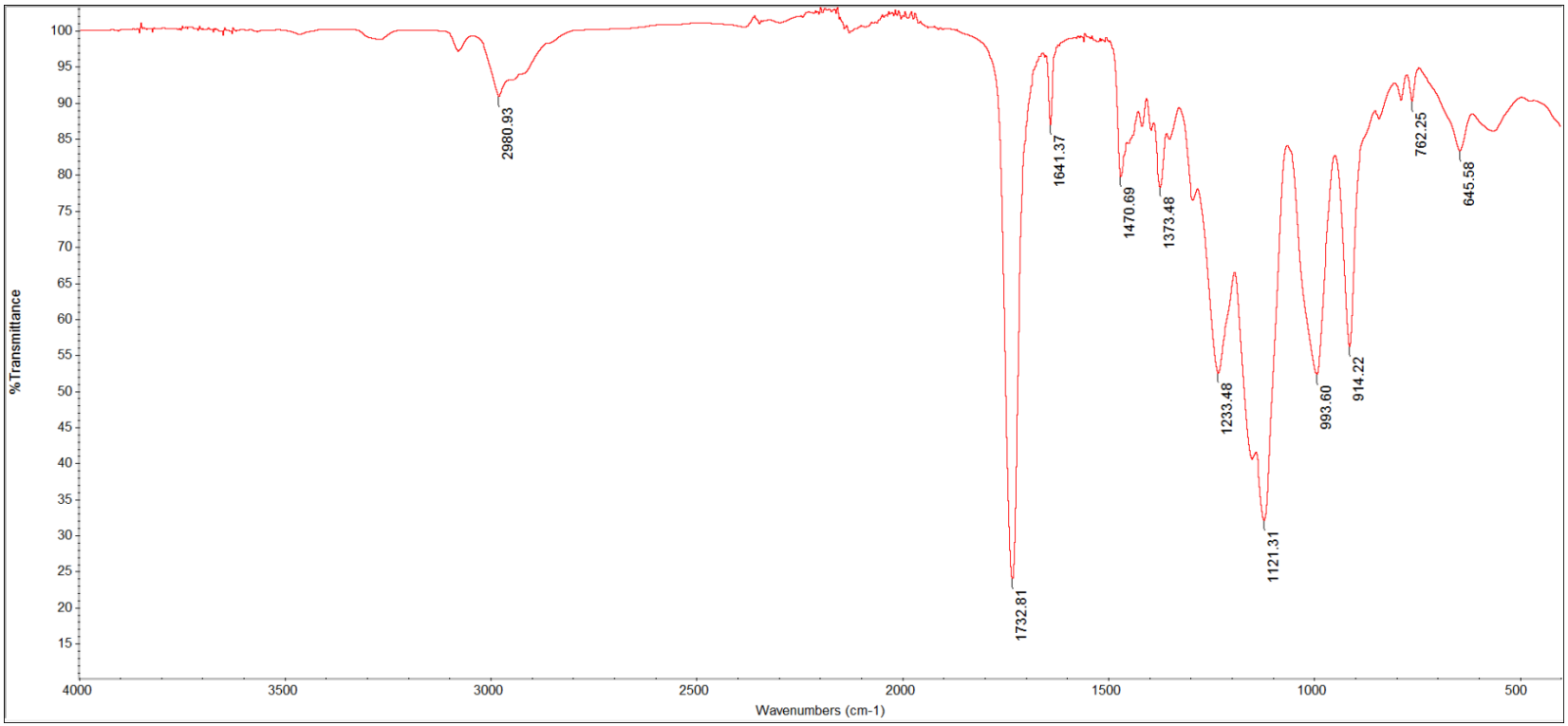

Figure A.4. FT-IR spectrum of 10.

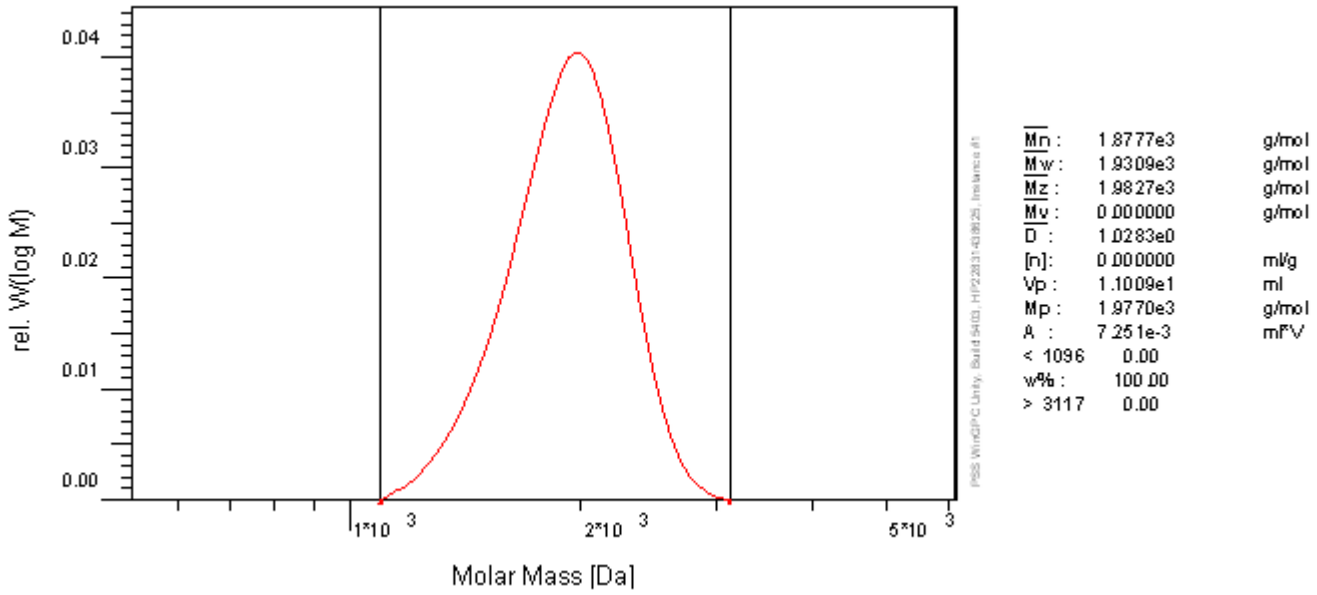

Figure A.5. GPC result of compund 10.

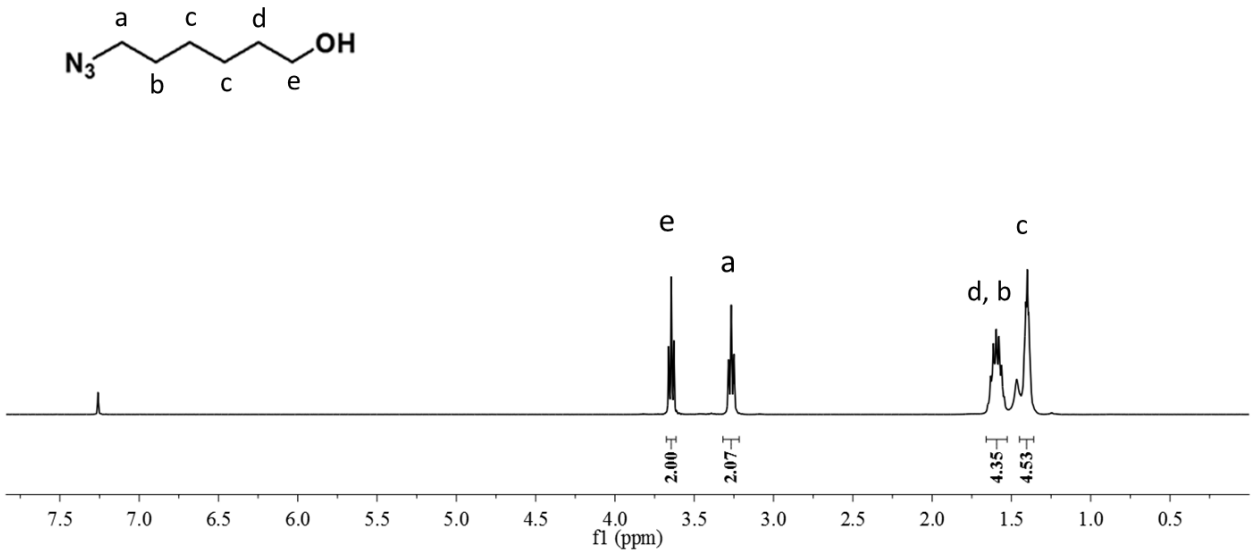

Figure A.6. ^{1}H NMR spectrum of 15.

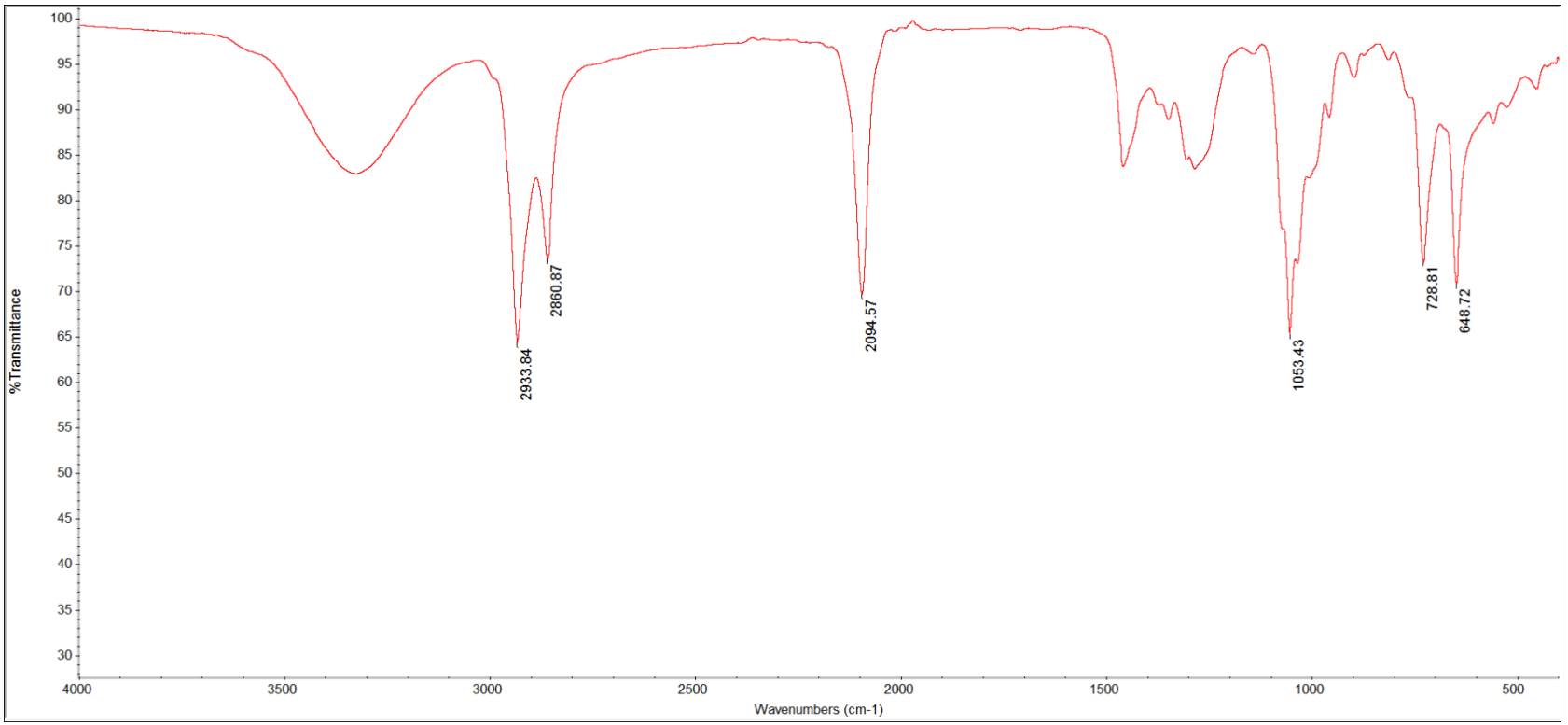

Figure A.7. FT-IR spectrum of 15.

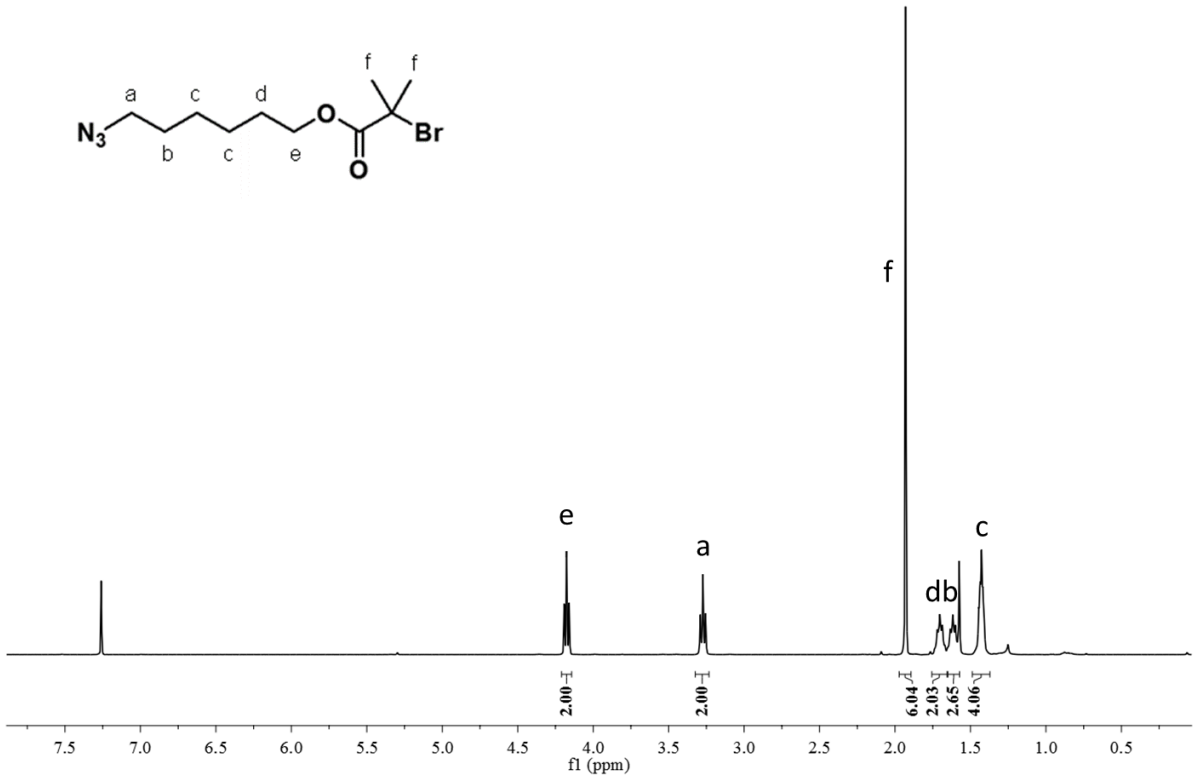

Figure A.8. ^{1}H NMR spectrum of 17.

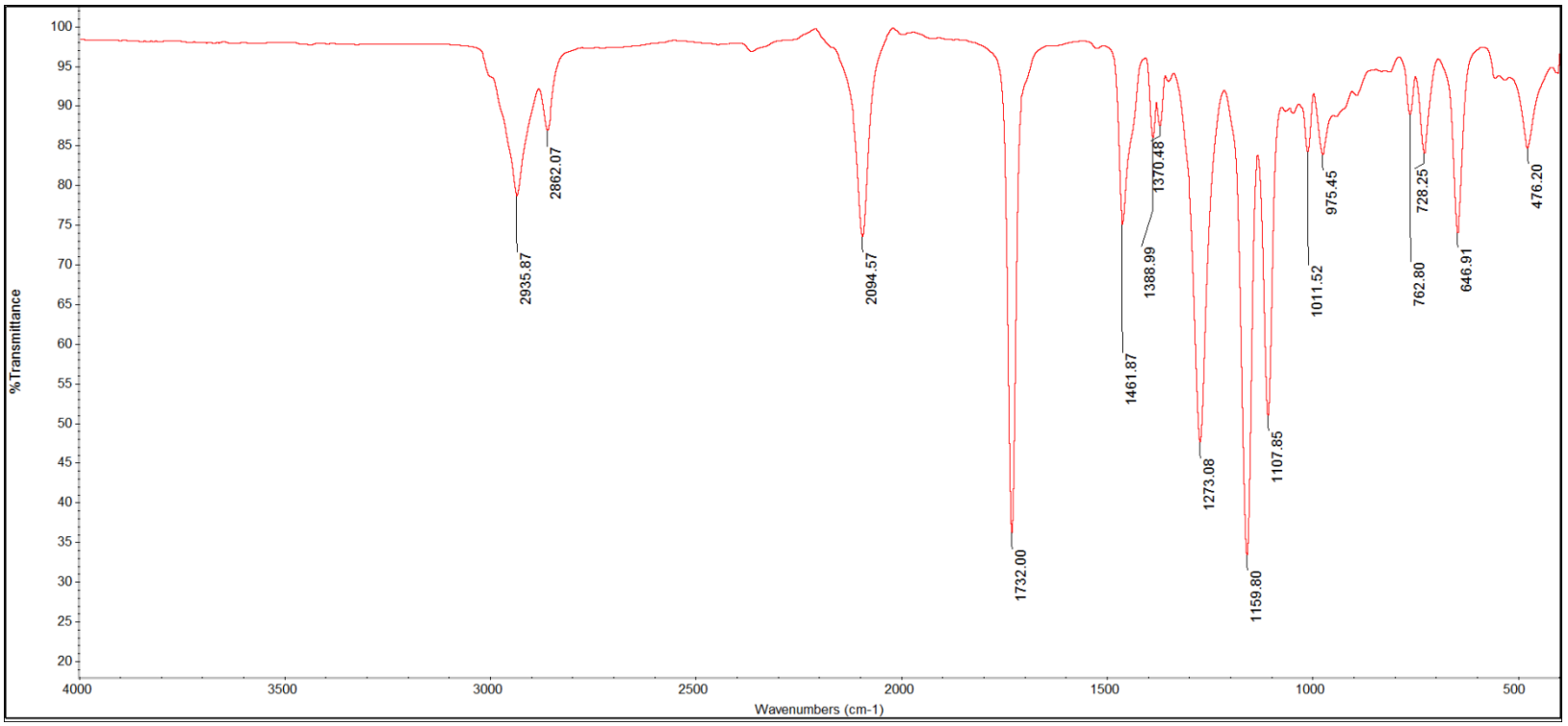

Figure A.9. FT-IR spectrum of 17.

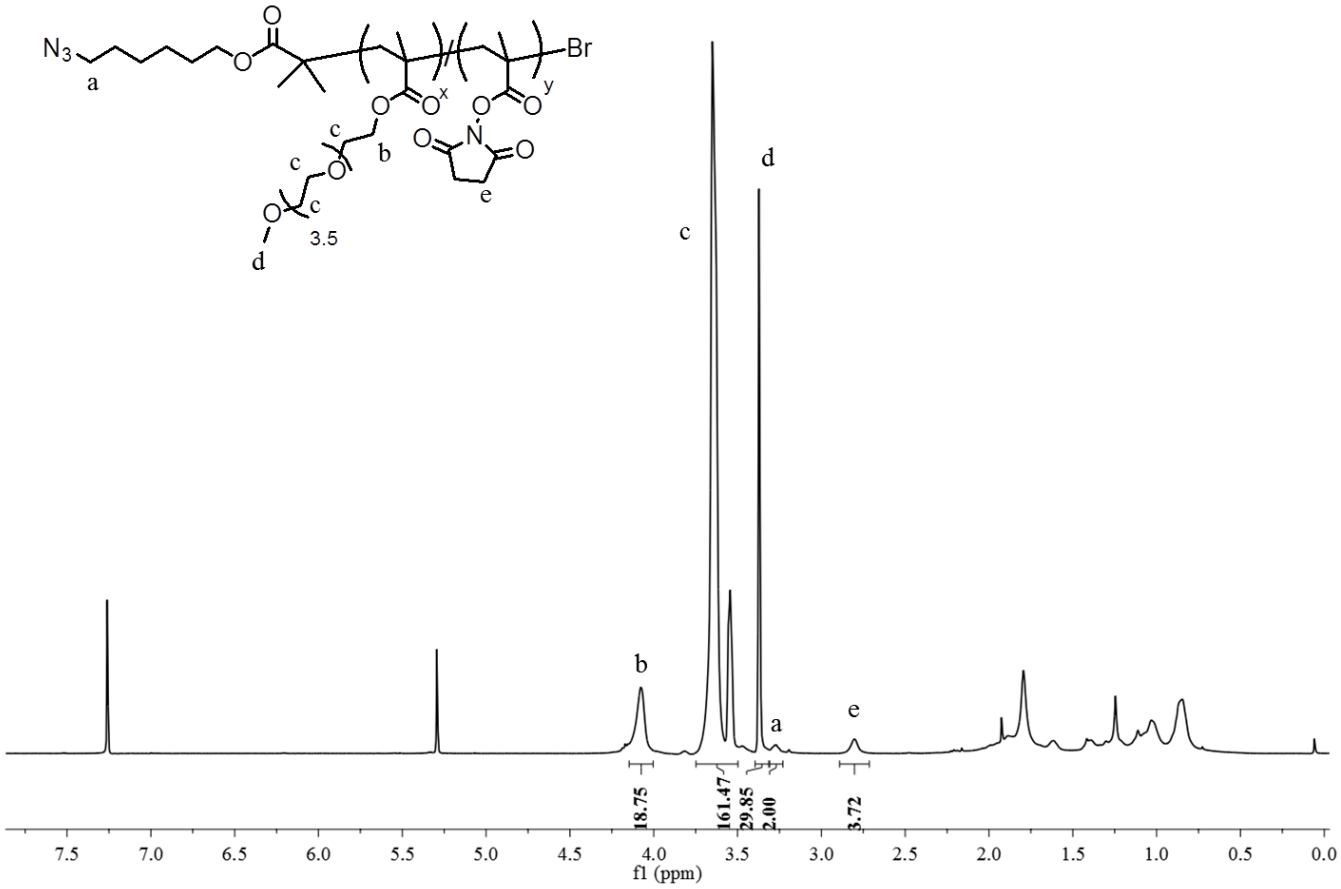

Figure A.10. ^{1}H NMR spectrum of P4 polymer (Mwt=3.3 kDa).

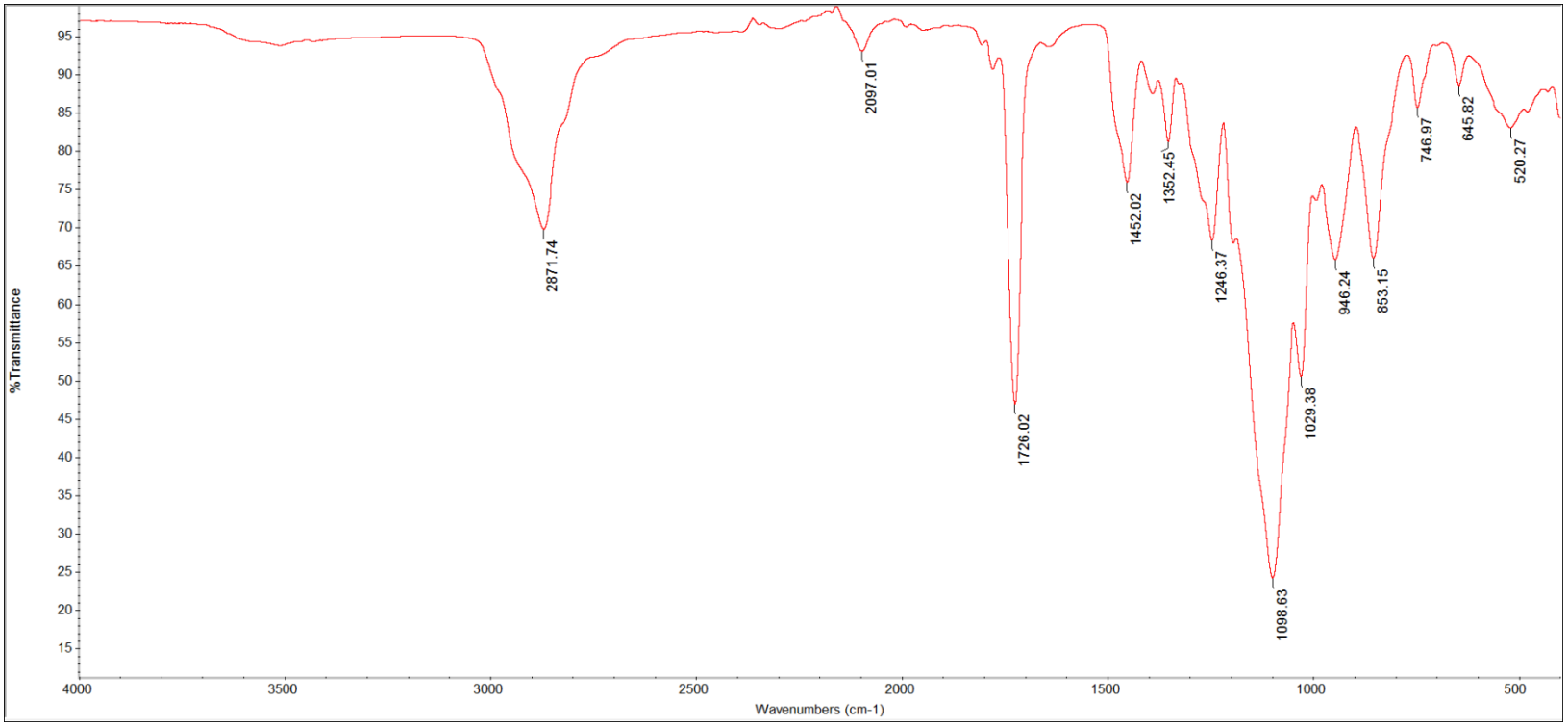

Figure A.11. FT-IR spectrum of P4.

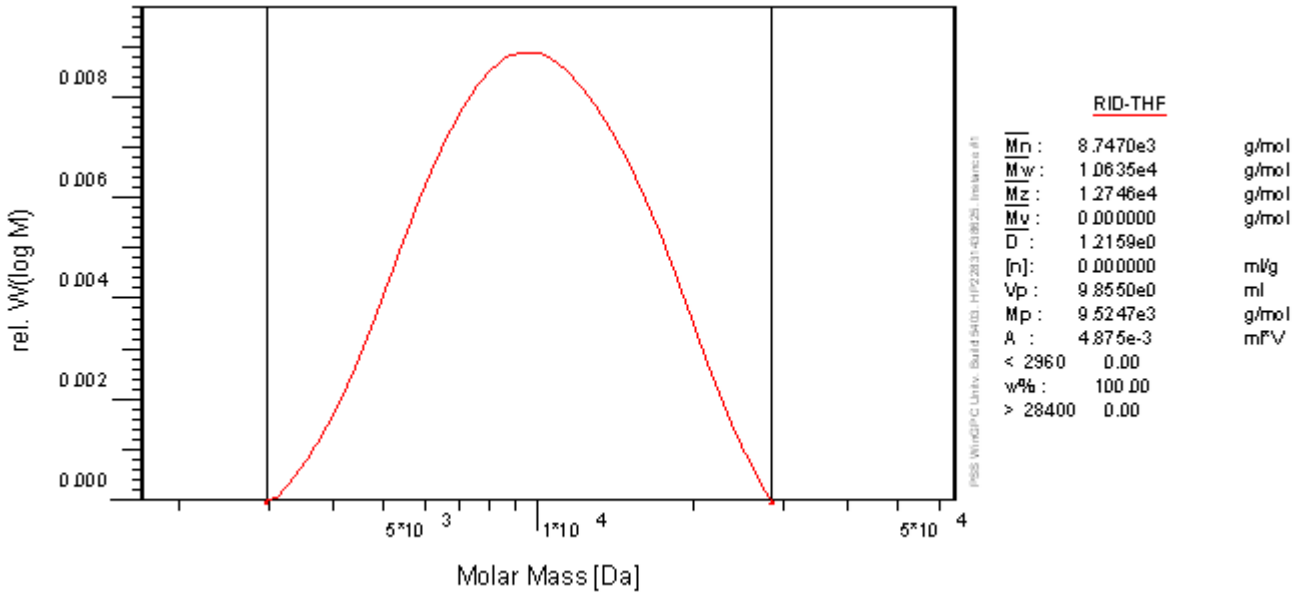

Figure A.12. GPC result of P4.

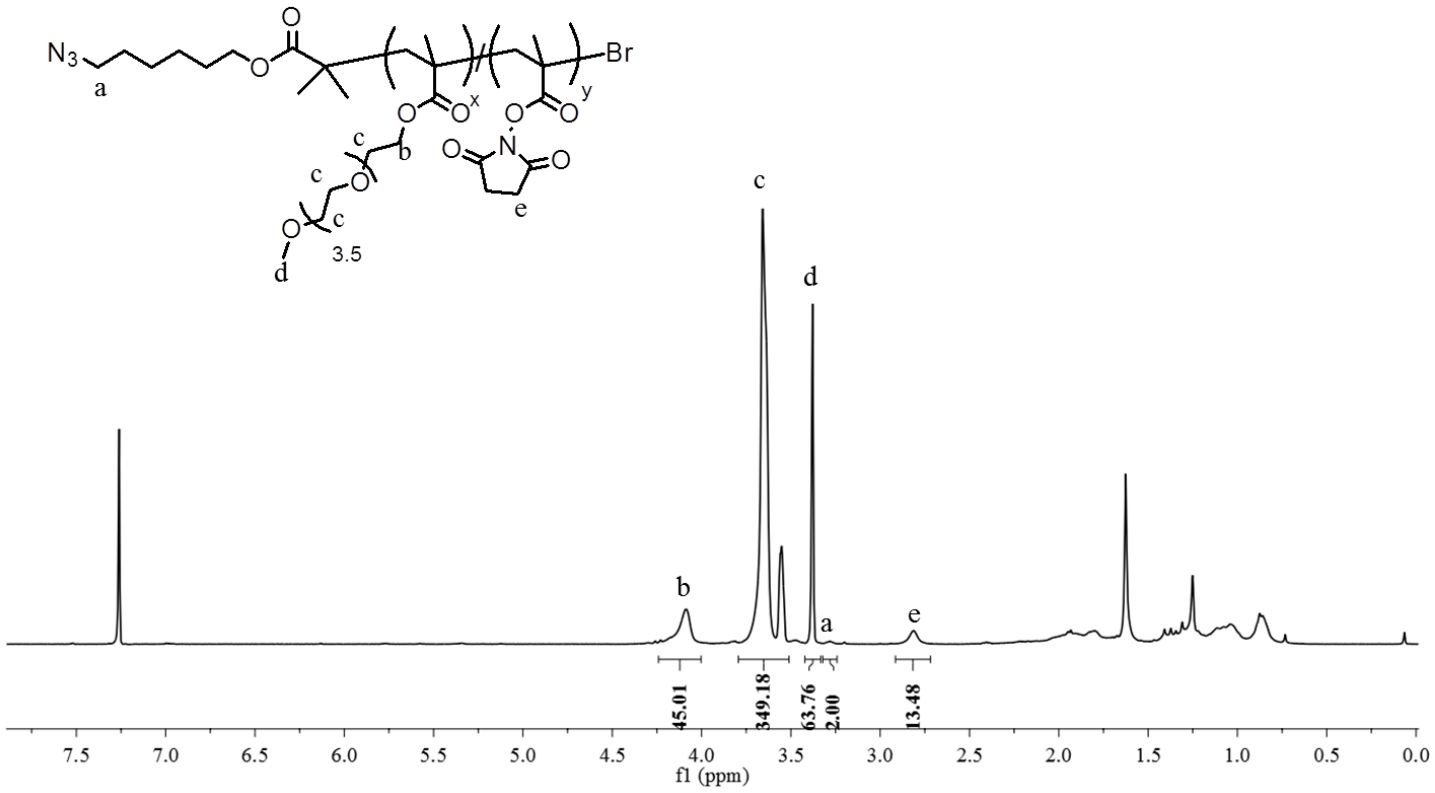

Figure A.13. ^{1}H NMR spectrum of P12 polymer (Mwt=7 kDa).

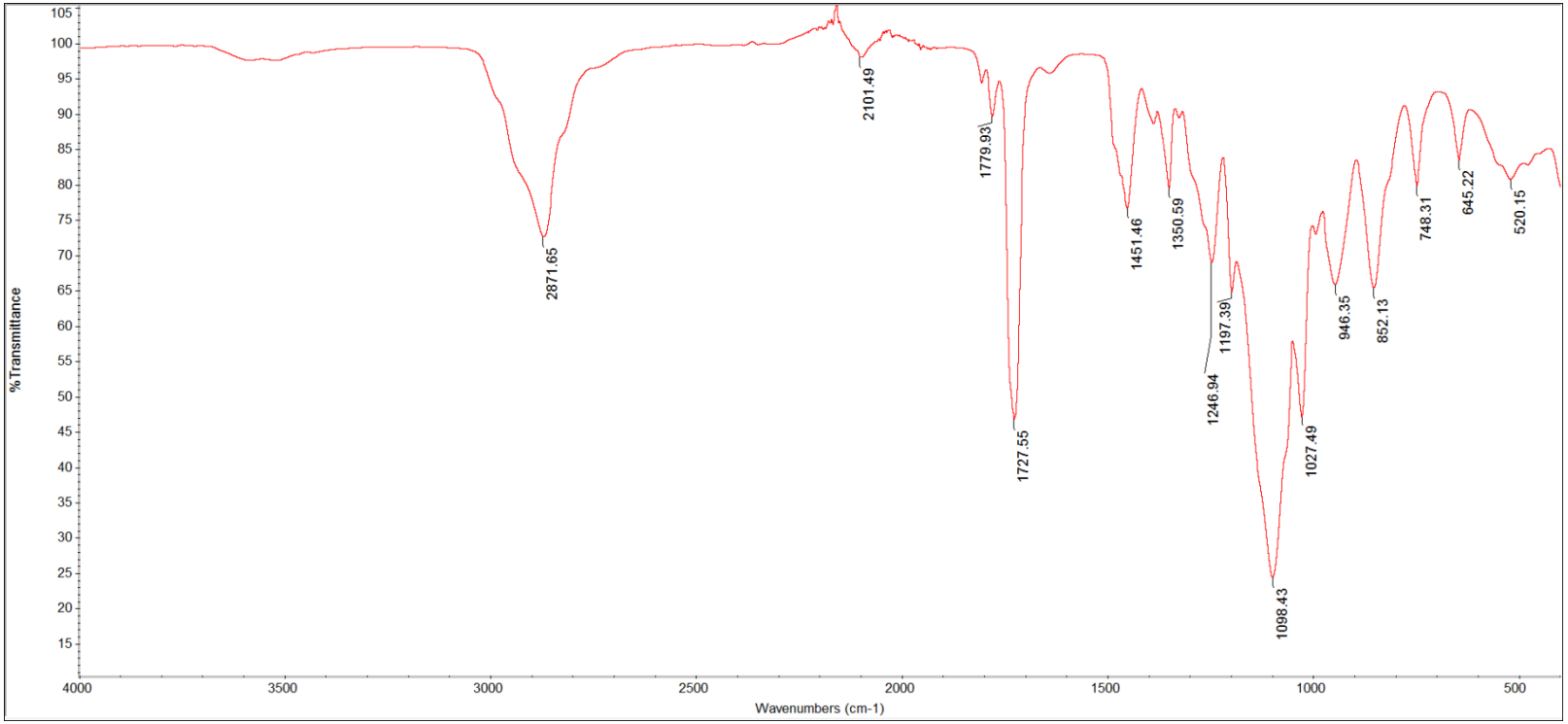

Figure A.14. FT-IR spectrum of P12.

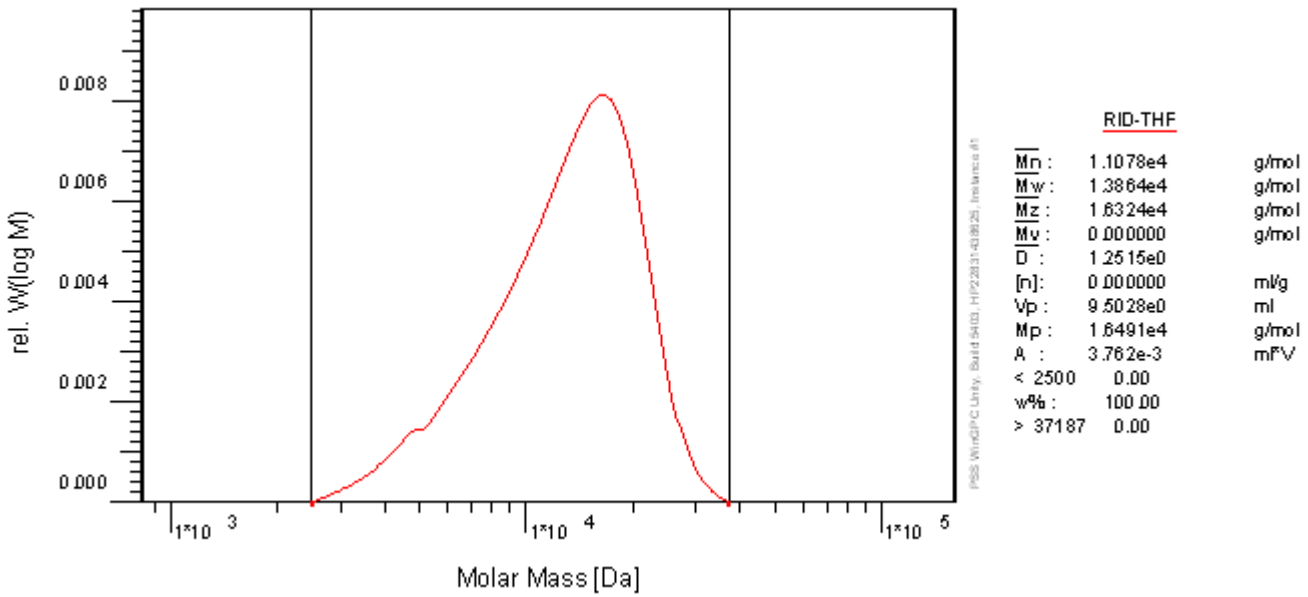

Figure A.15. GPC result of P12.

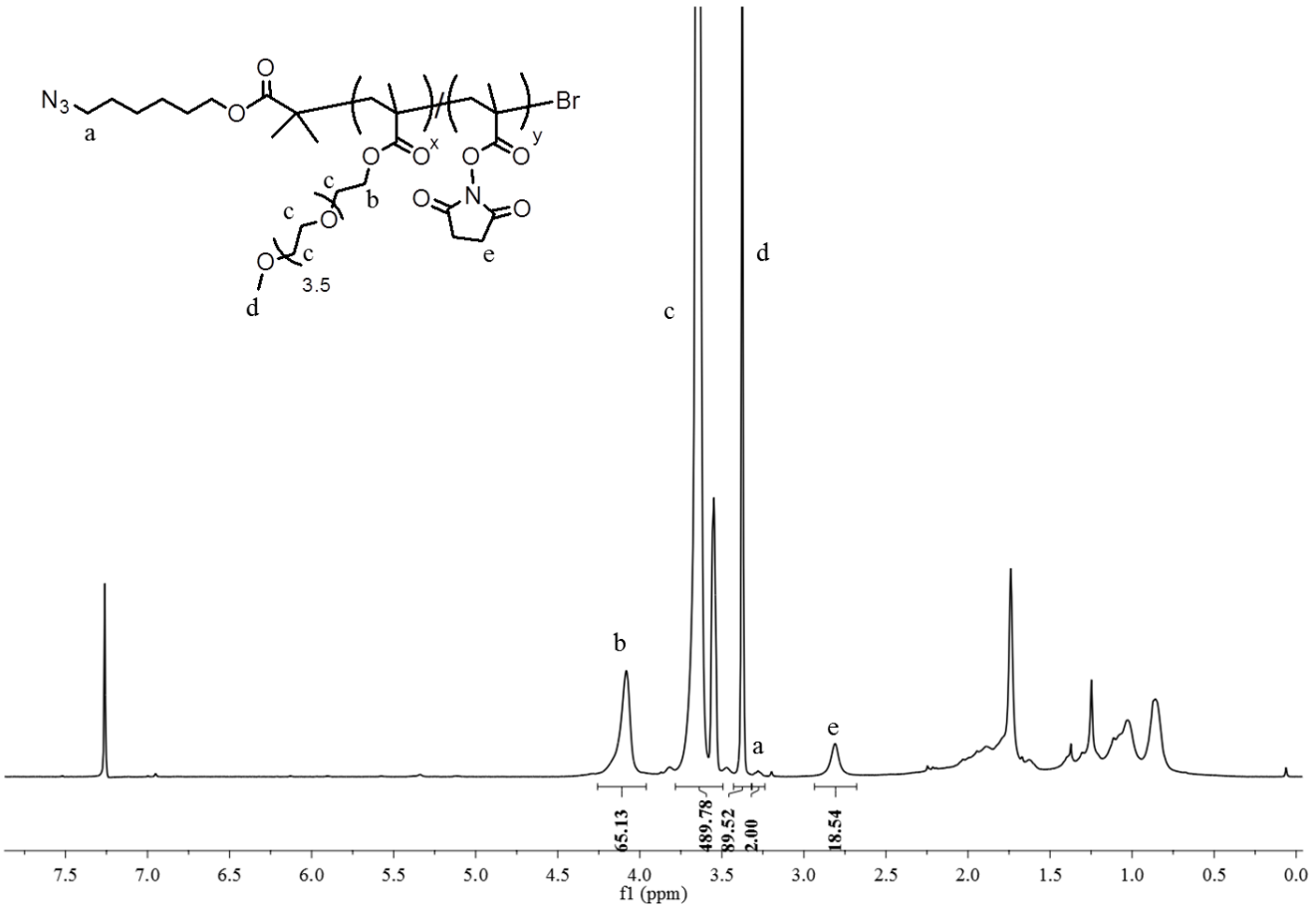

Figure A.16. ^{1}H NMR spectrum of P10 polymer (Mwt=10 kDa).

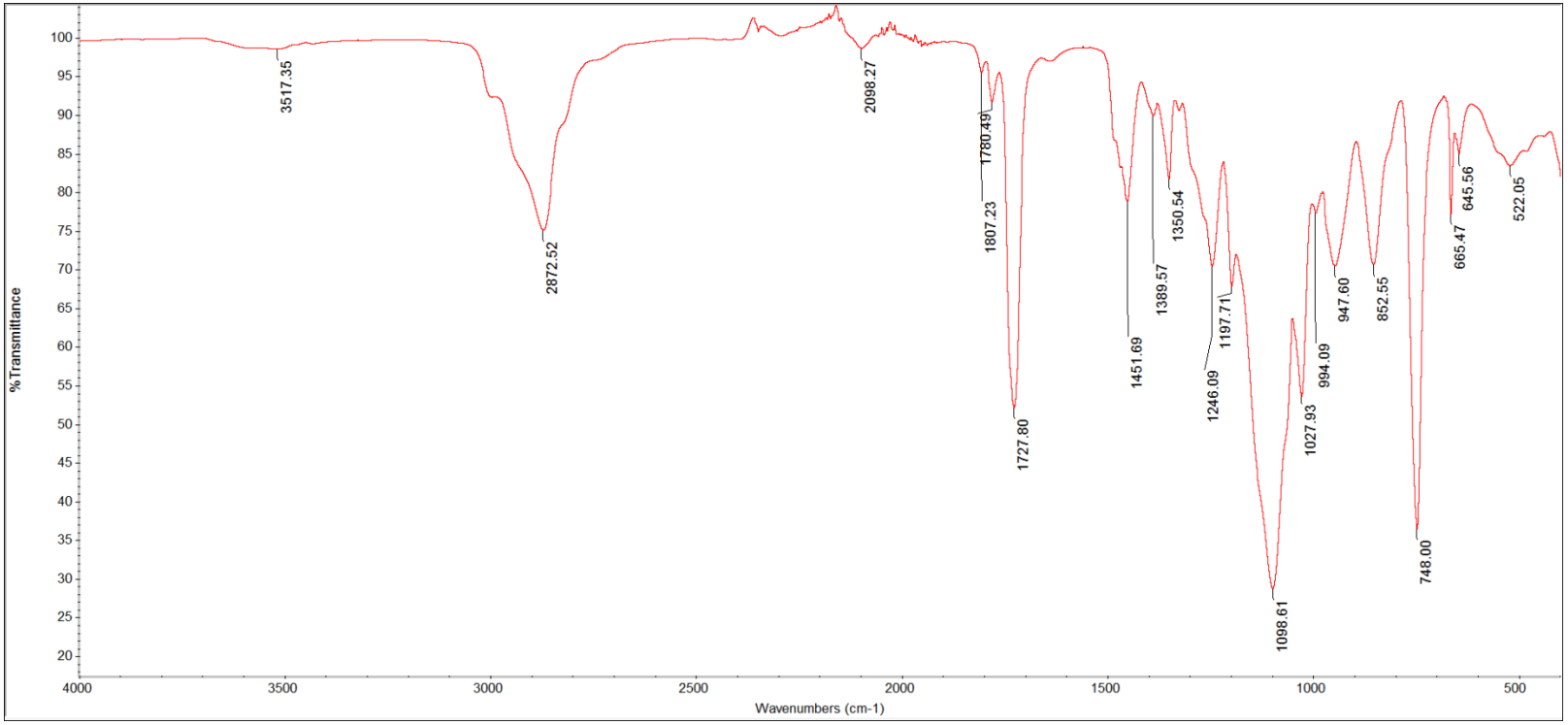

Figure A.17. FT-IR spectrum of P10.

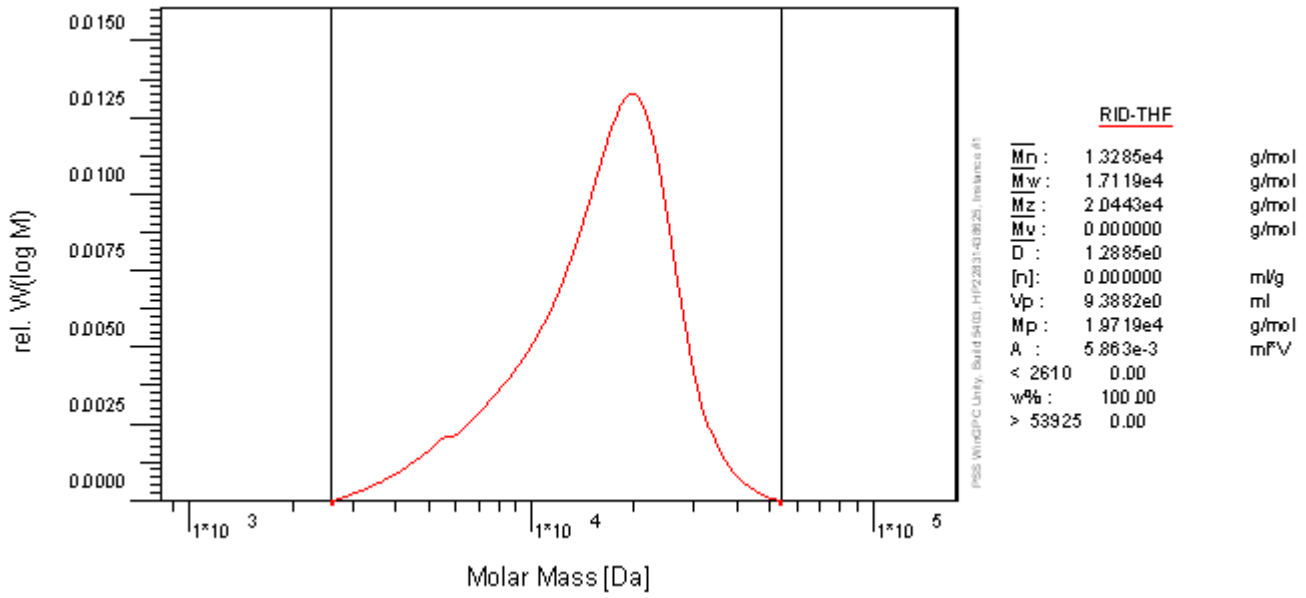

Figure A.18. GPC result of P10.

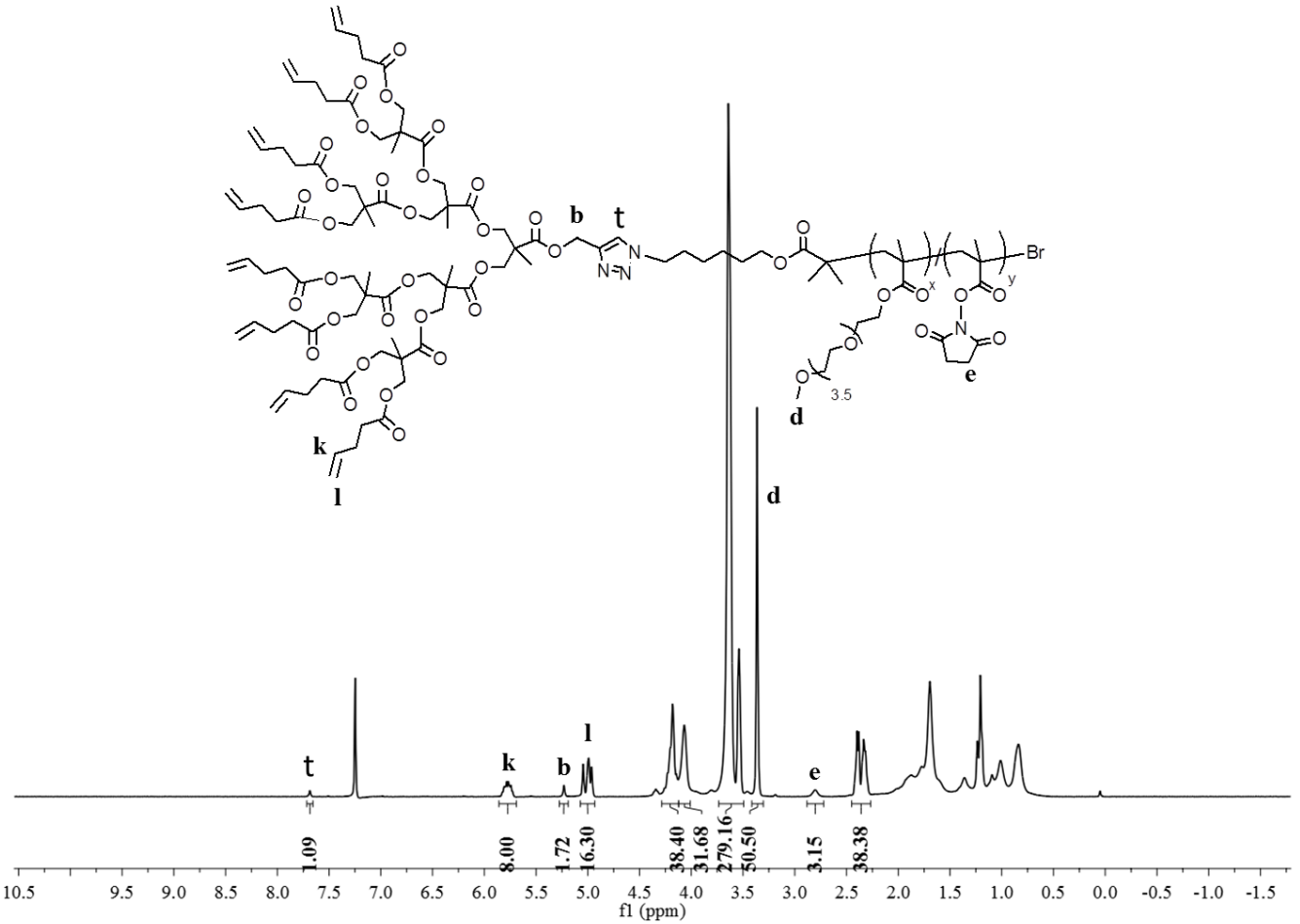

Figure A.19. ^{1}H NMR spectrum of C1.

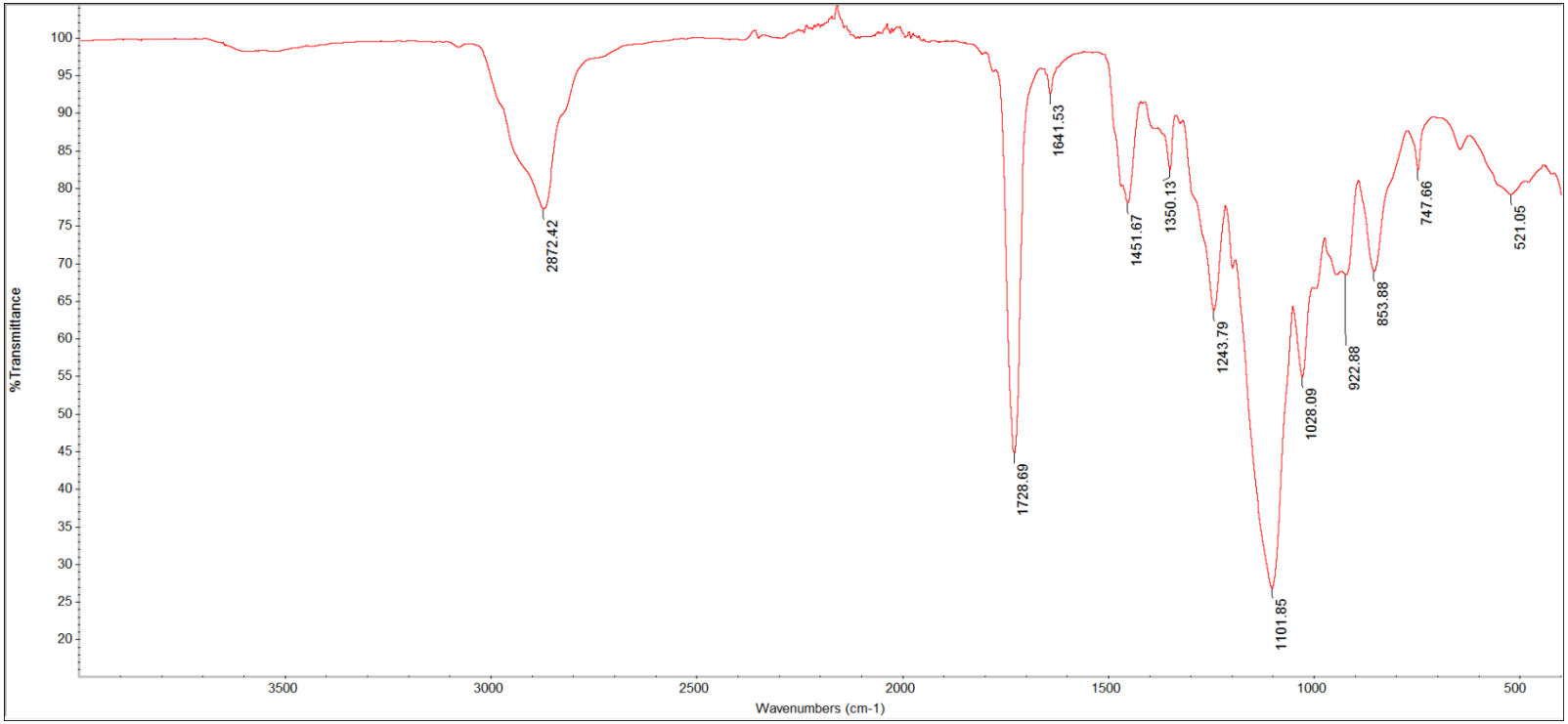

Figure A.20. FT-IR spectrum of C1.

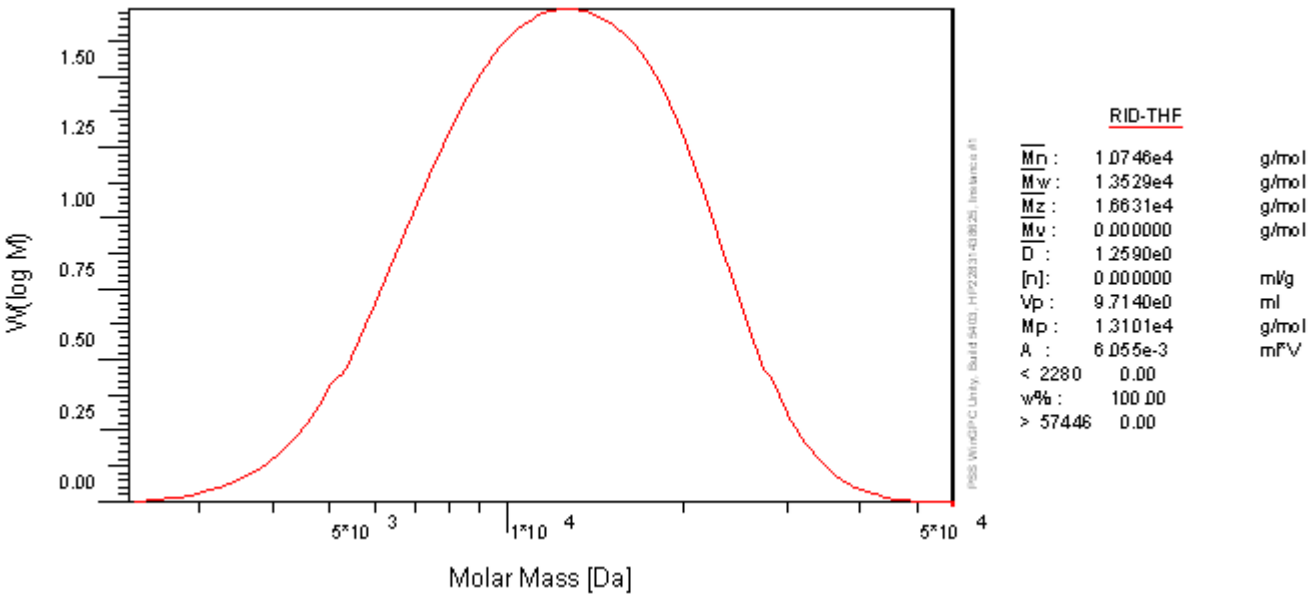

Figure A.21. GPC result of C1.

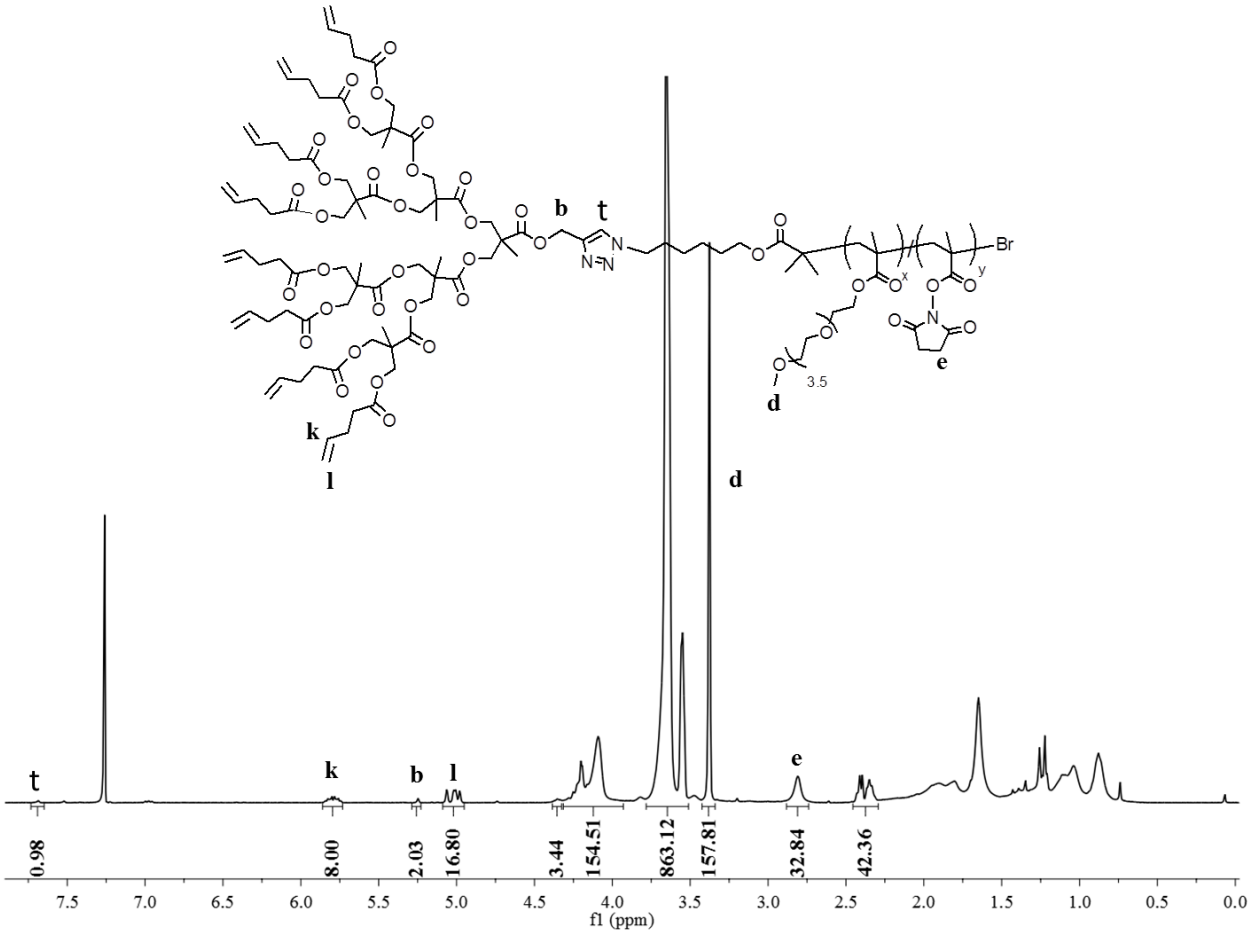

Figure A.22. ^{1}H NMR spectrum of C2.

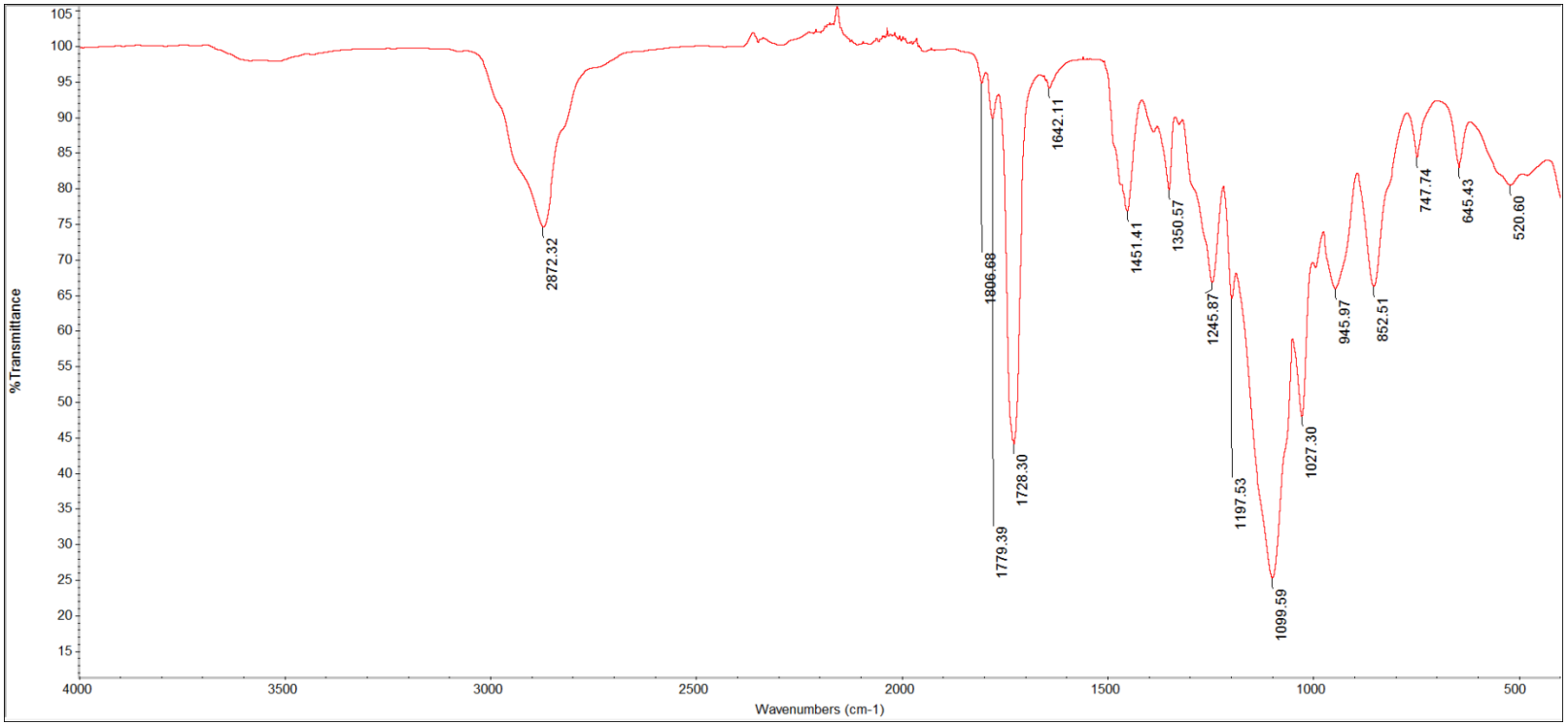

Figure A.23. FT-IR spectrum of C2.

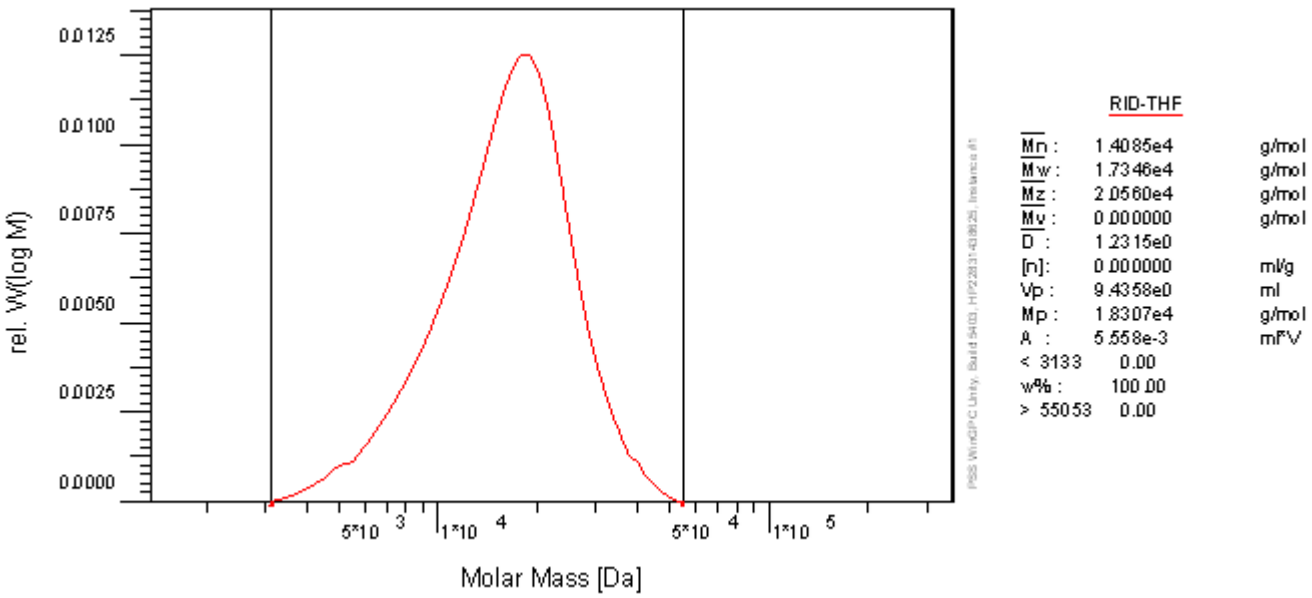

Figure A.24. GPC result of C2.

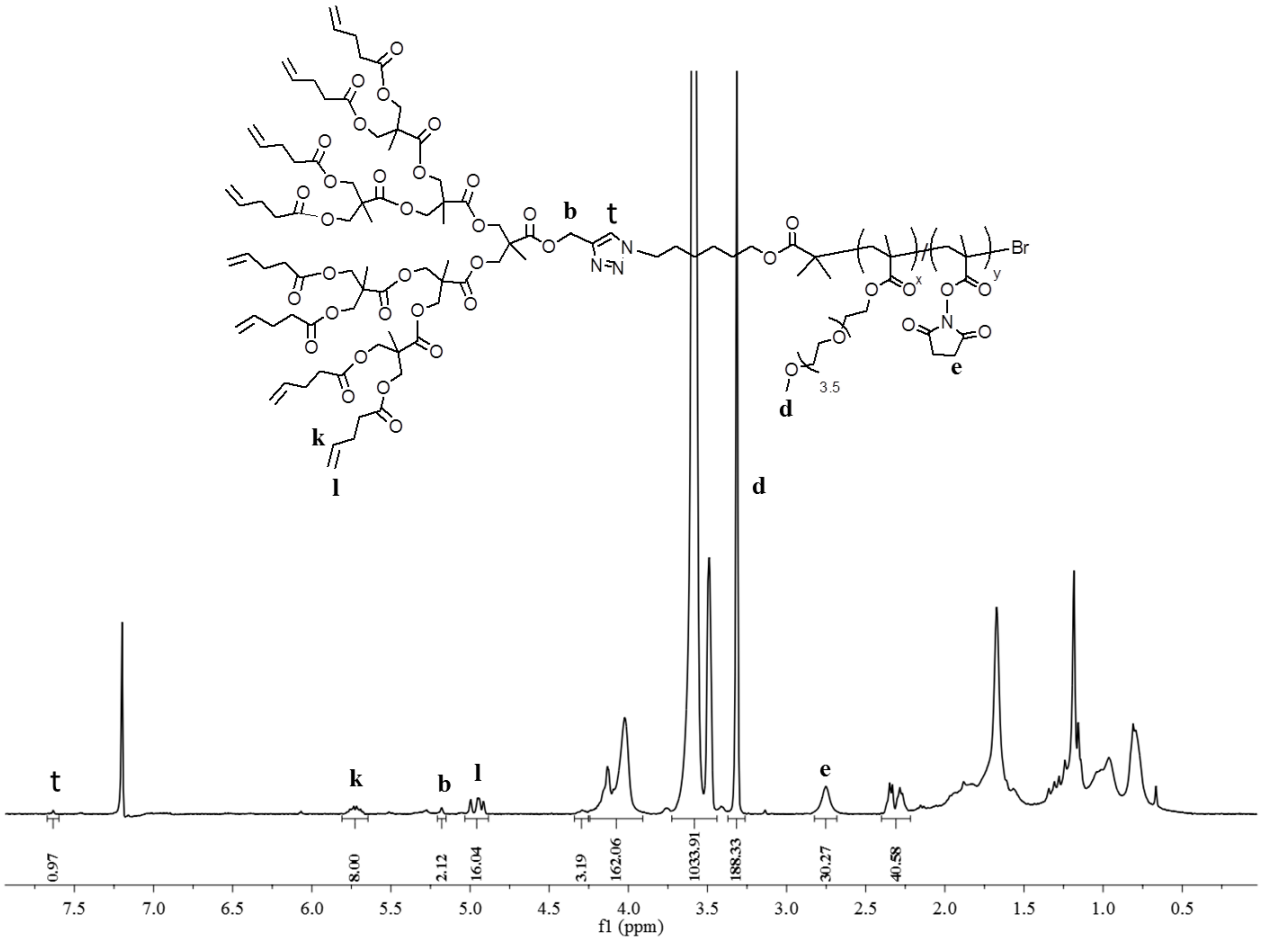

Figure A.25. ^{1}H NMR spectrum of C3.

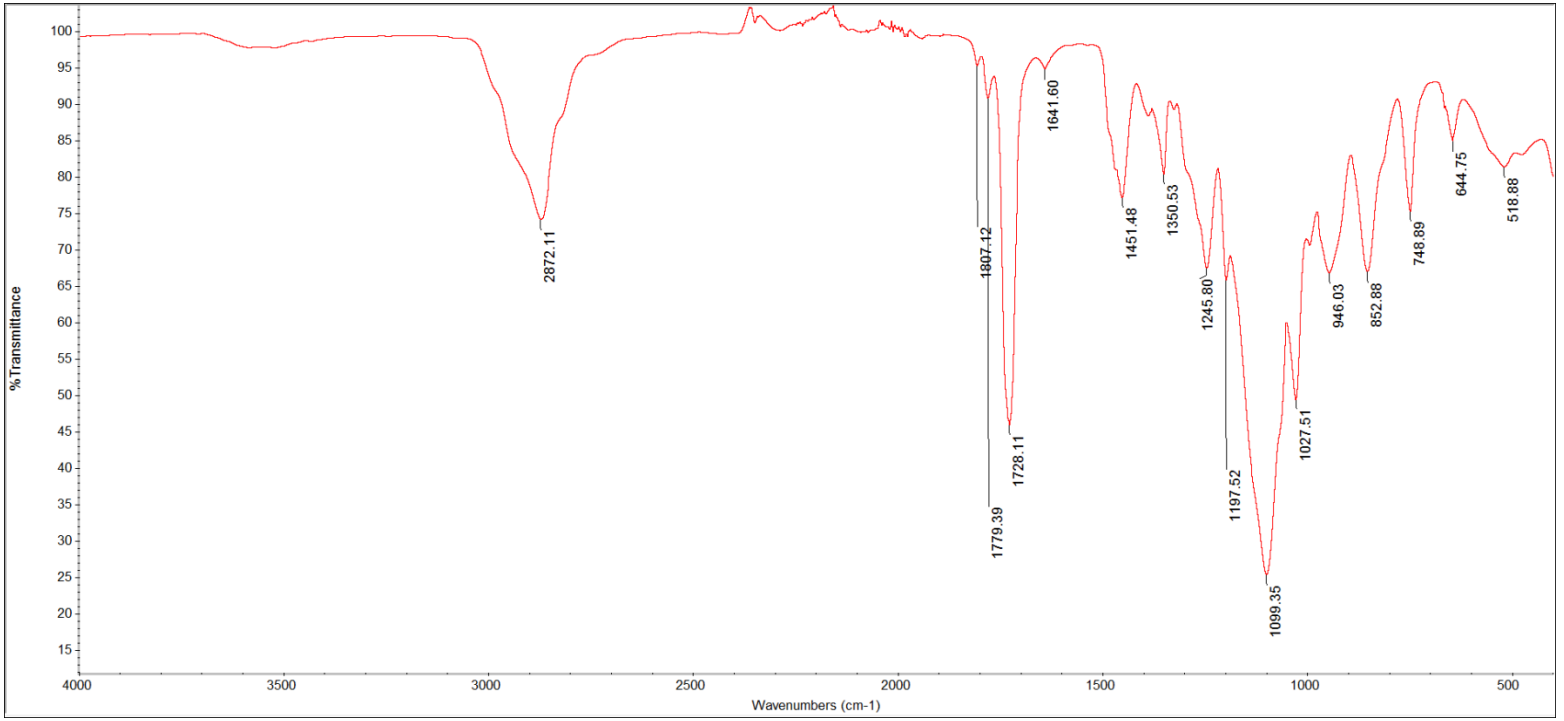

Figure A.26. FT-IR spectrum of C3.

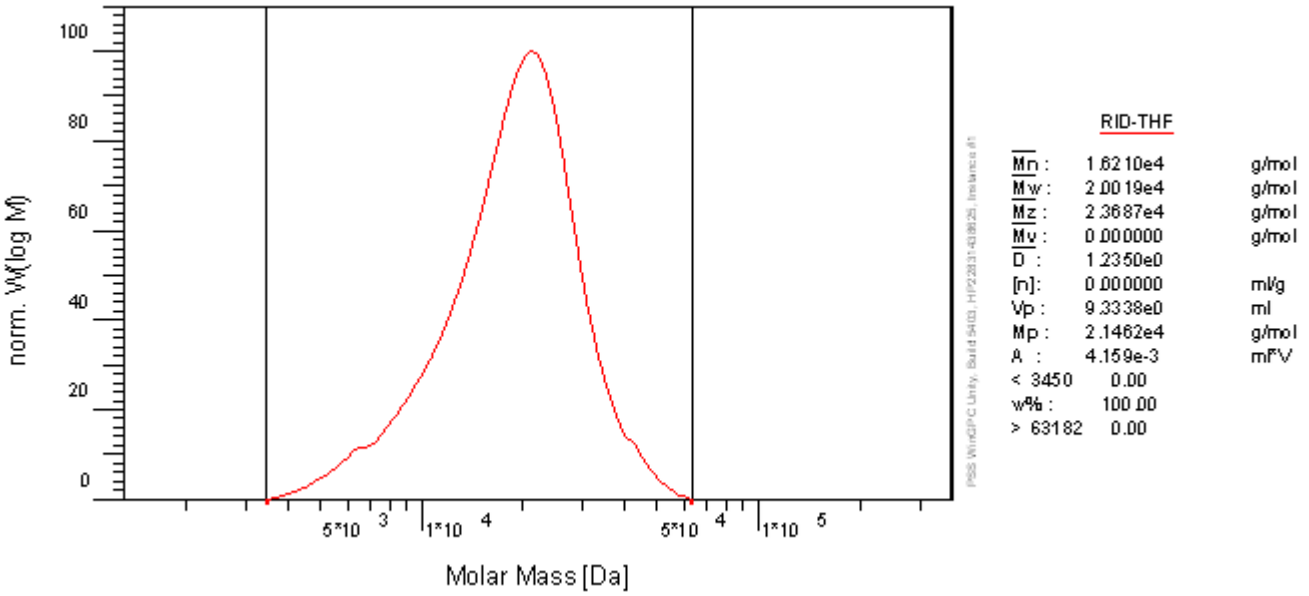

Figure A.27. GPC result of C3.

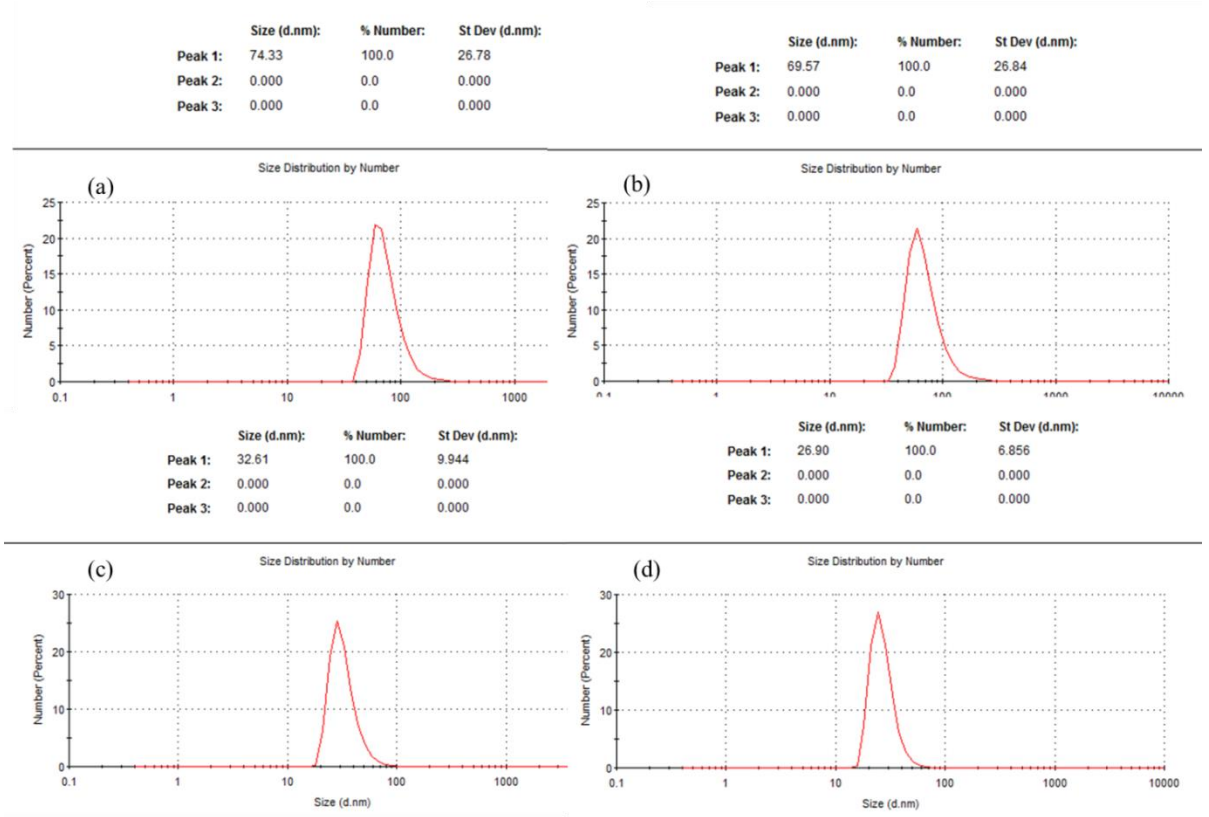

Figure A.28. Size distributions of (a) non-crosslinked empty, (b) non-crosslinked pyrene loaded, (c) crosslinked empty, (d) crosslinked pyrene loaded micelles assembled from C1 in water.

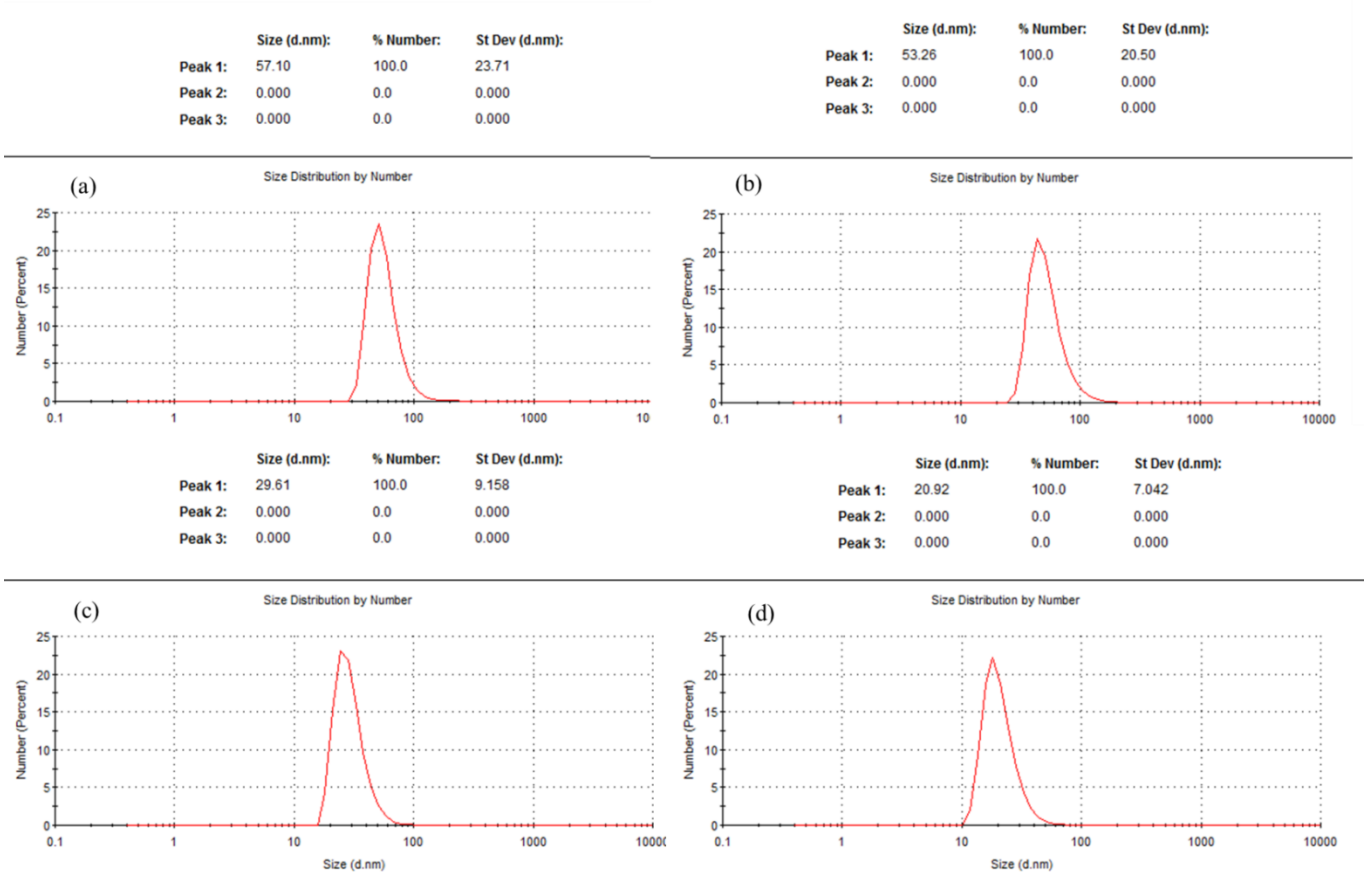

Figure A.29. Size distributions of (a) non-crosslinked empty, (b) non-crosslinked pyrene loaded, (c) crosslinked empty, (d) crosslinked pyrene loaded micelles assembled from C2 in water.

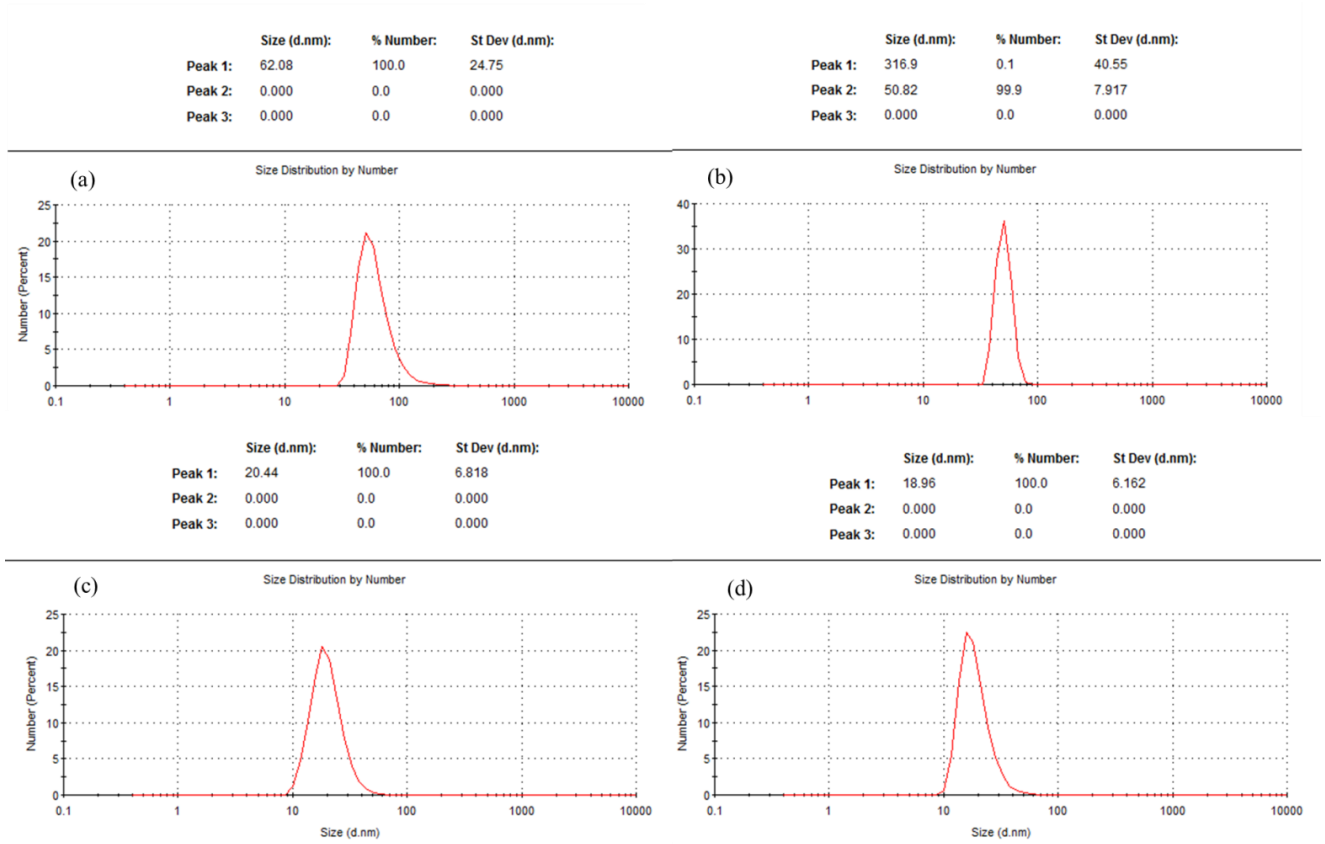

Figure A.30. Size distributions of (a) non-crosslinked empty, (b) non-crosslinked pyrene loaded, (c) crosslinked empty, (d) crosslinked pyrene loaded micelles assembled from C3 in water.

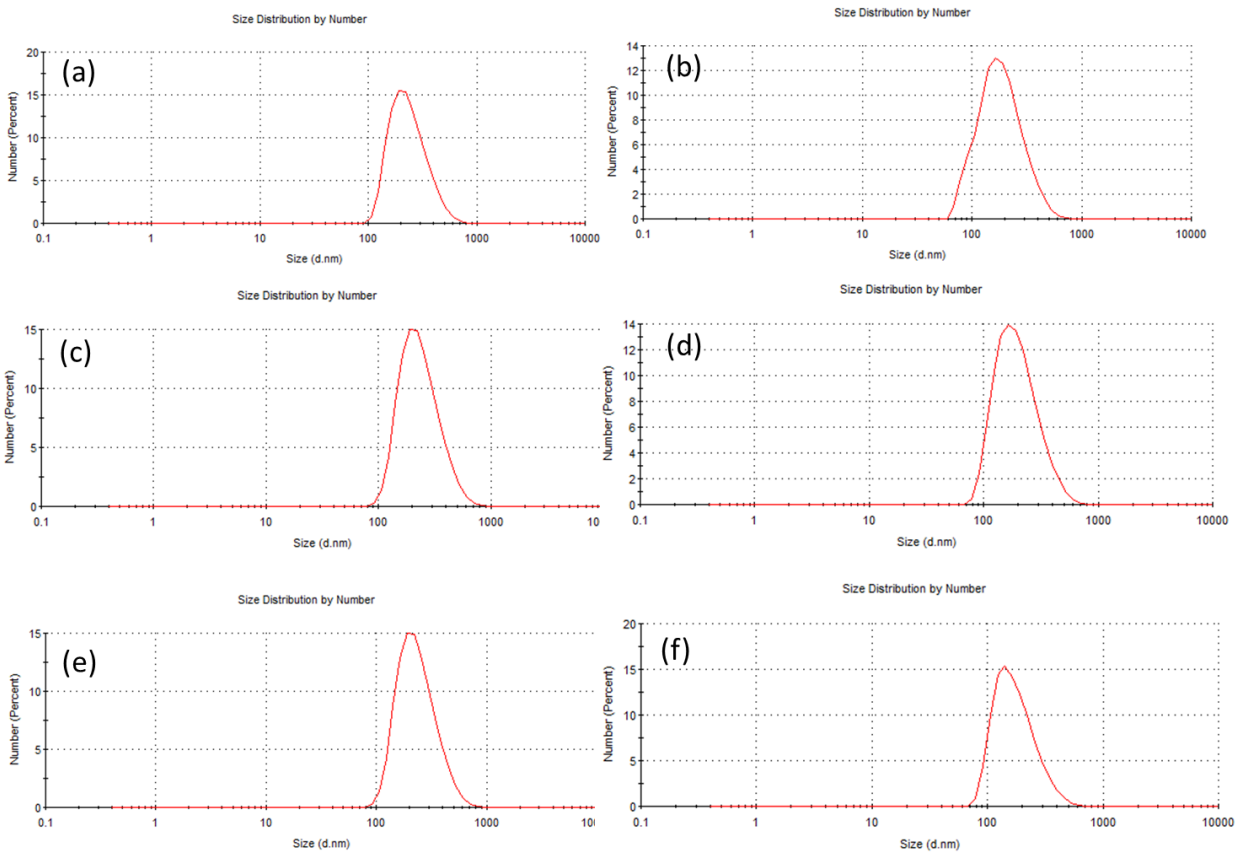

Figure A.31. Size distributions after THF addition to (a-c-d) crosslinked empty micelles assembled from C1, C2 and C3, (b-d-f) crosslinked pyrene loaded micelles assembled from C1, C2 and C3, respectively.

REFERENCES

1. Wild, C. P., "Future Research Perspectives on Environment and Health: The Requirement for a More Expansive Concept of Translational Cancer Research", *Environmental Health,* Vol. 10, pp. 1-4, 2011.

2. Jemal, A., F. Bray, M. M. Center, J. Ferlay, E. Ward, D. Forman, ''Global Cancer Statistics'', *CA: A Cancer Journal for Clinicians,* Vol. 61, pp. 69-90, 2011.

3. Bae, Y., H., K. Park, ''Targeted Drug Delivery to Tumors: Myths, Reality and Possibility'', *Journal of Control. Release,* Vol. 153, pp. 198-205, 2011.

4. Langer, R., ''Drug Delivery: Drugs on Target'', *Science,* Vol. 293, pp. 58–59, 2001.

5. Moghimi, S., A. Hunter, J. Murray, ''Long-Circulating and Target-Specific Nanoparticles: Theory to Practice'', *Pharmacological Reviews,* Vol. 53, pp. 283-318, 2001.

6. Cho, K., X. Wang, S. Nie, Z. Chen, D. Shin, ''Therapeutic Nanoparticles for Drug Delivery in Cancer'', *Clinical Cancer Research,* Vol.14, pp.1310-1316, 2008.

7. Duncan, R., ''The Dawning Era of Polymer Therapeutics'', *Nature Reviews Drug Discovery,* Vol. 2, pp. 347-360, 2003.

8. Chacko, R. T., J. Ventura, J. Zhuang, S. Thayumanavan, ''Polymer Nanogels: A Versatile Nanoscopic Drug Delivery Platform'', *Advanced Drug Delivery Reviews,* Vol. 64, pp. 836-851, 2012.

9. Hobbs, S. K., V. L. Monsky, F. Yuan, W. G. Roberts, L. Griffith, V. P. Torchilin, R. K. Jain, ‘‘Regulation of Transport Pathways in Tumor Vessels: Role of Tumor Type and Microenvironment’’, *Proceeding of the National Academy Sciences of the United States of America*, Vol. 95, pp. 4607-4612, 1998.

10. Seymour, L. W., K. Ulbrich, P. S. Steyger, M. Brereton, V. Subr, J. Strohalm, R. Duncan, ‘‘Tumor Tropism and Anti-Cancer Efficacy of Polymer-Based Doxorubicin Prodrugs in the Treatment of Subcutaneous Murine B16F10 Melanoma’’, *British Journal of Cancer*, Vol. 70, pp. 636-641, 1994.

11. Maeda, H., L. W. Seymour, Y. Miyatomo, ‘‘Conjugates of Anticancer Agents and Polymers: Advantages of Macromolecular Therapeutics in *vivo*’’, *Bioconjugate Chemistry*, Vol. 3, pp. 351-362, 1992.

12. Allen, T. M., P. R. Cullis, ‘‘Drug Delivery Systems: Entering the Mainstream’’, *Science*, Vol. 303, pp. 1818-1822, 2004.

13. Sutton, D., N. Nasongkla, E. Blanco, and J. Gao, “Functionalized Micellar Systems for Cancer Targeted Drug Delivery”, *Pharmaceutical Research*, Vol. 24, No. 6, pp. 1029-1046, 2007.

14. Nishiyama, N., K. Kataoka ‘‘Current State, Achievements and Future Prospects of Polymeric Micelles as Nanocarriers for Drug and Gene Delivery’’, *Pharmacology & Therapeutics*, Vol. 112, pp. 630-648, 2006.

15. Maysinger, D., A. Eisenberg, ‘‘Nano-Engineering Block Copolymer Aggregates for Drug Delivery’’, *Colloids Surfaces B: Biointerfaces*, Vol 16, pp. 3-27, 1999.

16. Torchilin, V., P., ‘‘Targeted Polymeric Micelles for Delivery of Poorly Soluble Drugs’’, *Cellular and Molecular Life Sciences*, Vol. 61, pp. 2549–2559, 2004.

17. Gong, J., M. Chen, Y. Zheng, S. Wang and Y. Wang, "Polymeric Micelles Drug Delivery System in Oncology", *Journal of Controlled Release*, Vol. 159, pp. 312-323, 2012.

18. Chris, O., V. Bult, M. Bos, G. Storm, J. F. Nijsen, W. E. Hennink, "Polymeric Micelles in Anticancer Therapy: Targeting, Imaging and Triggered Release", *Pharmaceutical Research,* Vol. 27, pp. 2569–2589, 2010.

19. Moghimi, S., A. Hunter, J. Murray, ''Long-circulating and target-specific nanoparticles: theory to practice'', *Pharmacological Reviews*, Vol. 53, pp. 283–318, 2001.

20. Haag, R., ''Supramolecular Drug-Delivery Systems Based on Polymeric Core–Shell Architectures'', *Angewandte Chemie International Edition*, Vol. 43, pp. 278-282, 2004.

21. Lavasanifar, A., X. B. Xiong, Z. Binkhathlan, O. Molavi, "Amphiphilic Block co-Polymers: Preparation and Application in Nanodrug and Gene Delivery", *Acta Biomaterialia,* Vol. 8, pp. 2017–2033, 2012.

22. Rapoport, N., ''Physical Stimuli-Responsive Polymeric Micelles for Anti-Cancer Drug Delivery'', *Progress in Polymer Science*, Vol. 32, pp. 962-990, 2007.

23. Sutton, D., N. Nasongkla, E. Blanco, J. Gao, ''Functionalized Micellar Systems for Cancer Targeted Drug Delivery'', *Pharmaceutical Research*, Vol. 24, pp. 1029-1046, 2007.

24. Lee, C. C., J. A. MacKay, J. M. J. Fréchet, F. C. Szoka, ''Designing Dendrimers for Biological Applications'', *Nature Biotechnology*, Vol. 23, pp. 1517-1526, 2005.

25. Boas, U., P. M. H. Heegaard, ''Dendrimer in Drug Research'', *Chemical Society Reviews*, Vol. 33, pp. 43-63, 2004.

26. Gillies, E. R., J. M. J. Fréchet, ‘‘Dendrimers and dendritic polymers in drug delivery’’, *Drug Discovery Today*, Vol. 10, pp. 35-43, 2005.

27. Liu, M., J. M. J. Fréchet, ‘‘Designing Dendrimers for Drug Delivery’’, *Pharmaceutical Science & Technology Today*, Vol. 2, pp. 393-401, 1999.

28. Lee, C. C., J. A. MacKay, J. M. J. Fréchet, F. C. Szoka, ‘‘Designing dendrimers for biological applications’’, *Nature Biotechnology*, Vol. 23, pp. 1517 – 1526, 2005.

29. She, W., K. Luo, C. Zhang, G. Wang, Y. Geng, Y. Li, B. He, Z. Gu, ‘‘The Potential of Self-Assembled, pH-Responsive Nanoparticles of mPEGylated Peptide Dendron Doxorubicin Conjugates for Cancer Therapy’’, *Biomaterials*, Vol. 34, pp. 1613-1623, 2013.

30. Gok, O., S. Yigit, M. M. Kose, R. Sanyal, A. Sanyal, ‘‘Dendron–Polymer Conjugates via the Diels–Alder “Click” Reaction of Novel Anthracene-Based Dendrons’’, *Polymer Chemistry*, Vol. 51, pp. 3191-3201, 2013.

31. Gillies, E.R., E. Dy, J. M. J. Fréchet, F. C. Szoka, ‘‘Biological Evaluation of Polyester Dendrimer: Poly(ethylene oxide) “Bow-Tie” Hybrids with Tunable Molecular Weight and Architecture’’, *Molecular Pharmaceutics*, Vol. 2, pp. 129-138, 2004.

32. Kempe, K., S. Onbulak, U. S. Schubert, A. Sanyal, R. Hoogenboom ‘‘pH Degradable Dendron-Functionalized poly(2-ethyl-2-oxazoline) Prepared by a Cascade “Double-Click” Reaction’’, *Polymer Chemistry*, Vol. 4, pp. 3236-3244, 2013.

33. Pati, D., N. Kalva, S. Das, G. Kumaraswamy, S. S. Gupta, A. V. Ambade, ‘‘Multiple Topologies from Glycopolypeptide-Dendron Conjugate Self-Assembly: Nanorods, Micelles, and Organogels’’, *American Chemical Society*, Vol. 134, pp. 7796-7802, 2012.

34. Gaucher, G., R. H. Marchessault, J. C. Leroux, ‘‘Polyester-Based Micelles and Nanoparticles for the Parenteral Delivery of Taxanes’’, *Journal of Controlled Release*, Vol. 143, pp. 2–12, 2010.

35. Bae, Y. H., H. Q. Yin, ‘‘Stability Issues of Polymeric Micelles’’, *Journal of Controlled Release*, Vol. 131, pp. 2–4, 2008.

36. Ferrari, M., ‘‘Cancer Nanotechnology: Opportunities and Challenges’’, *Nature Reviews Cancer*, Vol. 5, pp. 161–171, 2005.

37. Torchilin, V. P., ‘‘Multifunctional nanocarriers’’, *Advanced Drug Delivery Reviews*, Vol. 58, pp. 1532–1555, 2006.

38. Liu, Z., Z. Yu, W. He, S. Ma, L. Sun, F. Wang, ‘‘In-*vitro* Internalization and In-*vivo* Tumor Uptake of Anti-EGFR Monoclonal Antibody LA22 in A549 Lung Cancer Cells and Animal Model’’, *Cancer Biotherapy and Radiopharmaceuticals*, Vol. 24, pp.15–23, 2009.

39. Peppas, N. A., D. E. Owens, ‘‘Opsonization, Biodistribution, and Pharmocokinetics of Polymeric Nanoparticles’’, *International Journal of Pharmaceutics*, Vol. 307, pp. 93-102, 2006.

40. Owena, S. C., D. P. Y. Chana, M. S. Shoicheta, ‘‘Polymeric Micelle Stability’’, *Nano Today*, Vol. 7, pp. 53-65, 2012.

41. O’Reilly, R. K., C. J. Hawker, K. L. Wooley, “Crosslinked Block Copolymer Micelles: Functional Nanostructures of Great Potential and Versatility”, *Chemical Society Reviews*, Vol. 35, pp. 1068-1083, 2006.

42. Donald, E. O., N. A. Peppas, “Opsonization, Biodistribution, and Pharmacokinetics of Polymeric Nanoparticles”, *International Journal of Pharmaceutics*, Vol. 307, pp. 93 – 302, 2006.

43. Sungwon, K., Y. Shi, J. Y. Kim, K. Park, J. Cheng, "Overcoming The Barriers in Micellar Drug Delivery: Loading Efficiency, In Vivo Stability, and Micelle–Cell Inter-action", *Expert Opinion on Drug Delivery*, Vol. 7, pp. 49 – 62, 2010.

44. Allen, C., D. Maysinger, A. Eisenberg ''Nano-engineering block copolymer aggregates for drug delivery''. *Colloids Surf B: Biointerfaces*, Vol. 16, pp. 3-27, 1999.

45. Shuai, X. T., T. Merdan, A. K. Schaper, F. Xi, T. Kissel, ''Core-Crosslinked Polymeric Micelles as Paclitaxel Carriers, *Bioconjugate Chemistry*, Vol. 15, pp. 441-448, 2004.

46. Rijcken, C. J., C. J. Snel, R. M. Schiffelers, C. F. Nostrum, W. E. Hennink, ''Hydrolysable a Core-Crosslinked Thermosensitive Polymeric Micelles: Synthesis, Characterisation and in *vivo* Studies, *Biomaterials*, Vol. 28, pp. 5581-5593, 2007.

47. Talelli, M., M. Iman, A. K. Varkouhi, C. J. F. Rijcken, R. M. Schiffelers, T. Etrych, K. Ulbrich, C. F. Nostrum, T. Lammers, G. Storm, W. E. Hennink, ''Core-Crosslinked Polymeric Micelles with Controlled Release of Covalently Entrapped Doxorubicin, *Biomaterials,* Vol. 31, pp. 7797–7804, 2010.

48. Jin, S. K., J. H. Youk, "Preparation of Core Crosslinked Micelles Using a Photo Crosslinking Agent", *Polymer Communication*, Vol. 50, pp. 2204 – 2208, 2009.

49. Wu, Y., W. Chen, F. Meng, Z. Wang, R. Cheng, H. D. Liu, Z. Zhong, ''Core Crosslinked pH-Sensitive Degradable Micelles: A Promising Approach to Resolve the Extracellular Stability versus Intracellular Drug Release Dilemma'', *Journal of Controlled Release*, Vol. 164, pp. 338–345, 2012.

50. Li, Y., K. Xiao, J. Luo, W. Xiao, J. S. Lee, A. M. Gonik, J. Kato, T. A. Dong, K. S. Lam, ‘‘Well-defined, reversible disulfide cross-linked micelles for on-demand paclitaxel delivery’’, *Biomaterials*, Vol. 32, pp. 6633-6645, 2011.

51. Yoon, H. Y., H. Koo, K. Y. Choi, I. C. Kwon, K. Choi, J. H. Park, K. Kim, ‘‘Photo Crosslinked Hyaluronic Acid Nanoparticles with Improved Stability for in *vivo* Tumor-Targeted Drug Delivery’’, *Biomaterials*, Vol. 34, pp. 5273-5280, 2013.

52. Hoyleand, C. E., C. N. Bowman, ‘‘Thiol–Ene Click Chemistry’’, *Angewandte Chemie International Edition*, Vol. 49, pp. 1540 – 1573, 2010.

53. Lee, J. W., S. C. Han, J.H. Kim, W. S. Shin, S. H. Jin, ‘‘Synthesis of Symmetrical and Unsymmetrical PAMAM Dendrimers by Fusion between Azide- and Alkyne-Functionalized PAMAM Dendrons’’, *Bioconjugate Chemistry*, Vol. 18, pp. 579-584, 2007.

54. Polaske, N. W., D. V. McGrath, J. R. McElhanon, ‘‘Thermally Reversible Dendronized Step-Polymers Based on Sequential Huisgen 1,3-Dipolar Cycloaddition and Diels-Alder “Click” Reactions’’, *Macromolecules*, Vol. 43, pp. 1270-1276, 2010.

55. Seo, T., Z. Li, H. Ruparel, ‘‘Click Chemistry to Construct Fluorescent Oligonucleotides for DNA Sequencing’’, *Journal of Organic Chemistry*, Vol. 68, pp. 609-612, 2003.

56. Rostovtsev, V. V., L. G. Green, V. V. Fokin, K. B. Sharpless ‘‘A Stepwise Huisgen Cycloaddition Process: Copper(I)-Catalyzed Regioselective “Ligation” of Azides and Terminal Alkynes’’, *Angewandte Chemie, International Edition*, Vol. 41, pp. 2596-2599, 2002.

57. Altin, H., I. Kosif, R. Sanyal, ‘‘Fabrication of “Clickable” Hydrogels via Dendron-Polymer Conjugates’’, *Macromolecules*, Vol. 43, pp. 3801-3808, 2010.

58. Brett H., J. L. Mynar, C. J. Hawker, J. M. J. Fre´chet, “Dendronized Linear Polymers via “Click Chemistry””, *Journal of American Chemical Society,* Vol. 126, pp. 15020-15021, 2004.

59. Lowe, A. B., ‘‘Thiol-ene ‘‘click’’ reactions and recent applications in polymer and materials synthesis’’, *Polymer Chemistry*, Vol. 1, pp. 17-36, 2010.

60. Alice E. E., J. Harrell, V. Sathiyakumar, M. Meschievitz, J. Katz, K. Adcock, E. Harth, “Click” Reactions: Novel Chemistries for Forming Well-defined Polyester Nanoparticles”, *Macromolecules*, Vol. 43, pp. 5665 – 5671, 2010.

61. Eceoğlu, M., Core Crosslinked Polymeric Micelles from Dendritic Macromolecules as Drug Delivery Agents, Ms. Thesis, Graduate Program in Chemistry Boğaziçi University, 2012.

62. Giuseppe M., V. Ladmiral, L. Tao, D. M. Haddleton, “One-Pot Tandem Living Radical Polymerisation–Huisgens Cycloaddition Process (‘‘Click’’) Catalysed by N-Alkyl-2-Pyridylmethanimine/Cu(I)Br Complexes”, *Chemical Communications,* Vol. 16, pp. 2089 – 2091, 2005.

63. Peng W., M. Malkoch, J. N. Hunt, R. Vestberg, E. Kaltgrad, M. G. Finn, V. V. Fokin, K. B. Sharpless and C. J. Hawker, “Multivalent, Bifunctional Dendrimers Prepared by Click Chemistry”, *Chemical Communications*, Vol. 46, pp. 5775-5777, 2005.